Mechanisms of Neuroprotection Mediated by Oligodendroglial Exosomes

Dissertation zur Erlangung des Grades

Doktor der Naturwissenschaften

am Fachbereich Biologie

der Johannes-Gutenberg-Universität Mainz

von

Wen Ping Elsner (geb. Kuo)

geboren am 23.08.1983 in Hürth

Mainz, 2016

Dekan:

1. Berichterstatter:

2. Berichterstatter:

Tag der mündlichen Prüfung: 15.08.2016

TABLE OF CONTENT

1 ABSTRACT 1

2 INTRODUCTION 2

2.1 Neuron-Glia Interactions in the Central Nervous System 2

2.2 Friends for Life: Neuron-Glia Communication is Evolutionary Conserved 3

2.3 Oligodendrocytes: From OPCs to Myelinating Cells 4

2.3.1 The Significance of Myelin in Maintaining Axonal Integrity 7
2.3.2 Influence of Myelin on Axonal Transport 8
2.3.3 Myelin Diseases: Perturbed Axon-Glia communication? 9

2.4 Extracellular Vesicles: Intermediaries for Intercellular Communication 10

2.4.1 Composition of Exosomes 12
2.4.2 Exosome Biogenesis and Heterogeneity 12
2.4.3 Exosome Secretion and Uptake 14

2.5 The Ambivalence of Extracellular Vesicles: The Good and the Bad 15

2.6 Extracellular Vesicles in the Brain 16

2.6.1 EV-Mediated Neuron-Glia Interaction in Neuropathologies 17
2.6.2 Benefits of EV-Mediated Neuron-Glia Interaction 17
2.6.3 Reciprocal communication between oligodendrocytes and neurons via exosomes 18
2.6.4 Neuroprotective and Regenerative Potentials of EVs in the CNS 20

2.7 Aim of the Study 22

3 MATERIALS AND METHODS 23

3.1 Equipment, Materials, Buffers and Media 23

3.1.1 Equipment 23
3.1.2 Materials 24
3.1.3 Software 25
3.1.4 Buffers and Media 26

3.2 Antibodies 27

3.2.1 Primary Antibodies 27

3.2.2 Secondary Antibodies 28

3.3 Molecular Biology 28

3.3.1 Transformation into Competent Bacteria 28
3.3.2 Plasmid Preparation from Bacteria 29

3.4 Cell Culture 29

3.4.1 Isolation of Primary Oligodendrocytes using MACS Technology 29
3.4.2 Preparation of Primary Cortical Neurons 31
3.4.3 Preparation of Primary Hippocampal Neurons 32
3.4.4 Preparation of Primary Astrocytes 32
3.4.5 Oli-*neu* Cell Culture 33
3.4.6 HEK293T Cell Culture 33

3.5 Transfection 33

3.5.1 AMAXA Nucleofection 33
3.5.2 Bio-Rad GenePulser Electroporation 34

3.6 Immunocytochemistry 34

3.7 Protein Biochemistry 35

3.7.1 Cell Lysis 35
3.7.2 SDS-PAGE 35
3.7.3 Western Blotting 35

3.8 Exosome Preparation 36

3.9 Boyden Chamber Co-Culture System 36

3.10 Oxygen-Glucose Deprivation 37

3.11 MTT Viability Assay 37

3.12 Staining of the Mitochondrial Membrane Potential 38

3.13 Phospho-MAPK Array 38

3.14 Axonal Transport Analysis 38

3.14.1 Live-Cell Imaging 39
3.14.2 Kymograph Generation 40
3.14.3 Kymograph Analysis 40

4 RESULTS 42

4.1 Characterization of Isolated O4^{+}-Oligodendrocytes by Magnetic-activated Cell Sorting (MACS) 42

4.2 Stress-Relevant Proteins are Shipped to Neurons via Oligodendroglial Exosomes 44

4.3 Oligodendroglial Exosomes Facilitate Neuroprotection under Cellular Stress 45

4.3.1 Oxidative Stress 45
4.3.2 Nutrient Deprivation 48
4.3.3 Oxygen-Glucose Deprivation 50

4.4 Activation of Pro-Survival Signaling Pathways in Neurons by Oligodendroglial Exosomes 52

4.5 Oligodendroglial Exosomes Facilitate Axonal Transport under Oxidative Stress and Starvation Stress 55

4.6 Mutant Oligodendrocytes do not Mediate Neuroprotection 59

4.6.1 PLP^{null}- and CNP^{null}-Exosomes do not Support Neurons under Starvation Stress 60
4.6.2 Neuroprotective Effect of Oligodendroglial Exosomes: A Matter of Quality or Quantity? 61

4.7 PLP^{null}- and CNP^{null}-Exosomes do not Facilitate Axonal Transport under Starvation Stress 64

5 DISCUSSION 67

5.1 Characterization of High-purity OL Cultures to Study OL Exosomes 67

5.2 Exosomes Ameliorate Cellular Stress Tolerance in Neurons 68

5.3 Oligodendrocytes Shuttle Stress-protective Cargo to Neurons via Exosomes 69

5.4 Exosomes Activate Pro-Survival Signalling Pathways in Neurons 71

5.5 Axonal Transport Dynamics are Changed in Response to Oligodendroglial Exosomes 72

5.6 Comparison of Wildtype and Mutant Exosomes: Indications of Physiological Relevance? 74

5.7 *In vivo* evidence of exosome-mediated axon-myelin communication 76

5.8 Outlook 78

6 REFERENCES 80

7 APPENDIX 110

7.1 List of Abbreviations 110

7.2 List of Tables 112

7.3 List of Figures 113

8 PUBLICATIONS 115

9 ACKNOWLEDGEMENT 118

10 CURRICULUM VITAE 119

11 EIDESSTATTLICHE ERKLÄRUNG 122

1 Abstract

In the CNS, myelination acquires an intimate communication between oligodendrocytes and neurons not only for a fast saltatory conduction but also to maintain long-term axonal integrity. Recent evidence has emerged that oligodendrocytes are metabolically coupled to neurons to promote neuronal survival. However, this finding unravels only a small part of a complex mechanism mediated by oligodendrocytes providing trophic support to neurons. Exosomes are nano-sized, endosomal-derived vesicles carrying a specific set of lipids, proteins, and RNAs to target cells. We have recently provided evidence that neuronal electrical activity controls glial exosome release resulting in subsequent neuronal uptake and the modulation of neuronal gene expression. The presence of stress-relevant proteins in oligodendroglial exosomes suggests their neuroprotective potential upon horizontal transfer to neurons.

The present study deals with the role of oligodendroglial exosomes in glial support by analysing the underlying mechanisms of exosome-mediated neuroprotection. Functional assays revealed a role in neuroprotection by desensitising neurons towards cellular stress, such as oxidative stress and starvation stress. Using an *in vitro* model of brain ischemia, we further show that oligodendroglial exosomes are capable to relieve ischemic insult in neurons. Neuroprotection may be achieved by the transfer of protective cargo to neurons, potentially via the transfer of protective enzymes such as superoxide dismutase. Moreover, phosphorylation arrays revealed altered signal transduction pathways involved in cell survival upon exosome administration. A prerequisite of neuronal survival is the axonal transport of cytoplasmic components. In order to evaluate the exosomal influence on axonal transport, we analysed the movement of BDNF-containing vesicles in neurons by time-lapse microscopy. We found an increase of anterograde moving vesicles, but a reduced percentage of pauses exhibited during overall movement as well as a significantly lower number of static vesicles upon exosome treatment and stress exposure. It has been shown that axonal transport is affected in PLP and CNP-deficient mice. Intriguingly, exosomes derived from PLP and CNP null oligodendrocytes do not benefit neuroprotection, nor facilitate axonal transport.

In summary, our study indicates that oligodendroglial exosomes may complement the concept of glial support by promoting stress resilience in neurons.

2 Introduction

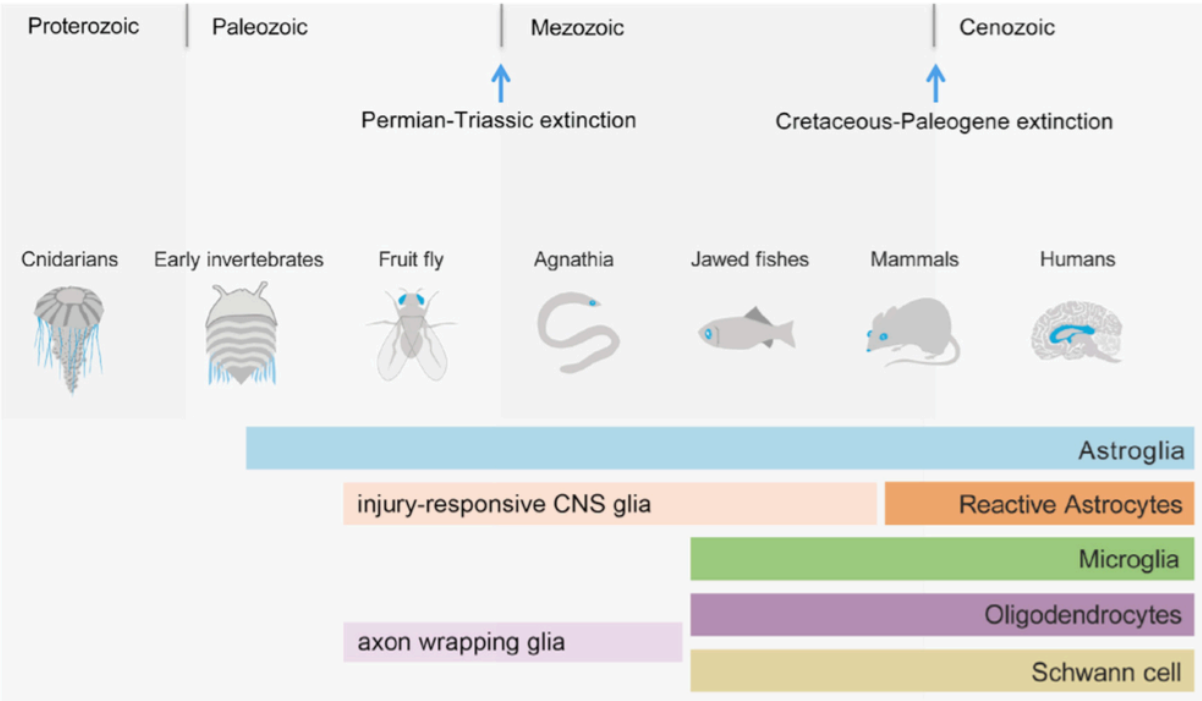

Figure 2-1 Glial phylogeny. The continuing timeline illustrates the evolutionary emergence of glial cells and their subpopulations, which correlates with growing complexity of the nervous system. The presence of oligodendrocytes has been reported first in jawed fishes. Illustration adapted from (Freeman and Rowitch, 2013).

2.1 Neuron-Glia Interactions in the Central Nervous System

The mammalian brain is a highly complex organ that is constructed by various types of neuronal and glial cells. While neurons guarantee the conversion and transmission of received information to neighbouring neurons via synaptic interconnections, glial cells representing the largest cell population in the brain contribute to homeostatic processes and the micro-architecture of the central nervous system (CNS). The necessity of glia is reflected in their diverse support functions that have given rise to the different glial subtypes. Accordingly, glial cells comprise the star-shaped astrocytes, predominantly controlling the ion and metabolic brain homeostasis, the highly ramified surveilling microglia representing the brain's immune defence, and the myelinating oligodendrocytes in the CNS insulating axonal segments for fast saltatory conductivity but also providing trophic support to neurons (Allen and Barres, 2009; Nave, 2010a). Reciprocal communication between neurons and oligodendrocytes is therefore

fundamental for the functional performance of the nervous system during development and throughout adult life (Fields and Stevens-Graham, 2002; Simons and Trajkovic, 2006).

2.2 Friends for Life: Neuron-Glia Communication is Evolutionary Conserved

The intimate association between neuron and glia has been evolved early during evolution. Representatives of the *Cnidarians*, such as the jellyfish, contain only rudimentary nerve nets and very simple light-sensing organelles which allow these multicellular animals to move (Figure 2-1) (Freeman and Rowitch, 2013). Increasing complexity of neuronal circuits finally resulted in the formation of glia to meet the new requirements. Among the most primitive animals *Acoelomorphs* appeared first in the phylogenetic order that possess glia-like cells with feasible supportive function for neurons (Bery et al., 2010). In higher invertebrates, such as *C. elegans* and *Drosophila*, glial functions have made a great leap forward as subdivision of glia occurs in order to expand in functionality. Certain functions are analogous to those defined for astrocytes in mammals including the guidance of axon outgrowth, dendrite morphogenesis, and trophic support required for neuronal survival (Edenfeld et al., 2005; Freeman and Doherty, 2006; Oikonomou and Shaham, 2011; Schirmeier et al., 2015; Shaham, 2006; Stork et al., 2012). In contrast, vertebrates have evolved larger brains with multiple cellular connectivities leading to the emergence of specialised glia, namely astrocytes, microglia, oligodendrocytes, and Schwann cells. The role of glia in vertebrates expanded significantly and comprises axonal insulation, metabolic regulation, ionic conductance, and synaptic efficacy to provide the ability to exhibit the most appropriate behaviour, incorporating flexibility of response (Laming et al., 2000). While glia make up to 15 % in *C. elegans* and *Drosophila*, in the human brain estimates ranges from 50 - 90 % suggesting a correlation of glia-to-neuron ratio with neuronal density and hence cognitive abilities rather than brain size (Allen and Barres, 2009; Freeman and Rowitch, 2013; Herculano-Houzel, 2014; Herculano-Houzel et al., 2015; Mota and Herculano-Houzel, 2014). The first has already been raised by various scientists declaring a higher demand and more assistance from glia to cater for the metabolic needs of larger neurons (Attwell and Laughlin, 2001; Hawkins and Olszewski, 1957; Tower, 1954). Consistently, this proposal matches the current understanding that both astrocytes and oligodendrocytes mediate metabolic support to neurons (Fünfschilling et al., 2012; Lee et al., 2012b; Magistretti, 2006; Magistretti and Allaman, 2015; Saab et al., 2016). Cellular composition of the grey matter of

human cerebral cortex revealed that the majority of glial cells are represented by oligodendrocytes (Pelvig et al., 2008). Myelination is one of the pivotal cell-cell interactions for normal brain development, involving extensive information exchange between differentiating oligodendrocytes and axons (Bercury and Macklin, 2015).

2.3 Oligodendrocytes: From OPCs to Myelinating Cells

The inception of myelination by oligodendrocytes marked an evolutionary milestone of brain development in vertebrates essential for motor, sensory, and higher-order cognitive function (Zalc et al., 2008). Oligodendrocytes produce myelin by elongating their plasma membrane to spirally enwrap axonal segments. This cellular process requires a precise orchestration of myelin production involving extensive changes in morphology and membrane architecture in oligodendrocytes.

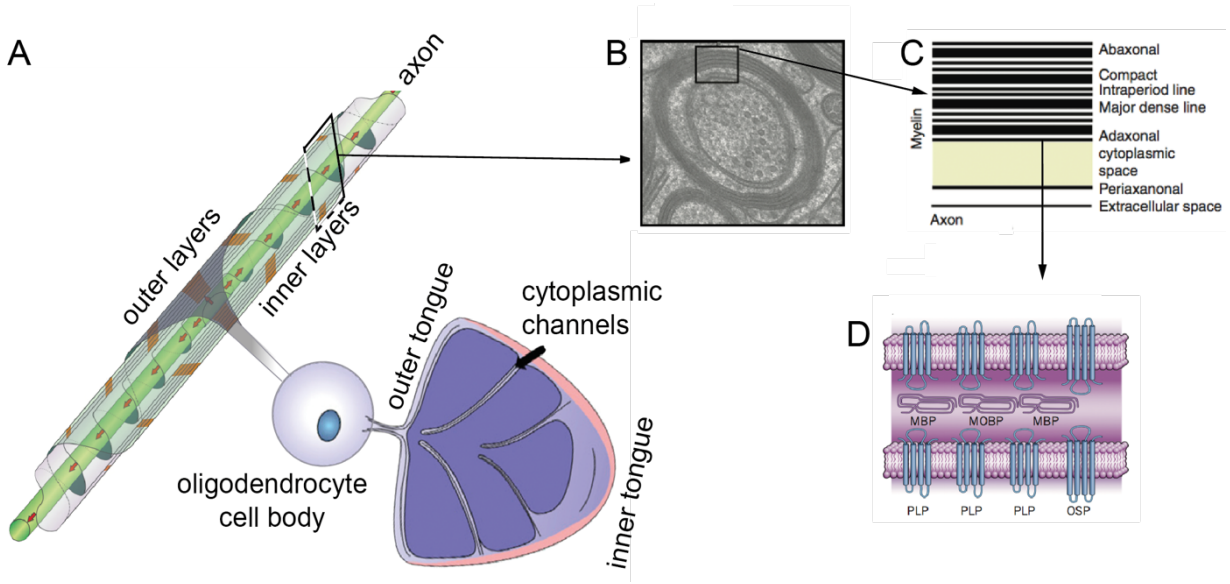

Figure 2-2 Emergence and structure of myelin. (A) Illustration of the myelination process. Axonal wrapping progresses as the myelin sheet grows at the leading edge of the inner tongue accompanied by the lateral extension of myelin membrane layers towards the nodal regions. (B) Electron microscopy picture depicts a cross-section of a myelinated axon. (C) Schematic illustration of the ultrastructure of myelin. (D) Protein composition in compact myelin. Modified from (Nave, 2010a; Simons and Nave, 2015; Snaidero et al., 2014)

Oligodendrocytes originate from oligodendroglial progenitor cells (OPC), which evolve in three waves from gliogenic ventricular zones (Menn et al., 2006; Rowitch and Kriegstein, 2010; Trotter et al., 2010). OPCs proliferate, migrate, and distribute across the entire CNS and some of them retain their stem cell-like potential throughout adulthood (Dawson et al., 2003; Hughes

and Appel, 2016). The vast majority of OPCs traverse a maturation process partitioned into different stages of morphological differentiation and express a number of stage-specific marker proteins and lipids, whereas NG2 and PDGFR-α are classical markers for OPCs and the expression of myelin proteins CNP (2',3'-Cyclic-nucleotide 3'-phosphodiesterase), PLP (proteolipid protein), MBP (myelin basic protein), MOG (myelin oligodendrocyte glycoprotein), and MAG (myelin-associated glycoprotein) appears as differentiation occurs (Figure 2-2 A) (Baumann and Pham-Dinh, 2001). Activity-dependent communication between axons and oligodendrocytes controls the emergence of new oligodendrocytes, myelin thickness, and the number of processes and myelin sheaths executed by single oligodendrocytes (Fields, 2015; Gibson et al., 2014; McKenzie et al., 2014; Mensch et al., 2015). Recent studies suggest that the distribution of OPCs allows an 'on-demand' generation of new oligodendrocytes in the adult CNS, which may be required for acquiring novel motor skills given that myelination correlates with cognitive ability and learning (Deoni et al., 2016; Hughes and Appel, 2016; McKenzie et al., 2014; Scholz et al., 2009). The differentiation program of OPCs underlies an extensive control mechanism encompassing the coordination of extrinsic signals including axonal electrical activity, intracellular pathways, micro RNAs (miRNA) and transcription factors (Emery, 2010; Gibson et al., 2014; Mitew et al., 2014; Wake et al., 2011). Interaction of cell adhesion molecules and signalling receptors mediates specific axon-glia recognition. For example, binding of the axonal cell adhesion molecule L1 activates the Src-family tyrosine kinase Fyn and facilitates the site-specific translation of MBP (White et al., 2008; White and Kramer-Albers, 2014). Integration of the manifold neuronal signals by oligodendrocytes controls cytoskeletal reorganization and cell polarization towards the axon-glia contact site to prepare the cells for myelin formation. Once the differentiation program has been turned on, the myelination process occurs at a very rapid pace. Time-lapse imaging of living zebrafishes demonstrated that myelination of single axonal segments has been completed after a few hours (Czopka et al., 2013). Proper myelination including compaction requires the synergy of intrinsic signals and bidirectional cellular interaction (Bechler et al., 2015; Lee et al., 2012a; Simons and Trajkovic, 2006).

Myelinated and non-myelinated segments, the so-called nodes of Ranvier, alternate along the axon to facilitate fast synaptic transmission and energy saving in neurons (Nave, 2010b). The wrapping process is propelled by the expansion of myelin at the tip of oligodendroglial

processes, the so-called leading edge, and the lateral growth of newly formed layers (Figure 2-2) (Snaidero et al., 2014; Snaidero and Simons, 2014). Increase of myelin thickness occurs along the internode followed by myelin compaction proceeding from the outer to the inner layer by the extrusion of cytoplasm, which finally gives rise to the characteristic structure of myelin (Figure 2-2 B – D). Dynamic movement of the non-adhesive leading edge is enabled by actin filament turnover, which is controlled by MBP (Nawaz et al., 2015; Zuchero et al., 2015).

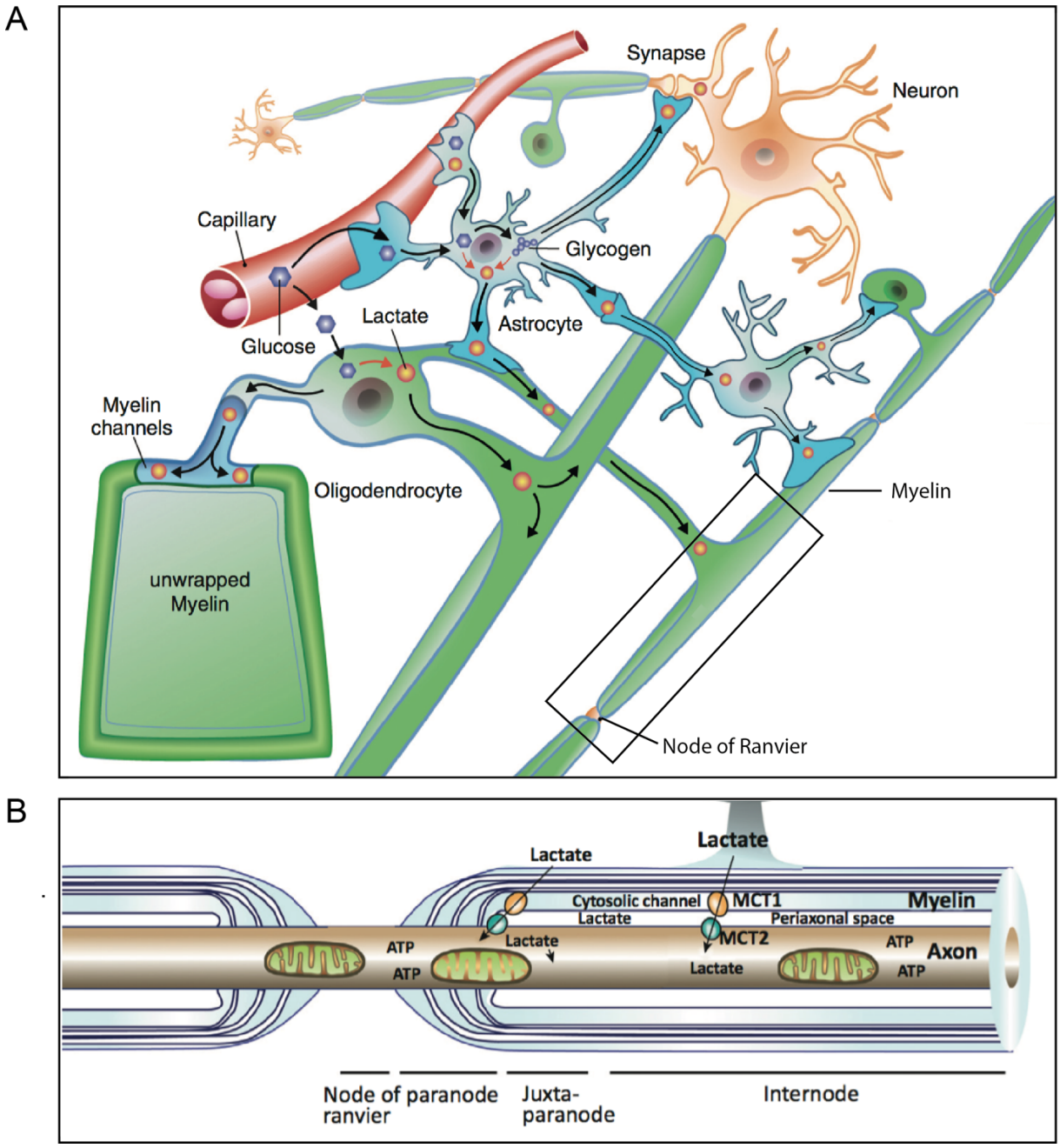

Figure 2-3 **Metabolic support of myelinated axons by glia.** (A) Axons are supplied with lactate deriving from glycolytic oligodendrocytes (green) and astrocytes (blue), which originates from glucose provided by both capillaries (red) and astrocytes. Modified from (Saab et al., 2013). (B) Lactate diffuses through myelinic channels towards the periaxonal site, where it is transported to the periaxonal space by MCT1. Neurons internalize lactate via MCT2 to fuel mitochondrial energy metabolism contributing to long-term axonal integrity. Adapted from (Morrison et al., 2013a).

Non-compacted regions comprise the innermost and outermost layer, which are connected via cytoplasmic channels representing trafficking routes for newly synthesized membrane to the growing tip (Nave and Werner, 2014). However, the majority of the channels close as myelination progresses, but some of the radial cytoplasmic channels retain as functional connections most probably for the distribution of glial metabolites and vesicular trafficking to the axonal compartment to provide long-term trophic support (Simons and Nave, 2015).

2.3.1 The Significance of Myelin in Maintaining Axonal Integrity

The role of oligodendrocytes encompasses not only myelin assembly to provide electrical insulation but also maintenance of functional integrity and long-term survival of axons (Nave, 2010b). This becomes evident by reflecting the anatomy of long-projecting neurons that can extend meters in length, of which the axon accounts for up to 99 % of the cell's cytoplasm (Edgar and Nave, 2009; Morrison et al., 2013b). Thus, neurons are challenged by a metabolic problem of equilibrating the physiological energy balance along the entire axon to maintain presynaptic compartments as well as the axonal membrane potential (Trevisiol and Nave, 2015). Since their access to extracellular metabolites is constrained by the surrounding myelin sheaths, trophic support by glia is conceivable. Indeed, recent studies have unravelled a glia-dependent axonal support mechanism in which energy metabolites are shuttled to neurons via monocarboxylate transporter 1 (MCT1) (Figure 2-3) (Fünfschilling et al., 2012; Lee et al., 2012b). While MCT2 is found on axons, MCT1 is predominantly expressed in oligodendroglia and is essential for axonal survival as MCT1 deficiency results in axonal degeneration *in vitro* and *in vivo* (Lee et al., 2012b; Rinholm et al., 2011). Consistently, conditional mutation of cytochrome oxidase (COX) in oligodendroglial mitochondria elevates extracellular lactate levels in mice anesthetised with isoflurane most likely due to the increased export of lactate from mutated oligodendrocytes forced to utilize non-oxidative metabolism (Fünfschilling et al., 2012). Intriguingly, upon anaesthesia disruption the levels of lactate diminished rapidly,

presumably due to rapid uptake by neurons. Thus, oligodendrocytes adjust their metabolism after the completion of myelination reminiscent to the Warburg effect to efficiently provide lactate to axons for mitochondrial ATP production (Saab et al., 2013). The production of lactate in oligodendrocytes is supported by glucose transporter 1 (GLUT1) trafficking and glucose import, which is regulated by oligodendroglial NMDA receptors (Saab et al., 2016). This phenomenon represents a metabolic coupling of oligodendrocytes with axonal compartments, a mechanism particularly exploited by cancer cells to adapt to harsh microenvironmental conditions during tumour development (Brahimi-Horn et al., 2007; Gatenby and Gillies, 2004). Lactate shuttling is also known from the interaction between astrocytes and neurons (**Figure 2-3** A), which differs in many ways as it is primarily thought to support cortical glutamatergic synapses (Magistretti and Allaman, 2015; Tress et al., 2012). Moreover, execution of trophic support has also been reported by Schwann cells, which supply energy-rich metabolites to peripheral neurons (Beirowski, 2013; Beirowski et al., 2014). In invertebrates, glia has been mostly associated with blood-brain-barrier (BBB) formation, neurotransmitter transport, and phagocytic functions (Limmer and Klambt, 2014). Recent findings in *Drosophila* also showed that glycolytically active glial cells supply neurons with metabolites and knockdown of glycolytic genes in glia, but not in neurons, leads to severe neurodegeneration (Volkenhoff et al., 2015). In summary, the concept of glial support for the axonal compartment is a prerequisite for the integrity of the neuronal network and represents an evolutionary conserved mechanism.

2.3.2 Influence of Myelin on Axonal Transport

The organised transport of cellular components throughout the neurons is crucial for neuronal growth, function, and long-term maintenance. The two major mechanisms of the transport machinery comprise the molecular motor proteins kinesin and dynein, and microtubules (MT). While kinesins are mostly responsible for anterograde transport pointing towards the synapse, dyneins mediate transport of most cargoes towards the soma (retrograde). Based on the bulk speed and cargo movement, a distinction is made between slow and fast axonal transport (FAT). FAT carry membranous cargoes such as vesicles and mitochondria at speeds of ~ 1 µm/s, whereas cytoskeleton components move in slow axonal transport at speeds of 1 mm/day (De Vos et al., 2008). Defective axonal transport and neurodegenerative diseases could potentially result from disruptions of any of these components (Duncan and Goldstein, 2006; Morfini et al., 2009). Accumulating studies link myelination to axonal transport as myelin signals

phosphorylation of various axon proteins involved in transport (de Waegh and Brady, 1990; Sanchez et al., 2000). For example, slowing of neurofilament transport is regulated by oligodendrocytes to expand radial expansion of axon calibre for fast axonal conduction (Garcia et al., 2003; Hoffman et al., 1984; Monsma et al., 2014; Witt and Brady, 2000). Mitochondrial trafficking is crucial for neuronal survival as it supplies ATP for axonal transport (Schwarz, 2013). Distribution and motility of mitochondria is modulated by electrical activity and myelination. Mitochondria are mostly present within internodes, where they move at higher velocities but slow down when traversing nodal regions (Misgeld et al., 2007). These modulations of movement probably represent a response to the change in energy supply. Recently, identification of glycolytic enzymes bound to the surface of vesicles moving along axons suggests an ATP producing mechanism that drives FAT of these vesicles independent of mitochondria (Zala et al., 2013). Since glia and neurons are glycolytically coupled, it remains unclear whether this on-board energy production is required for axonal transport *in vivo* (Fünfschilling et al., 2012; Lee et al., 2012b; Maday et al., 2014).

2.3.3 Myelin Diseases: Perturbed Axon-Glia communication?

The significance of axon-glia interaction for proper brain function becomes evident when scrutinising myelin diseases. The neurotrophic role of oligodendroglia has been initially demonstrated in mouse models lacking the oligodendrocyte-specific *PLP1* gene encoding for the tetraspan membrane protein PLP and its isoform DM20, the most abundant myelin proteins. In humans, mutations or deletion of the *PLP1* gene cause Pelizaeus-Merzbacher Disease (PMD) or X-linked spastic paraplegia type 2 (SPG-2), respectively (Regis et al., 2009). Intriguingly, point mutations of the gene cause protein misfolding resulting in lethal dysmyelination in mice and men. In contrast, *PLP1*^{null} mutant mice lacking PLP generate almost inconspicuous myelin sheaths with only subtle abnormalities in terms of myelin ultrastructure and motor development (Rosenbluth et al., 2006). However, at older age PLP^{null} mutant mice develop axonopathies leading to the appearance of axonal swellings due to the accumulation of organelles and phosphorylated neurofilaments (Griffiths et al., 1998). The emergence of axonal swellings is associated with the impairment of fast anterograde and retrograde transport followed by distal Wallerian degenerations, progressive ataxia, and finally premature death of neurons without obvious myelin loss (Edgar et al., 2004; Edgar and Nave, 2009;

Griffiths et al., 1998). Similarly, Cnp1^{null} mutant mice lacking the myelin protein CNP, which resides in the non-compacted myelin as a membrane-anchored protein, develop progressive axonopathy and die prematurely even earlier than PLP^{null} mutant mice (Edgar et al., 2009; Lappe-Siefke et al., 2003). CNP has been suggested to bind to RNA and tubulin and prevent premature myelin compaction during development (Bifulco et al., 2002; Lee et al., 2005; Simons and Nave, 2015). Although both PLP^{null} and CNP^{null} mutant mice exhibit similar pathologies, they seem to act in different pathways since PLP- and CNP- double knockouts develop a more severe axonal phenotype than either single mutant (Edgar et al., 2009; Edgar and Nave, 2009). However, the mechanism by which the absence of one myelin protein causes axonopathy has not yet been elucidated. The majority of peroxisomes in white matter tracts are associated with oligodendrocytes. Conditional knockout of peroxin-5 (PEX5) in oligodendrocytes and Schwann cells leads to malfunction of peroxisomes in mice, which die prematurely due to axonal swellings and subsequent Wallerian degeneration (Kassmann et al., 2007; Kassmann et al., 2011). On the other hand, shiverer mice lacking MBP exhibit a strong dysmyelination, while axons remain intact (Griffiths et al., 1998).

Comparison of different myelin disease models creates the impression that for axonal integrity no myelin appears to be better than defective myelin. Since disease onset in mutant mice occurs despite normal myelin morphology the answer to this problem might be found in oligodendrocytes, which occupy a crucial role in maintaining the integrity of the myelinated axon. This aspect is further supported by functional perturbation of non-myelinating Schwann cells causing progressive degeneration of C-fibres and sensory neuropathy (Chen et al., 2003). Taken together, such mouse models deliver valuable insights into the pathomechanism of human myelin diseases.

2.4 Extracellular Vesicles: Intermediaries for Intercellular Communication

Intercellular communication is a prerequisite for the development and adaptation of multicellular organisms. Exchange of soluble factors as well as direct cell interaction via gap junctions and adhesion molecules represent classical mechanisms of intercellular exchange. The discovery of extracellular vesicles (EVs) implied a new mode of intercellular interaction carrying cell type-specific membrane and cytosolic components (Colombo et al., 2014; Kowal et al., 2014; Lo Cicero et al., 2015b). Based on their molecular origin, EVs are further subdivided

into exosomes and microvesicles (MVs). While MVs pinch off directly from the plasma membrane and exhibit a heterogenous size distribution ranging from 100 – 1000 nm in diameter, exosomes with a more defined size of 30 – 100 nm originate from the endosomal system (Minciacchi et al., 2015; Stoorvogel et al., 2002; Thery et al., 2009). The secretion of EVs is a highly conserved process exploited by cells from different organisms from simple prokaryotes to complex eukaryotes. Since they are released by almost all cell types, EVs are abundantly present in diverse body fluids, such as blood, amniotic fluid, urine, breast milk, and cerebrospinal fluid (Cocucci et al., 2009; Keller et al., 2007; Pisitkun et al., 2004; Raposo and Stoorvogel, 2013; Street et al., 2012). Functional interactions of EVs with cells have first been reported for the promotion of sperm cell motility by proteasomes (Raposo and Stoorvogel, 2013; Stegmayr and Ronquist, 1982). In the late 1980's, studies of the maturation process of reticulocytes revealed the presence of exosomes responsible for the removal of obsolete transferrin receptors and plasma membrane remodelling (Colombo et al., 2014; Harding et al., 1983; Pan et al., 1983; Pan and Johnstone, 1983; Pan et al., 1985). But subsequent investigations revealed a much broader spectrum of action for EVs rather than simply function as a waste disposal. Their hallmark bases on the capacity to transport bioactive molecules between neighbouring or remote cells (Tetta et al., 2013; Thery et al., 2002; Yanez-Mo et al., 2015). Besides bioactive lipids and proteins, EVs also contain mRNA and miRNA allowing the shuttle of genetic information resulting in a transient or persistent modulation of target cells (Valadi et al., 2007). However, the vesicular cargo exhibits a dynamic feature as it changes depending on the physiological state of the donor cells. Numerous studies now demonstrate the wide-ranging effects of EVs on fundamental biological processes in a pleiotropic manner. EVs are not only involved in essential physiological processes, such as immune surveillance, stem cell maintenance, tissue repair, and blood coagulation, but also in disease pathogenesis (Del Conde et al., 2005; Gatti et al., 2011; Raposo et al., 1996; Ratajczak et al., 2006). The role of EVs in disease is best described in tumour biology: EVs have been implicated in stimulating tumour progression by initiating pre-metastatic niche formation (Bobrie et al., 2012b; Costa-Silva et al., 2015; Hoshino et al., 2015; Peinado et al., 2012; Tkach and Thery, 2016).

2.4.1 Composition of Exosomes

Among all EVs, exosomes are the vesicles that harvested most attention over the past few years. Exosomes can be purified from cell culture supernatant or biological fluids classically by differential centrifugation or novel alternative purification methods, such as polymer-based precipitation or immunocapture by antibody-coated beads (Colombo et al., 2014). Comparability of data sets requires the standardization of analysis criteria based on the well-defined exosomal characteristic pattern (Van Deun et al., 2014; Witwer et al., 2013): In contrast to the previous definition of a cup-shaped structure due to fixation artefacts, exosomes appear as round vesicles limited by a bilayer as observed by cryo-electron microscopy (Brouwers et al., 2013; Raposo et al., 1996; Raposo and Stoorvogel, 2013). Density-dependent purification methods like sucrose gradients allow the discrimination from other EVs as exosomes typically float between 1.13 – 1.19 g/ml (Thery et al., 2006). Although loading of exosomal cargo varies with respect to the mode of biogenesis, cell type, and physiological conditions, which have been summarised in different databases, such as Vesiclepedia, they also carry a common set of proteins and lipids reflecting their endosomal origin (Abels and Breakefield, 2016; Kalra et al., 2012; Simons and Raposo, 2009). These proteins comprise components of the exosomal sorting complex required for transport (ESCRT), proteins responsible for formation and release, as well as tetraspanins, such as CD63, CD81, and CD9. Furthermore, proteins involved in signal transduction (EGFR), antigen presentation (MHC I and MHC II) and other transmembrane proteins also belong to the exosomal inventory (Abels and Breakefield, 2016). For analytical purposes, Hsp70, Alix, TSG101, flotillin, and tetraspanins are well-accepted exosome markers. In addition to proteins, exosomes are also enriched in lipids including sphingomyelin, cholesterol, ganglioside GM3, disaturated lipids, phosphatidylserine, and ceramide as well as genetic material like mRNA and miRNA (Llorente et al., 2013; Skog et al., 2008; Subra et al., 2007; Trajkovic et al., 2008; Valadi et al., 2007).

2.4.2 Exosome Biogenesis and Heterogeneity

Exosomes arise from the endocytic pathway by inward budding of the limiting membrane of late endosomes (LE) leading to the appearance of so-called multivesicular bodies (MVBs). Sorting of cytosolic proteins, nucleic acids, and lipids occurs during this process (Abels and Breakefield, 2016; Colombo et al., 2014). These MVBs can either coalesce with lysosomes for

degradation or fuse with the plasma membrane to discharge the intraluminal vesicles (ILVs) to the extracellular space as exosomes. Formation and sorting of exosomes occurs in two alternative processes: The ESCRT-dependent or independent pathway. The ESCRT-dependent mechanism relies on the recruitment of ESCRT-0, I, II, and III complexes to the site of ILV formation, which leads to the binding and sorting of ubiquitinated proteins by ESCRT-0, I, and II complexes followed by the initiation of the budding process (Hurley, 2008; Hurley et al., 2010; Katzmann et al., 2001). Alix recruits ESCRT-III complex, which associates with TSG101 bound to ESCRT-I, to finalize budding (Henne et al., 2013). Another ESCRT-dependent pathway bases on the interaction of syntenin with Alix to facilitate ILV formation, which is controlled by ARF6 and PLD2 but also depends on the availability of heparin sulphate, syndecans, Alix, and ESCRTs (Baietti et al., 2012; Ghossoub et al., 2014). Finally, release of syntenin-1-, syndecan-, and CD63-positive exosomes is mediated by heparanase via the enzymatic digestion of heparin sulphate chains on syndecans (Roucourt et al., 2015).

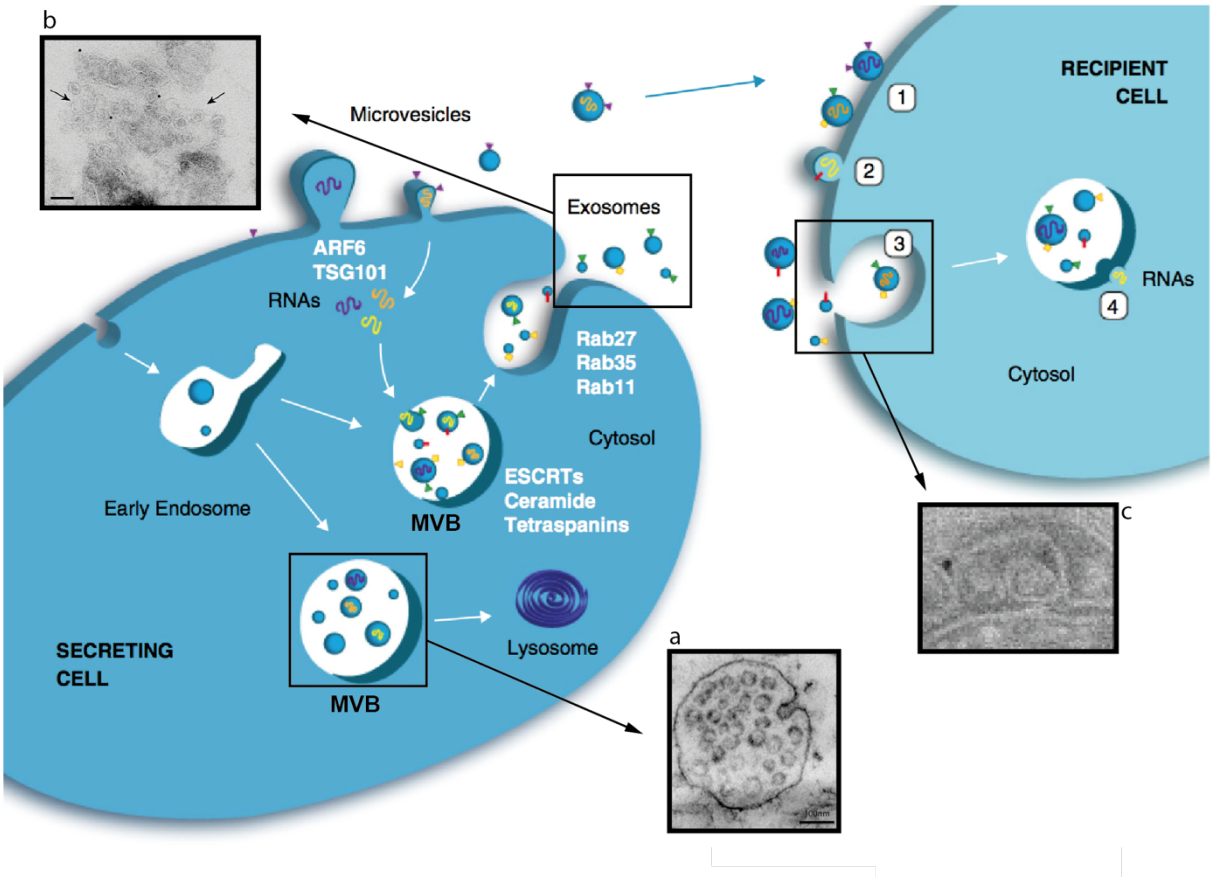

Figure 2-4 **Exosome biogenesis and internalization.** While MVs bud directly from the plasma membrane, exosome formation occurs upon invagination of the limiting membrane of MVBs, a mechanism controlled by ESCRT complexes or ceramides and tetraspanins. Subsequently, during a process mediated by different Rab GTPases, MVBs fuse with the plasma membrane and discharge its content as exosomes into the extracellular space. Exosomes as well as MVs containing a specific set of proteins and RNAs are shuttled to target cells for internalization in different ways: (1) Stably attachment of vesicles might modify target cell surface properties or induce signalling pathways followed by either fusion (2) or endocytosis (3) of the vesicles. In the latter case, exosomes might back-fuse with the endosomal membrane and unload its cargo into the cytosol (4). EMs represent MVB formation (a), exosome secretion (b), and internalization (c) by target cell. Adapted from (Lo Cicero et al., 2015a). EMs adapted from (Chivet et al., 2012; Fruhbeis et al., 2013a; Krämer-Albers et al., 2007).

On the other hand, formation of ILVs during the ESCRT-independent pathway requires the neutral sphingomyelinase (nSMase) catalysing the formation of the sphingolipid ceramide, which facilitates membrane curvature through its cone-shaped structure (Trajkovic et al., 2008). Additionally, exosome biogenesis through this pathway is also associated with various tetraspanins, such as CD63 and CD81, as well as TSG101 and the oligodendrocyte-specific tetraspan PLP. Rana et al. have shown that the interaction of tetraspanins with other transmembrane and cytosolic proteins contributes to exosome release (Rana et al., 2012).
Exosomal subpopulations might exist as inhibition of either pathway does not entirely inhibit exosome secretion (Bobrie et al., 2012a; Simons and Raposo, 2009; Smith et al., 2015; Willms et al., 2016). Comprehensive comparison indeed revealed heterogenous populations of EV subtypes including exosomes (Kowal et al., 2016). Exosomal RNAs are distinct from the cytosolic pool and occur to be selectively sorted, which may involve ESCRT-II complex as it also binds mRNA (Irion and St Johnston, 2007). miRNA sorting into exosomes is supported by a specific RNA-motif, which is recognized by the sumoylated nuclear ribonucleoprotein A2B (hnRNPA2B1) (Villarroya-Beltri et al., 2013). Recently, Argonaute 2 (Ago2) has been found to be sorted via KRAS-MEK signalling to exosomes, which in turn regulates the exosomal loading of miRNAs (Kunadt et al., 2015; McKenzie et al., 2016).

2.4.3 Exosome Secretion and Uptake

Different mechanisms controlling exosome release have been identified mostly involving small Rab GTPases. Rab11 and Rab35, for example, mediate the release of exosomes containing PLP, Wnt, flotillin, and TfR in oligodendrocytes and an erythroleucemic cell line, whereas Rab27a and b promote the docking of CD63-, Tsg101-, and Alix-containing exosomes (Hsu et al., 2010; Ostrowski et al., 2010; Savina et al., 2005). RalA regulates both MVB formation and fusion by targeting ARF6 and PLD within the syndecan-syntenin-pathway and by its interaction with the

t-SNARE protein SYX-5, respectively (Corrotte et al., 2010; Hyenne et al., 2015; Vitale et al., 2005). Exosome secretion occurs constitutively under normal conditions, but can also be increased by certain stimuli. Extrinsic signals such as neurotransmitter signalling, depolarization, and γ-irridiation influence exosome production by regulating intracellular Ca^{2+} influx (Faure et al., 2006; Fruhbeis et al., 2013a; Krämer-Albers et al., 2007; Lachenal et al., 2011; Yu et al., 2006). Exosomes but also MVs are internalized by recipient cells either by fusion with the plasma membrane to release its cargo directly into the cytosol or via endocytosis (Mulcahy et al., 2014). The latter can be categorized into different types of endocytic processes, such as clathrin-mediated endocytosis, and requires its back-fusion with the endosomal membrane to submit its content (Raposo and Stoorvogel, 2013). Target cell selection and uptake might be mediated by tetraspanins or tetraspanin-integrin-complexes (Rana et al., 2012; Rana and Zoller, 2011). High resolution imaging of exosome uptake revealed that the vast majority surfs along filopodia to enter the target cell, a mechanism reminiscent to virus entry (Heusermann et al., 2016). Upon internalization, exosomes shuttle within endocytic vesicles in close proximity to the endoplasmic reticulum (ER) before being sorted to lysosomes for cargo delivery. Thus, as similarities between exosomes and viruses have already been pointed out before, this mechanism emphasizes the common feature of exosomes and viruses (Schneider and Simons, 2016).

2.5 The Ambivalence of Extracellular Vesicles: The Good and the Bad

Studies of the physiological role of EVs *in vitro* and *in vivo* offer great insight into the rather ambivalent functions of EVs that ranges from beneficial to detrimental effects on health. In the immune system, EVs represent potential modulators of the adaptive immune response and effectors in immune system regulation (Bobrie et al., 2011; Raposo et al., 1996; Zitvogel et al., 1998). The exosomal potential in regeneration has been substantiated in exosome-treated infarcted hearts resulting in improved cardiac functions (Barile et al., 2014; Yu et al., 2013). Exosomal miRNAs released by endothelial cells stalled atherosclerotic lesion formation mitigating myocardial infarction (Hergenreider et al., 2012). Epidermal keratinocytic exosomes contribute to melanogenesis by modulating pigmentation of neighbouring melanocytes (Lo Cicero et al., 2015a). EV secretion has also been reported in stem cells suggesting their role in maintaining pluripotency and proliferation (Ratajczak et al., 2006; Yuan et al., 2009). On the

downside, EVs also participate in tumour biology by facilitating invasion and dissemination of cancer cells (Lo Cicero et al., 2015b) (Peinado et al., 2012; Shimoda et al., 2014). For example, EVs derived from stromal cells may support tumour growth in breast cancer (Boelens et al., 2014). In turn, breast cancer cells are able to store glucose by suppressing glucose uptake of non-tumor cells in pre-metastatic niches (Fong et al., 2015). EVs supporting tumour progression may also mediate angiogenesis (Tadokoro et al., 2013; van Balkom et al., 2013). At last, EVs have also been involved in inter-parasite communication as well as parasite-host-communication which led to pathogen progression (Marcilla et al., 2014).

2.6 Extracellular Vesicles in the Brain

EVs have been emerged as important intermediaries in reciprocal communication in the brain. Accumulating studies demonstrated the secretion and the subsequent uptake of EVs by neural target cells, and furthermore their transition to the CSF. This type of communication has been shown to exert functional impact on physiological processes, such as neural development and maintenance, progression of neuropathology, but also neuroprotection and regeneration (Budnik et al., 2016; Kramer-Albers and Hill, 2016). Their physiological role has been convincingly affirmed by *in vivo* studies performed in *Drosophila* and *C. elegans*, which additionally emphasized their evolutionary conservation. In *C. elegans*, EV-shedding from ciliated sensory neurons has been shown to control male mating (Wang et al., 2015; Wang et al., 2014). At the *Drosophila* neuro-muscular junction (NMJ), exosomal transfer of the Wnt-binding protein Evi (Evenless interrupted) and Synaptotagmin 4 (Syt4) from presynaptic boutons is required for synaptic maturation and plasticity and its activity-dependent release is regulated by Rab11 and Syntaxin1A (Koles et al., 2012; Korkut et al., 2009; Korkut et al., 2013). Consistently, EV secretion in mammalian neurons also depends on electrical activity and increases after depolarization (Escudero et al., 2014; Faure et al., 2006; Lachenal et al., 2011). EM analysis of hippocampal neurons revealed an augmented number of MVBs at somato-dendritic sites (Chivet et al., 2012). Furthermore, GluR2/3 AMPA receptor subunits, the neuronal cell adhesion molecule L1, as well as the p75 neurotrophin receptor ($p75^{NTR}$) have been identified in neuronal exosomes (Escudero et al., 2014; Lachenal et al., 2011). In mammals, neuronal EVs participate in interneuronal communication and supporting synaptic

plasticity (Budnik et al., 2016; Chivet et al., 2013; Chivet et al., 2014; Goldie et al., 2014; Lachenal et al., 2011).

2.6.1 EV-Mediated Neuron-Glia Interaction in Neuropathologies

The onset of neurodegenerative diseases is often linked to gene mutations that provoke misfolding and aggregation of encoded proteins (Budnik et al., 2016). Subsequent disease progression correlates with the spreading of the affected proteins from cell to cell reminiscent to the mode of prion propagation (Grad et al., 2015). A number of neurodegenerative disorders have been associated with misfolded proteins such as Aß and tau in Alzheimers disease (AD), α-synuclein in Parkinson disease (PD), and TAR DNA-binding protein 43 (TDP-43) and SOD1 in amyotrophic lateral sclerosis (ALS) (Clavaguera et al., 2009; Grad et al., 2011; Luk et al., 2012). These proteins have been identified in EVs and can be spread intercellularly across different brain regions (Coleman and Hill, 2015; Grad et al., 2011). For example, mutant SOD1 is released via exosomes by mutant SOD1-expressing astrocytes and transferred to neurons causing neuronal degeneration (Basso et al., 2013). Furthermore, neuron-astrocyte interaction also contributes to neurodegeneration in HIV-associated neurological disorders by the miR-29b shuttle via exosomes upon HIV Tat (trans-activator of ranscription) and morphin exposure (Hu et al., 2012). Microglial MVs may contribute to AD pathogenesis by converting extracellular Aß into its neurotoxic forms and subsequent transmission to neurons (Joshi et al., 2014). Likewise, spreading of tau in the brain is facilitated by microglial exosomes, which can be prevented by the inhibition of exosome secretion (Asai et al., 2015). In contrast, microglia-derived EVs also function in mitigating the toxic effect of Aß by its elimination via exosomes, which is additionally confirmed by a reduced exosome production in old AD mice resulting in plaque deposition (Joshi et al., 2015; Yuyama et al., 2012; Yuyama et al., 2015). Thus, in terms of AD microglial EVs are involved in both disease propagation and neuroprotection.

EVs released by cells in the CNS represent valuable biomarkers for neurodegenerative diseases, since they are drained into body fluids such as blood, urine, and CSF (Colombo et al., 2012).

2.6.2 Benefits of EV-Mediated Neuron-Glia Interaction

Modulation of neuronal excitability has also been associated with EVs derived from glial cells. Upon ATP stimulation of P_2X_7-receptors microglia secrete IL-1ß-containing MVs to enhance

excitatory transmission by stimulating the production of ceramide and sphingosine (Antonucci et al., 2012; Darios et al., 2009; Turola et al., 2012). Transfer of vesicular endocannabinoids from microglia to GABAergic neurons inhibits presynaptic neurotransmission upon binding to cannabinoid receptor type 1 (CB1) (Gabrielli et al., 2015). Both stimulatory pathways occur independent from each other suggesting a role of microglia-derived EVs in regulating the balance between excitation and inhibition (Antonucci et al., 2012; Budnik et al., 2016; Gabrielli et al., 2015; Turola et al., 2012). Regulation of extracellular glutamate level in the brain is mediated by shuttling miRNA-124a-containing exosomes from cortical neurons to astrocytes, which results in an the upregulation of excitatory amino acid transporter 2 (EAAT2/GLT1) and augmented glutamate uptake in target astrocytes (Morel et al., 2013). Stimulation of microglia with serotonin triggers microglial exosome release via 5-HT receptor (Glebov et al., 2015). These exosomes carry an insulin depending enzyme that is known for degrading amyloid-ß (Aß), a neurotoxin linked to AD. This finding might explain the association of high concentration of serotonin with a reduced Aß level in mouse models of AD (Cirrito et al., 2011). Another stimulant of EV secretion in microglia is WNT3A, a signalling molecule implicated in development but also in neurodegeneration (Hooper et al., 2012). Indication for the presence of MCT1, and thus lactate, in microglial exosomes, emphasizes their potential function as energy supplier for neurons (Potolicchio et al., 2005). Recent studies pointed out the role of exosomes derived in synaptic pruning. Accordingly, exosomes derived from differentiated PC12 cells after depolarization were applied to a microglial cell line culture, which upregulated complement factors to facilitate synapse elimination (Bahrini et al., 2015). Due to the presence of synapsin 1 and Heat shock cognate/ Heat shock protein 70 (Hsc/Hsp70) in EVs derived from astrocytes, they have been implicated in neuroprotection and neurite outgrowth (Taylor et al., 2007; Wang et al., 2011).

2.6.3 Reciprocal communication between oligodendrocytes and neurons via exosomes

Profiling of exosomes derived from oligodendrocytes verified exosomal properties in terms of size, density, and content that is enclosed by a lipid-rich myelin-sheath like membrane comprised of galactocerebroside, sulfatide, and cholesterol (Krämer-Albers et al., 2007). In addition to the common exosomal proteins, oligodendroglial exosomes also contain myelin proteins such as PLP, CNP, MAG, and MOG as well as the NAD-dependent deacetylase sirtuin-

2 (SIRT2), proteins involved in stress protection, and glycolytic enzymes (Frohlich et al., 2014; Krämer-Albers et al., 2007). Furthermore, exosome-associated mRNAs and miRNAs have been detected (Fruhbeis et al., 2013a). PLP is a tetraspan related to tetraspanins, which are involved in the ESCRT-independent exosome biogenesis. Indeed, formation of PLP-containing exosomes is operated by the same mechanism by which sphingomyelinase and ceramide control the invagination of the limiting membrane of MVBs (Trajkovic et al., 2008). The subsequent exosome secretion in oligodendrocytes relies on the activity of the small GTPase protein Rab35 controlling the fusion with the plasma membrane (Hsu et al., 2010). Microglia and neurons have been identified as the main target cells of oligodendroglial exosomes. While Microglia internalize oligodendrocyte-derived exosomes via macropinocytosis for degradation without provoking an immune response, neurons internalize exosomes via clathrin- and dynamin-dependent endocytosis (Fitzner et al., 2011; Fruhbeis et al., 2013a). EM images demonstrate the presence of exosomes within MVBs located at the periaxonal site adjacent to the axonal membrane. These observations point out a potentially intriguing role of exosomes in reciprocal communication between neurons and oligodendrocytes. Indeed, exosome release by oligodendrocytes is coupled to neurotransmitter signalling. Thus, electrically active neurons release glutamate, which induces Ca^{2+}-influx upon the activation of the glutamatergic receptors NMDA and AMPA present on the plasma membrane of oligodendrocytes (Fruhbeis et al., 2013a; Karadottir and Attwell, 2007). Elevation of cytosolic Ca^{2+} triggers fusion of MVBs discharging exosomes into the extracellular space or periaxonal site, as neurons internalize exosomes at both somatodendritic and axonal compartments (Figure 2-5). Using the Cre-loxP system, we demonstrated the functional retrieval of the exosomal content by neurons upon internalization. Consistently, stereotactically injected exosomes bearing the Cre recombinase induced recombination by reporter activation in recipient neurons *in vivo*. However, the significance and impact of the oligodendroglial exosomes on neuronal physiology remains unclear and requires further investigation to unravel its function. The presence of various proteins facilitating stress tolerance in these exosomes favours the idea of their involvement in neuroprotection. So far, oligodendroglial exosomes have only been reported to functionally inhibit differentiation and myelin formation (Bakhti et al., 2011). This autoinhibition has been linked to a control mechanism of premature myelination in the absence of neurons as inhibition diminishes upon incubation with conditioned neuronal medium.

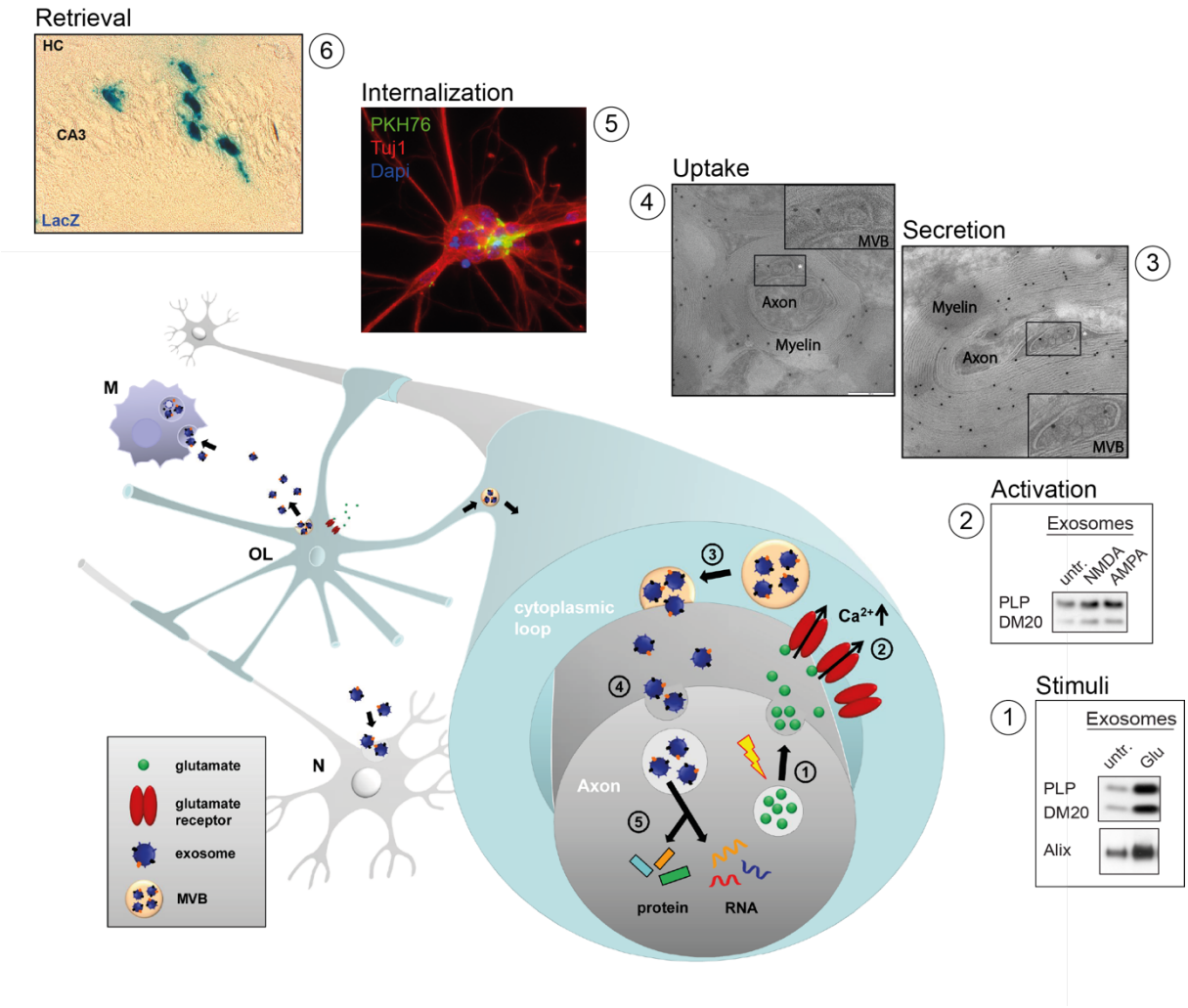

Figure 2-5 Reciprocal communication between neurons and oligodendrocytes. (1) Electrical active axons release glutamate, which activates oligodendroglial NMDA and AMPA receptor (2) resulting in Ca^{2+} entry. Elevated level of intracellular Ca^{2+} triggers fusion of MVBs (3) leading to the release of exosomes (4). Internalization of exosomes by neurons occurs at both the soma and periaxonal site (5), where the exosomal content is finally retrieved (6). This hypothetical model bases on results obtained from different experiments performed *in vitro* and *in vivo*, which have been integrated in addition to the cartoon. Modified from (Fruhbeis et al., 2013b; Krämer-Albers et al., 2007).

2.6.4 Neuroprotective and Regenerative Potentials of EVs in the CNS

Cell communication mediated by EVs between neural cells but also the periphery possesses remarkable neuroprotective and neuroregenerative potential (Kramer-Albers and Kuo-Elsner, 2016). Exosomal sorting of α-synuclein involves the ATPase zinc ion pump in MVBs and supports neuronal survival by the removal of α-synuclein (Emmanouilidou et al., 2010; Kong et al., 2014). Schwann cells support nerve regeneration in response to nerve injury by the exosomal release of $p75^{NTR}$ inducing dedifferentiation (Lopez-Verrilli et al., 2013). Treatment of dorsal ganglion root neurons with these exosomes enhances the axon regeneration rate. Simultaneously, RhoA

activity in growth cones is effectively decreased to offset inhibition of axon elongation and growth cone collapse. *In vivo* experiments confirmed the regenerative properties by the application of SC-derived exosomes after sciatic nerve crush. Furthermore, muscle-derived EVs are also capable to benefit neurons by promoting cell survival and neurite outgrowth (Madison et al., 2014).

EV-mediated pro-neuronal activity has been suggested to emerge from conversation between cells from the CNS with the periphery as they have been suggested to cross the BBB (Kramer-Albers and Kuo-Elsner, 2016; Ridder et al., 2014). For example, MSCs harbour regenerative effects as MSC-based therapies have demonstrated clinical and preclinical efficacy, which is partially attributable to their EVs (Doeppner et al., 2015; Kim et al., 2016; Rani et al., 2015; Wei et al., 2013; Xin et al., 2013a; Xin et al., 2013b). Furthermore, EVs harvested from human adipose tissue MSCs carrying the Aß-degrading enzyme neprilysin decrease both secreted and intracellular Aß in cell culture suggesting a potential approach to treat AD (Katsuda et al., 2013). Recently, an altered miRNA profile in Purkinje neurons in the cerebellum has been reported upon internalization of EVs produced by hematopoietic cells in the periphery (Ridder et al., 2014). This modulatory effect was triggered to a greater extent upon peripheral inflammation and also transmitted to other neuronal populations such as cortical and hippocampal neurons without activating microglia. Pro-myelinating activity in slice cultures has been suggested for EVs derived from dendritic cells exposed to IFN-γ (Pusic et al., 2014). Similarly, EVs isolated from the serum of young mice are enriched in miR-219, which promotes differentiation of myelinating oligodendrocytes (Pusic and Kraig, 2014). Application of these EVs to demyelinated rat hippocampal slices or systemic administration to aged rats improve remyelination and enhance myelination, respectively (Pusic et al., 2016). Neuroimmune function has been reported for MVs derived from microglia containing IL-1ß, which is activated upon high levels of extracellular ATP released from astrocytes or injured tissues resulting in the initiation of an acute inflammatory response (Bianco et al., 2005). EVs collected from neural stem cells (NSC), which were exposed to pro-inflammatory cytokines contain IFN-γ bound to its receptor, propagate immunomodulatory signals within the host environment and exert functional recovery upon systemic application in different neural diseases (Cossetti et al., 2014).

Taken together, EV-mediated communication between neural cells and also with cells from the periphery highlights the potential of EVs as therapeutic agents for neural injury.

2.7 Aim of the Study

The concept of glial support of axon function has first been described in mouse models lacking the myelin proteins PLP and CNP and could be supported by studies showing the supply of axons with metabolites by oligodendrocytes (Edgar et al., 2004; Fünfschilling et al., 2012; Griffiths et al., 1998; Lee et al., 2012b). However, the underlying mechanism has yet not been sufficiently elucidated. Recently, we have provided evidence for exosome transmission from oligodendrocytes to neurons suggesting a new route of horizontal transfer in the CNS (Fruhbeis et al., 2013a). Oligodendrocytes release exosomes into the periaxonal space in response to neuronal electrical activity and glutamate signalling and modulate neuronal gene expression upon internalization (Frohlich et al., 2014). Association of PLP, CNP, and different beneficial factors with oligodendroglial exosomes suggests their possible role in trophic support, and thus their potential to complement the concept of glial support (Krämer-Albers et al., 2007).

The present study aims to unravel the functional impact of oligodendroglial exosomes on neuronal physiology. Using different approaches, we first investigated the transfer of stress-relevant proteins. To validate the functional effect of oligodendroglial exosomes, we performed metabolic assays and a kinase screen during cellular stress. PLP and CNP null mutant mice exhibit normal myelination but develop axonal swellings followed by perturbations in axonal transport with fatal consequences for the mice (Edgar et al., 2004; Griffiths et al., 1998). Disruption of axonal transport is a hallmark and precipitating factor of neurodegenerative diseases. Hence, analysis of axonal transport shall provide further indications of the role of exosomes on neuronal physiology. Preliminary investigations reveal a reduced exosome secretion in PLP and CNP knockout oligodendrocytes (data unpublished). We therefore examined the role of exosomes on neuronal viability and axonal transport in a comparative study using exosomes derived from wildtype as well as mutant oligodendrocytes.

3 Materials and Methods

3.1 Equipment, Materials, Buffers and Media

3.1.1 Equipment

Table 3.1 Microscopes

Microscope	Manufacturer
DM6000	Leica, Wetzlar
DMLB	Leica, Wetzlar
DM-IL	Leica, Wetzlar
TCS SP5	Leica, Wetzlar
Axiovert 200M	Zeiss, Jena

Table 3.2 Centrifuges

Centrifuge	Manufacturer
Biofuge 17RS	Haraeus, Hanau
Z 383 K	Hermle, Wehingen
3K20	Sigma-Aldrich, Munich
Optima™ MAX-E	Beckman, Munich
Rotors: TLA-55, TLS-55	Beckman, Munich

Table 3.3 Cell culture equipment

Cell culture equipment	Manufacturer
Nucleofector II	AMAXA, Köln
GenePulser Xcell	Bio-Rad, München
SterilGARD III Advance Class II Bio-logical Safety Cabinet	The Baker Company, Sanford, USA
C200 Incubator	Labotect, Göttingen
CO2 incubator MCO-20AIC	Sanyo Electric Co. Ltd., Moriguchi, Japan
Water bath Z 383K	Hermle, Wehingen
MACS gentle tissue dissociator	Miltenyi Biotec, Bergisch Gladbach
MACS Multistand	Miltenyi Biotec, Bergisch Gladbach
Midi MACS Separator	Miltenyi Biotec, Bergisch Gladbach
MACSMix Tube Rotator	Miltenyi Biotec, Bergisch Gladbach

Table 3.4 Other lab equipment

Device	Manufacturer
NanoDrop 1000 Spectrometer	Peqlab, Erlangen
Photospectrometer Ultrospect 2100 pro	GE Healthcare, München
Infinite M200 Pro	Tecan
Optimax TR X-ray film processor	MS Laborgeräte, Wiesloch
Mini PROTEAN Electrophoresis System	Bio-Rad, München
Mini Trans-Blot Electrophoretic Transfer Cell System	Bio-Rad München
Electrophoresis chamber NuPAGE	Invitrogen, Karlsruhe
LM10	NanoSight, Malvern, UK
Epson Perfection 1660	Epson, Suwa, Japan

3.1.2 Materials

Table 3.5 Chemicals

Chemicals	Cat. no.	Manufacturer
DibutyrylRcAMP (dbcAMP)	#D0627	Sigma-Aldrich, München
Sodiumbutyrate	#30341-0	Sigma-Aldrich, München
Hydrogen peroxide	#8070.2	Roth, Karlsruhe
Complete Protease Inhibitor Cocktail Tablets	#11697498001	Roche, Mannheim
Halt Phosphatase Inhibitor Cocktail	#78420	Pierce
DAPI	#D9542	Sigma Aldrich, München
Opti-Prep Density GradientSolution 60 %	#D1556	Sigma Aldrich, München
Roti-Histofix 4%	#P087.4	Roth, Karlsruhe

Table 3.6 Kits

Kits	Cat. no.	Manufacturer
PureLink HiPure Plasmid Maxiprep Kit	#K2100G07	Invitrogen, Karlsruhe
AMAXA Basic NucleofectorKit for Primary Neurons	VPI – 1003	Lonza, Köln
Neural Dissociation Kit	#130-092-628	Miltenyi Biotec, Bergisch Gladbach

MitoCapture Mitochondrial Apoptosis Detection Fluorometric Kit	#K250-25, -100	BioVision, Milpitas, USA
Human Phospho-MAPK Array Kit	#ARY002B	R&D Systems, Minneapolis, USA

Table 3.7 Marker

Marker	Cat. no.	Manufacturer
Precision Plus Protein Standards Dual Color	#161-0374	Bio-Rad, München

Table 3.8 Other Materials

Other Materials	Cat. no.	Manufacturer
Amersham Hyperfilm ECL	#28906837	GE Healthcare, München
Luminata Crescendo ECL	#WBLUR0100	Millipore, Billerica, USA
Immobilon-P transfer membrane	# IPVH00010	Millipore, Billerica, USA
Glass ware	VWR, Darmstadt	
Plastic ware	Nunc, Langenselbold BD Falcon, Heidelberg Sarstedt, Nümbrecht	
Six-well Companion Plates	#353502	BD Falcon, Heidelberg
Six-well Cell Culture Inserts	#353102	BD Falcon, Heidelberg
Glass Bottom µ-Dish35 mm, high	#81158	Ibidi, Martinsried

3.1.3 Software

Table 3.9 Software

Software	Manufacturer
Microsoft Office 2011	Microsoft, Redmond Washington, USA
Microsoft Office 2016	Microsoft, Redmond Washington, USA
Endnote X7	Wintertree Software Inc., Kanada
Illustrator CS6	Adobe, München
Photoshop CS6	Adobe, München
ImageJ 1.44a	NIH, Bathesda, Maryland
LAS AF Lite	Leica, Wetzlar
NTA 2.3	NanoSight, Malvern, UK
MetaMorph	MetaMorph Inc., Nashville, USA
SPSS Statistics 19	SPSS Inc., Stanford, USA

3.1.4 Buffers and Media

Table 3.10 Buffers, media, and solutions

Buffers, media, solutions	Composition
10 x Poly-L-Lysine (PLL)	0.1 % PLL (Sigma, #P1524) in ddH2O
Sato 1.5 % HS (Oli-neu culture medium)	13.4 g/l DMEM (Invitrogen, #52100-039), 2 g/l NaHCO3, 0.01 g/l transferrin, 100 µg/l insulin, 100 µM putrescine, 200 nM progesterone, 500 nM TIT, 220 nM Sodium-selenite, 520 mM L-thyroxine, 1.5% (v/v) horse serum
Cryoprotective medium	RPMI 1640 70%; FCS 20%; DMSO 10%
HBSS+	500 ml HBSS (1x) + 7.5 ml 10% MgSO4
Trypsin/EDTA (low)	HBSS; 0.01% trypsin; 0.02% EDTA
PBS 10% HS	PBS; 10% horse serum
Neurobasal plating medium	Neurobasal (#1309101 Gibco); 20 ml/l B27 (#17504044 Invitrogen); 0.5 mM LG-lutamine; 10 ml/l 100x Pen-Strep (63.2 µg/ml Penicillin – K-salt; 135 µg/ml Streptomycin sulfate); 12.5 µM Glutamate
Neurobasal feeding medium	Neurobasal (#1309101 Gibco); 20 ml/l B27 (#17504044 Invitrogen); 0.5 mM LGglutamine; 10 ml/l 100x PenGStrep (63.2 µg/ml Penicillin G KGsalt; 135 µg/ml Streptomycin sulfate)
NeuroMACS cultivation medium	NeuroMACS (#130-093-570, Miltenyi Biotec); 20 ml/l NeuroBrew21 w/o vitamin A (#130-093-566); 10 ml/l 100x Pen-Strep (63.2 µg/ml Penicillin G K-salt; 135 µg/ml Streptomycin sulfate);
DMEM 10% FCS	13.4 g/l DMEM (#52100G039 Invitrogen); 2 g/l NaHCO3; 10 ml/l 100x Pen-Strep (63.2 µg/ml Penicillin G K-salt; 135 µg/ml Streptomycin sulfate); 100 ml/l fetal calf serum
DMEM 1 - 10% HS	13.4 g/l DMEM (#52100G039 Invitrogen); 2 g/l NaHCO3; 10 ml/l 100x Pen-Strep (63.2 µg/ml Penicillin G K-salt; 135 µg/ml Streptomycin sulfate); 1 – 10 % (v/v) horse serum
PBS (1x)	150 mM NaCl; 8 mM Na2HPO4; 1.7 mM NaH2PO4; adjust pH to 7.2
PBST	PBS (1x); 0,1% Tween 20
LB medium	10 g/l NaCl; 10 g/l trypton; 5 g/l yeast extract
LB agar	2,25 g agar; 150 ml LB medium
MTT	5 mg MTT in 1 ml 1x PBS
Solubilization buffer	10 % (w/v) SDS; 40 % (v/v) DMF; 20 % (v/v) conc. acetic acid; solved in dH_2O (pH 4)
Triton lysis buffer	50 mM Tris/HCl (pH 7,2); 150 mM NaCl; 1% Triton XG100; Roche® Complete protease inhibitor cocktail was added prior to use
4x sample buffer	200 mM TrisGHCL (pH 6.8); 8 % SDS; 0.4 % bromphenol blue; 40 % glycerol; 400mM DTT (if reducing conditions are desired)

Stacking gel buffer	1 M Tris (pH 6,8)
Separation gel buffer	1.5 M Tris (pH 8,8)
Stacking/separation gel for SDS-PAGE	Gels were prepared according to Tables A8G9 and A8G10 (Volume 3, A8.43) „Molecular Cloning – A Laboratory Manual“, Sambrook und Russell, 2001, Cold Spring Harbour Press, New York, USA
5x SDS electrophoresis buffer	125 mM Tris; 1.25 M glycine; 0.5 % SDS; adjust pH to 8.3
Western blot transfer buffer	24 mM Tris; 192 mM glycine; 20 % ethanol
Blocking solution (protein biochemistry)	PBST; 4 % milk powder
ECL solution	Solution A: 0.1 M TrisGHCl (pH 8.6), luminol 0,25 g/l Solution B: 1.1 g/l paraGhydroxy coumaric acid Development: Combine 1ml solution A + 100 µl solution B + 0.3 µl H2O2
Permeabilization buffer	PBS; 0.1 % Triton XG100
Blocking solution (immunocytochemistry)	PBS; 10 % horse serum
Mounting medium	2.4 g Moviol 4G88; 6 g glycerol; 6 ml ddH_2O; 12 ml 0.2 M Tris (pH 8.5)

3.2 Antibodies

3.2.1 Primary Antibodies

Table 3.11 Primary antibodies

Antigen	Clone	Host/species	Dilution	Manufacturer
Akt		rabbit	1:1000 (WB)	Cell Signalling
Akt (phosphorylated)		rabbit	1:400 (WB)	R&D Systems
AIP-1/Alix		mouse	1:250 (WB)	BD
Erk1/2		rabbit	1:5000 (WB)	Cell Signalling
Erk1/2 (phosphorylated)		mouse	1:1000 (WB)	Cell Signalling
Flotillin		mouse	1:250 (WB)	BD
GAPDH		rabbit	1:5000 (WB)	Bethlyl
GFAP		rabbit		
GFP		rabbit	1:2000 (WB)	Abcam
Hsp70		mouse	1:1000 (WB)	BD
Iba1		rabbit	1:1000 (WB)	Proteintech
MBP	12	rat	1:500 (WB)	AbdSerotech
O4	81	mouse	Undiluted (IF)	Hybridoma

PLP	aa3	rat	1:10 (WB)	Hybridoma, M.B. Lees, Waltham, USA
SOD1		rabbit	1:2000 (WB)	Abcam
Tsg101	4A10	mouse	1:250 (WB)	GeneTex
Tubulin alpha	DM1A	mouse	1:5000 (WB)	
Tubulin ß III	TUJ1	rabbit	1:1000 (IF) 1:2500 (WB)	Covance

3.2.2 Secondary Antibodies

Table 3.12 Secondary antibodies

Host species	Target species	Conjugation	Application	Manufacturer
goat	mouse	HRP	1:10000	Dianova
goat	rat	HRP	1:10000	Dianova
goat	rabbit	HRP	1:10000	Dianova
goat	mouse	Alexa488	1:400	Invitrogen
goat	rabbit	Cy3	1:800	Dianova

3.3 Molecular Biology

Plasmids used for experiments described in the present thesis comprise human WT SOD1-EGFP and BDNF-mCherry, which were kindly provided by Albrecht Clement and Frederic Saudou, respectively (Witan et al., 2008; Zala et al., 2013).

3.3.1 Transformation into Competent Bacteria

For reproduction, plasmids were mixed with competent bacteria E. coli Top10 F' (Invitrogen) after being thawn on ice for 30 min. Subsequently, bacteria were heat-shocked at 42 °C for 1 minute before adding 1 ml of antibiotic-free LB medium. The suspension was incubated at 37 °C for 30 min and plated on agar plates containing adequate antibiotics for selection. Agar plates were incubated at 37 °C over night allowing bacteria to grow.

3.3.2 Plasmid Preparation from Bacteria

Single colonies were transferred to 200 ml LB medium containing selective antibiotics and were constantly shaked at 37 °C over night. Plasmid extraction was performed by using the *PureLink™ Hipure Plasmid Maxiprep Kit* (Invitrogen) according to the manufacturer's protocol. Isolated plasmids were eluted in 200 µl of nuclease-free ddH_2O.

3.4 Cell Culture

Primary cells were prepared from C57Bl/6-N mouse strain. Primary and Oli-*neu* cells were cultured at 37 °C, 95% humidity, and 8 % CO_2. HEK293T cells were cultured under the same conditions but at 5 % CO_2.

All cells were plated on poly-L-lysine (PLL) coated culture dishes. Accordingly, PLL were applied to dishes and incubated at 37 °C for up to 24 h. Subsequently, dishes were washed twice using ddH_2O.

3.4.1 Isolation of Primary Oligodendrocytes using MACS Technology

Table 3.13 Composition of enzyme mix 1 and 2

Enzyme mix 1 (per 400 mg brain tissue)		Enzyme mix 2 (per 400 mg brain tissue)	
Enzyme P	Buffer X	Enzyme A	Buffer Y
50 µl	1900 µl	10 µl	20 µl

Primary oligodendrocytes were isolated from brain tissues of P7 postnatal mice (C57/Bl6). Dissection of the brain have been performed under sterile conditions. Before starting the preparation, enzyme mix 1 provided in the MACS Neural Dissociation Kit (P) was prepared and transferred to C-tubes for pre-heating at 37 °C (see Table 3.13). A maximum of 1600 mg mouse brain can be processed in one C-tube, which corresponds to 6 brains of P7 pups. Centrifuge was kept at room temperature (RT). For sacrificing the mice, heads were cut close to the brain stem and placed in a petri dish with HBSS. To remove the brain, the scalp was cut along the midline until the olfactory bulb and the skin was flapped aside. Subsequently, an incision was made on the left and right side of the scull. Using forceps, the scull was folded up to uncover the brain, which was carefully removed and transferred into the C-tube containing appropriate

amount of pre-warmed enzyme mix 1. Brain tissues were dissociated using a 5 ml pipette allowing better enzymatic digestion of the tissue. C-tubes were attached onto the Gentle MACS Tissue Dissociator with the MACS program m_brain_01 ran twice per C-tube followed by the incubation on the MACS Mix Tube Rotator with continuous rotation within the incubator at 37 °C for 15 min. Meanwhile, the appropriate amount of enzyme mix 2 was prepared as indicated in Table 3.13. The C-tubes were again attached onto the Gentle MACS Tissue Dissociator and the program m_brain_02 was run twice, before the addition of enzyme mix 2 and subsequent careful mixing by inverting the tube. At this point, the suspension appears less viscous. The cell suspension was again incubated in the incubator as previously described and attached onto the Gentle MACS Tissue Dissociator for the last time (2x program m_brain_03). The tube was briefly centrifuged to collect the suspension at the bottom of the tube (300 x g, 5 min at RT). The tissue pellet was resuspended in 10 ml of pre-warmed DMEM per C-tube. First, 5 ml of the suspension was passed through a 70 µm cell strainer placed on a 50 ml falcon. After washing the strainer with 5 ml of fresh DMEM, the remaining 5 ml of suspension was applied onto the cell strainer. This procedure was repeated using a 40 µm cell strainer to remove any undigested tissue or debris. After centrifugation at 300 xg for 10 min at RT, cells were resuspended in 20 ml of DMEM per tube and cell number was subsequently determined. On average, the protocol yields 9 to 10 x 10^6 cells per brain. Centrifugation was repeated and the cell pellet was resuspended in a total of 100 µl of DMEM + 1 % HS and anti-O4 MicroBeads per 10^7 cells (90 µl DMEM + 1 % HS and 10 µl of anti-O4 MicroBeads) followed by the incubation at 4 °C for 15 min to facilitate binding of antibodies to the specific cell population.

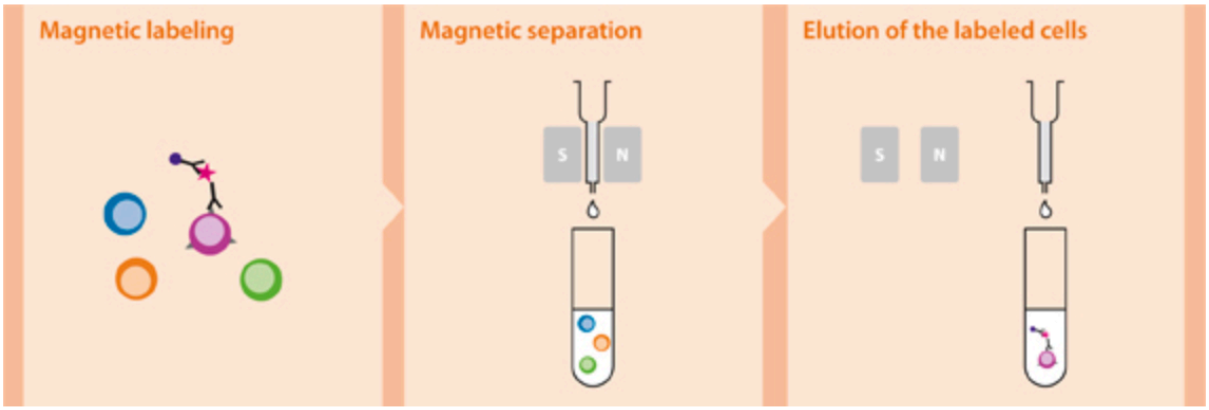

Figure 3-1 Cell sorting using MACS MicroBeads.

Labelling of $O4^+$ OL occurred at this stage and cells were prepared for magnetic separation (Figure 3-1). Cells were washed by adding 1 -2 ml of DMEM + 1 % HS per 10^7 cells and centrifuged at 300 x g and 4 °C for 10 min. After the supernatant was completely aspirated, cells were resolved in 500 µl of DMEM + 1 % HS per 10^7 cells.

MACS LS Separation Columns were attached to the MACS magnet and the addition of 3 ml of DMEM + 1 % HS activated the magnetic LS column. The cell suspension containing OL labelled by anti-O4 antibodies coupled to magnetic beads was subsequently applied to the LS column. During this process magnetic-labelled cells were retained in the columns due to the magnetic field, while the remaining O4-negative cell fraction passes through (Figure 3-1). Before eluting cells, the column was washed three times with 3 ml of DMEM + 1 % HS. Detachment of the LS column from the magnet allowed to flush out $O4^+$ OL with 5 ml of fresh DMEM + 1 % HS using the plunger provided into a new falcon. Selected cells were counted and plated onto culture dishes (Nunc) previously processed and coated with poly-L-lysine (see section 3.4). Cells were plated as followed: 2.5 – 3 x 10^6 OL were plated on a 6 cm culture dish (Nunc) and 0.15 x 10^6 on a 24-well or coverslip with a diameter of 11 mm.

One hour after plating $O4^+$ cells, the medium was replaced by NeuroMACS cultivation medium (Table 3.10) containing 1 ml/l PDGF. After 24 h, the conditioned medium was collected and centrifuged at 300 x g and RT for 5 min to remove dead cells and debris. In the meantime, cells were washed twice with pre-warmed DMEM before adding back the conditioned medium to the cells.

For preparing exosome isolation, culture medium was replaced by fresh medium at 2 – 3 DIV and collected after 48 h at 4 – 5 DIV for exosome isolation.

3.4.2 Preparation of Primary Cortical Neurons

Primary cortical neurons were prepared from E15 mouse embryos. After preparing the embryos from the uterus, brains were carefully extracted and meninges removed. The cortical hemispheres were dissected from the remaining brain tissue and the olfactory bulbs and subjected for digestion with 1 % trypsin at 37 °C for 4 min. Cortices were washed twice with HBSS+ and transferred to 0.05 % DNAse for mechanical dissociation using Pasteur pipettes. Cells were resuspended through decreasing diameters until suspension appeared homogenous. After washing the cells twice with HBSS+ and subsequent centrifugation at 130 x

g and 4 °C for 10 min, the cells were plated onto PLL coated culture dishes in Neurobasal plating medium at densities indicated in **Table 3.14**. To maintain neuronal cultures, half of the culture medium was exchanged every 4 - 5 days to Neurobasal feeding medium.

Table 3.14 Density of Neuronal Cultures

Culture dish/ coverslip	Cell number
coverslip (11 mm)	0.15×10^6
6-well	0.7×10^6
6 cm	2.8×10^6

3.4.3 Preparation of Primary Hippocampal Neurons

Primary hippocampal neurons were prepared from E18 mouse embryos. To access the hippocampus, brains were first extracted from embryos removed from the uterus. After peeling off the meninges, the hippocampus was carefully prepared using fine forceps. Dissociation procedure is the same as described for cortical neurons (see section 3.4.2). Single cells suspension was subjected to transfection using the AMAXA Nucleofector and cultured as described for cortical neurons. Preparation of hippocampal neurons from one brain yielded about $0.5 – 1 \times 10^6$ cells.

3.4.4 Preparation of Primary Astrocytes

Primary astrocytes from E15 mouse embryonic brains were isolated from mixed neural cultures, which were cultured following the protocol from (Trotter and Schachner, 1989) originally describing the preparation of primary oligodendrocytes. Briefly, whole brains were extracted from mouse embryos E15 and dissociated as described for cortical neurons (see section 3.4.2). After determining the cell number, cells were plated onto PLL coated culture flasks (70 cm^2, Nunc) at a density of $3 – 3.5 \times 10^7$ cells in 10 ml DMEM + 10 %. After 5 DIV, neurons were removed by a complement mediated immune cytolysis using M5 antibody (358 hybridoma supernatant, diluted 1:10) and guinea pig complement (diluted 1:15). Subsequently, cells were washed using DMEM + 10 % HS to remove dead cells and cultured in DMEM + 10% HS. Culture medium was changed to fresh DMEM + 10 % HS and insulin added (0.5 µg/ml) after 2 days. At 8 DIV, microglia and OL grown on the astrocyte layer were removed by intensely

shaking the culture flask. To detach astrocytes from the flask bottom, pre-warmed trypsin/EDTA was added followed by a strong shaking-off method for 4 min. Trypsin reaction was stopped by the addition of an equal amount of PBS + 10 % HS (4 °C). cell suspension was centrifuged at 130 x g and 4 °C for 10 min and plated onto PLL coated culture dishes in DMEM + 10 % HS at a density of 3.5 x 10^5 cells/6-well.

3.4.5 Oli-*neu* Cell Culture

The oligodendroglial cell line Oli-*neu* was generated from primary mouse OPCs by transferring the t-*neu* oncogene using replication deficient retroviruses. t-*neu* is expressed under the control of the thymidine kinase promoter in Oli-*neu* cells and maintains the proliferative state of the cells (Jung et al., 1995). Differentiation of Oli-*neu* cells cultured on PLL coated culture dishes in Sato + 1.5 % HS can be induced by the daily application of 1 mM dbcAMP. To passage the cells, detachment of cells was mediated by the incubation of trypsin/EDTA for 4 min. Reaction was stopped by adding the same amount of PBS + 10 % HS (4 °C) and cells were centrifuged at 130 x g and 4 °C for 10 min. To freeze cells for long-term storage, cell pellet was resuspended in cryoprotective medium at – 80 °C and stored in liquid nitrogen.

3.4.6 HEK293T Cell Culture

HEK293T cells derive from human embryonic kidney cells and were cultured in DMEM + 10 % FCS in non-coated culture dishes. Passaging and freezing procedure corresponds to the protocol used for Oli-*neu* cells. HEK298T cells were plated at a density of 0.35 x 10^6 cells/6-cm culture dish for exosomes preparation after 48 h.

3.5 Transfection

3.5.1 AMAXA Nucleofection

Primary hippocampal neurons prepared according to section 3.4.3 were transfected with the BDNFmCherry plasmid by electroporation using the AMAXA Nucleofector 2D device. 1.5 x 10^6 cells were pelleted (130 x g, 4 °C for 10 min) and resuspended in 100 µl nucleofector solution provided by the AMAXA Basic Nucleofector Kit and thoroughly mixed with 4 µg DNA. The

mixture of cells and DNA was transferred to an electroporation cuvette provided by the kit and attached to the Nucleofector device for electroporation using the program O-005. After electroporation, 500 µl of Neurobasal plating medium was added to the cell suspension and the whole sample containing the cells was distributed on three PLL coated video microscopy dish for live-cell imaging. To remove dead cells and debris, culture medium was replaced by fresh medium after 4 h.

3.5.2 Bio-Rad GenePulser Electroporation

Oli-*neu* cells were transfected with plasmids using the Bio-Rad GenePulser Xcell. 1.3 – 1.8 x 10^6 cells in 600 µl were transferred to a 4 mm electroporation cuvette containing 5 µg DNA followed by thorough mixing. The cuvette containing the cells was attached to the GenePulser device for pulsing (exponential decay program; 220 V, 950 µF) followed by an incubation time of 5 min at RT. Cells were plated on a PLL coated 6cm culture dish containing Sato + 1.5 % HS. After 2 – 4 h medium was changed to fresh Sato + 1.5 % HS containing 1 mM dbcAMP and 2 mM sodiumbutyrate.

3.6 Immunocytochemistry

For immune-staining, cells were grown on PLL coated coverslips. All steps were performed at RT. Coverslips were washed once with 1x PBS to remove residual medium and cell debris. After fixing the cells in 4 % paraformaldehyde for 20 min, cells were washed three times with PBS. To allow antibodies to bind to proteins located intracellularly, cells were permeabilized with 0.1 % tritonX100 in PBS for 2 min followed by three washing steps with PBS. Subsequently, cells were incubated in PBS + 10 % HS (blocking solution) to block unspecific binding sites for at least 30 min. Primary antibodies were diluted in blocking solution and incubated for 1 h. After a three times washing step with PBS, secondary antibodies diluted in blocking buffer were applied for 30 min, before washing the cells again for three time with PBS. For nuclei staining, 4'6-diamidino-2-phenylindole (DAPI) was used for 2 min followed by a three additional washing steps. Finally, coverslips were briefly submerged in ddH_2O for the removal of residual buffer salts and mounted in moviol on object slides.

3.7 Protein Biochemistry

3.7.1 Cell Lysis

Cells were washed twice with cold 1x PBS before being scraped off on ice in cold triton lysis buffer (4 °C) containing Complete Protease Inhibitor Cocktail (Roche) using a rubber policeman. Lysates were incubated on a rotation wheel at 4 °C for 45 min and subsequently centrifuged (300 x g, 4 °C, 10 min) to remove cellular debris and nuclei. Lysates were stored at – 20 °C.

3.7.2 SDS-PAGE

Sodium Dodecyl Sulfate Polyacrylamide Gel Electrophoresis (SDS-PAGE) allows the separation of proteins. Protein samples were loaded on a SDS gel consisting of a stacking and a separation phase with different polyacrylamide concentrations according to 'Molecular Cloning – A Laboratory Manual' (Sambrook and Russell, 2001). Preparation and running of the gel were carried out using the Bio-Rad Mini Protean electrophoresis system. Alternatively, NuPAGE pre-cast gradient (4 – 12 %) gels (Invitrogen) with MOPS buffer were used according to the manufacturer's protocol. Protein samples were prepared by the addition of 4x sample buffer before loading onto the gel together with the pre-stained marker (bio-Rad) for protein size determination.

3.7.3 Western Blotting

After separation by SDS-PAGE, proteins were blotted from the gel on a polyvinylidene fluoride (PVDF) membrane (Immobilon-P transfer membrane, 0.45 µm pore size, Millipore) using the Bio-Rad Mini Trans-Blot Electrophoretic Transfer Cell system for 3 h at 300 mA or 12 h at 60 mA. After blotting, membranes were briefly washed in dH_2O and incubated in blocking solution (4 % milk powder in PBST) for at least 30 min to block unspecific antibody binding to the membrane. Primary antibodies were applied in blocking solution over night at 4 °C on a shaker. Before applying secondary antibodies coupled to horse radish peroxidase (HRP) diluted in blocking solution, the membrane was washed four times with PBST for 7 min. After a 30 min incubation time, secondary antibodies were removed and membrane was again washed four times for 7 min using PSBT. Finally, proteins were visualized on X-Ray films by enhanced chemiluminiscence (ECL) reaction. For storage, membranes were kept at – 20 °C. Proteins were

visible after developing the hyperfilms and can be subjected for quantitative analysis using the ImageJ software.

3.8 Exosome Preparation

Exosomes can be isolated from body fluids or tissue culture supernatants by differential centrifugation including different centrifugation steps. All steps were performed on ice or 4 °C. The first centrifugation step is carried out at 130 x g for 10 min to deplete dead cells. After transferring the supernatant to a fresh tube, centrifugation at 10000 x g was performed for 30 min to remove cell debris and bigger vesicles, such as microvesicles. This 10000 x g supernatant contains exosomes and was used for treating neurons for example during the starvation paradigm. Finally, exosomes were pelleted from the supernatant at 100000 x g for 2 h and were defined as 'crude exosomes'. For better dissolving and more gentle pelleting, exosomes were sedimented onto a sucrose cushion (1.8 M sucrose in TBS). Further purification of exosomes and discrimination from vesicles other than exosomes, the exosome-containing sucrose cushion was carefully applied on top of a continuous sucrose gradient. The gradient was generated by overlaying equal amounts of 1.8 M and 0.3 M sucrose in an ultracentrifugation tube and kept horizontally at 4 °C for 1 h. After centrifugation at 100000 x g for at least 16 h, 12 fractions were collected from top to bottom using a 1 ml pipette. Using a refractometer, the density of each fraction was determined before centrifuging all single fraction at 100000 x g for 1 h to pellet exosomes. Due to their characteristic density, exosomes are typically contained in fractions with densities around 1.13 – 1.19 g/ml.

3.9 Boyden Chamber Co-Culture System

Boyden chambers allow a contact-free co-culture of different cells and simultaneously the exchange of particles, such as exosomes, through the 1 m pores of the filter membrane, while retaining whole cells. For viability assay using MTT, primary OL were cultured on the porous membrane of the inserts (1 x 10^6 cells/insert) and neurons were plated onto the 6-well plates (0.7 x 10^6 cells/well) in Neurobasal feeding medium. At 5 DIV, inserts containing OL were transferred to the well plate with cortical neurons and both cells were co-cultured for 48 h. Oxidative stress was performed by the application of 25 or 50 µM H_2O_2 for 1 h to neurons after removing OL. Cell viability was determined by MTT assay. Starvation stress was initiated by

replacing the culture medium to Neurobasal feeding medium lacking B27 in both OL and neurons before co-culture. MTT was performed after 48 h when OL were removed.

3.10 Oxygen-Glucose Deprivation

Primary cortical neurons (10 DIV; 0.7 10^6/ 6-well) were cultured with $O4^+$ OL (1 x 10^6/insert) in Boyden chambers for 48 h in neuronal feeding medium or with blank inserts containing oligodendrocyte-conditioned medium. Before oxygen–glucose deprivation (OGD) exposure, the culture media was replaced by glucose-free Neurobasal and cells were transferred to an anaerobic chamber saturated with 95% N_2 and 5% CO_2 at 378C. The co-cultures remained in an oxygen-free atmosphere for 2 h in order to mimic an ischaemic condition. Simultaneously, control cultures were grown under normoxic conditions in glucose-containing feeding medium. To allow subsequent reoxygenation, cells exposed to the OGD were returned to glucose-containing feeding medium and kept under normoxic conditions for 1 h. Medium exchange was equally performed in the normoxic and OGD group. Neuronal viability was determined by the MTT assay.

3.11 MTT Viability Assay

Analysis of cell viability was performed by MTT (3-(4,5-dimethylthiazol-2-yl)-2,5-diphenyltetrazoliumbromid) assay. The MTT substrate is dissolved in 1x PBS (5 mg/ml) and applied to cultured cells at a final concentration of 15 % of the culture medium. For example, primary cortical neurons cultured in 12-well plates at a density of 0.35 x 10^6 cells/well in 1 ml culture medium were treated with 150 µl of MTT solution and incubated for 2 h at 37 °C in the incubator. The quantity of formazan is directly proportional to the number of viable cells and measured at 562 nm after lysing cells by adding solubilisation buffer at the same volume of the culture medium (1:1). MTT is converted by living cells with active metabolism into a purple coloured formazan product involving the with NADH by transferring electrons to MTT (Figure 3-2).

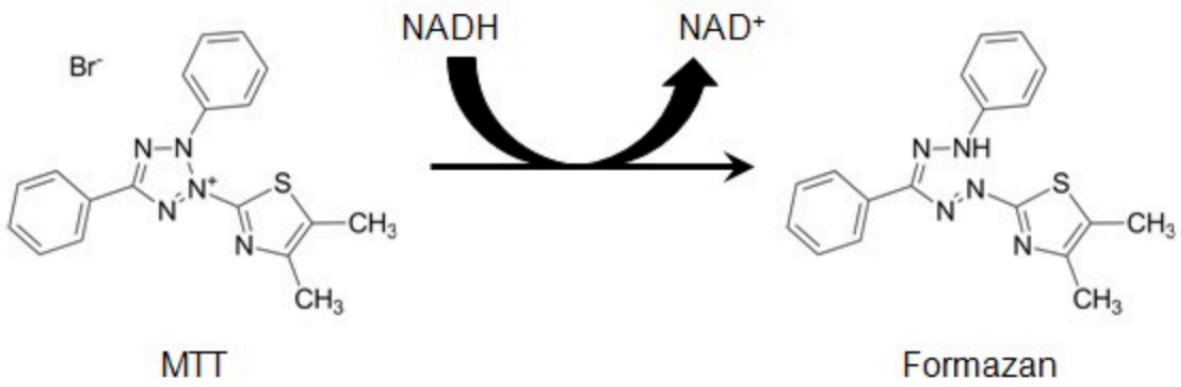

Figure 3-2 Conversion of MTT to formazan. Adapted from (Riss et al., 2004).

3.12 Staining of the Mitochondrial Membrane Potential

Visualization of the mitochondrial membrane potential was performed by using *MitoCapture ™* according to the manufacturer's protocol. Primary cortical neurons were plated in a 6-well companion plate with coverslips used for Boyden chamber co-culture. *MitoCapture ™* is a cationic dye, which aggregates in healthy cells due to mitochondrial transmembrane potential resulting in red fluorescent staining. In dead cells, it stays in its monomeric form and emits in green.

3.13 Phospho-MAPK Array

Using the Phospho-MAPK Array kit, we determined the phosphorylation state of various proteins upon exosomes treatment of neuronal cultures. Experimental performance and evaluation were carried out according to the manufacturer's protocol.

3.14 Axonal Transport Analysis

Axonal transport of BDNF-positive vesicles was analysed in hippocampal neurons expressing BDNFmCherry. After plating, the movement of BDNFmCherry containing vesicles was recorded at 2 or 3 DIV. The effect of exosomes under normal conditions was investigated by their application 30 min prior to video microscopy. Exosomes were previously isolated from cultures by differential centrifugation. Oxidative stress conditions were performed by subjecting hippocampal neurons to 15 µM H_2O_2 for 1 h after the pre-incubation with isolated exosomes by differential centrifugation for 12 h prior to imaging. In the starvation paradigm, neurons

were pre-cultured in conditioned full medium containing exosomes (10.000 x g supernatant) for 12 h. Subsequently, nutrient-deprivation was initiated by replacing the medium with conditioned starvation medium lacking B27-supplemet but including exosomes 3 h prior to video microscopy.

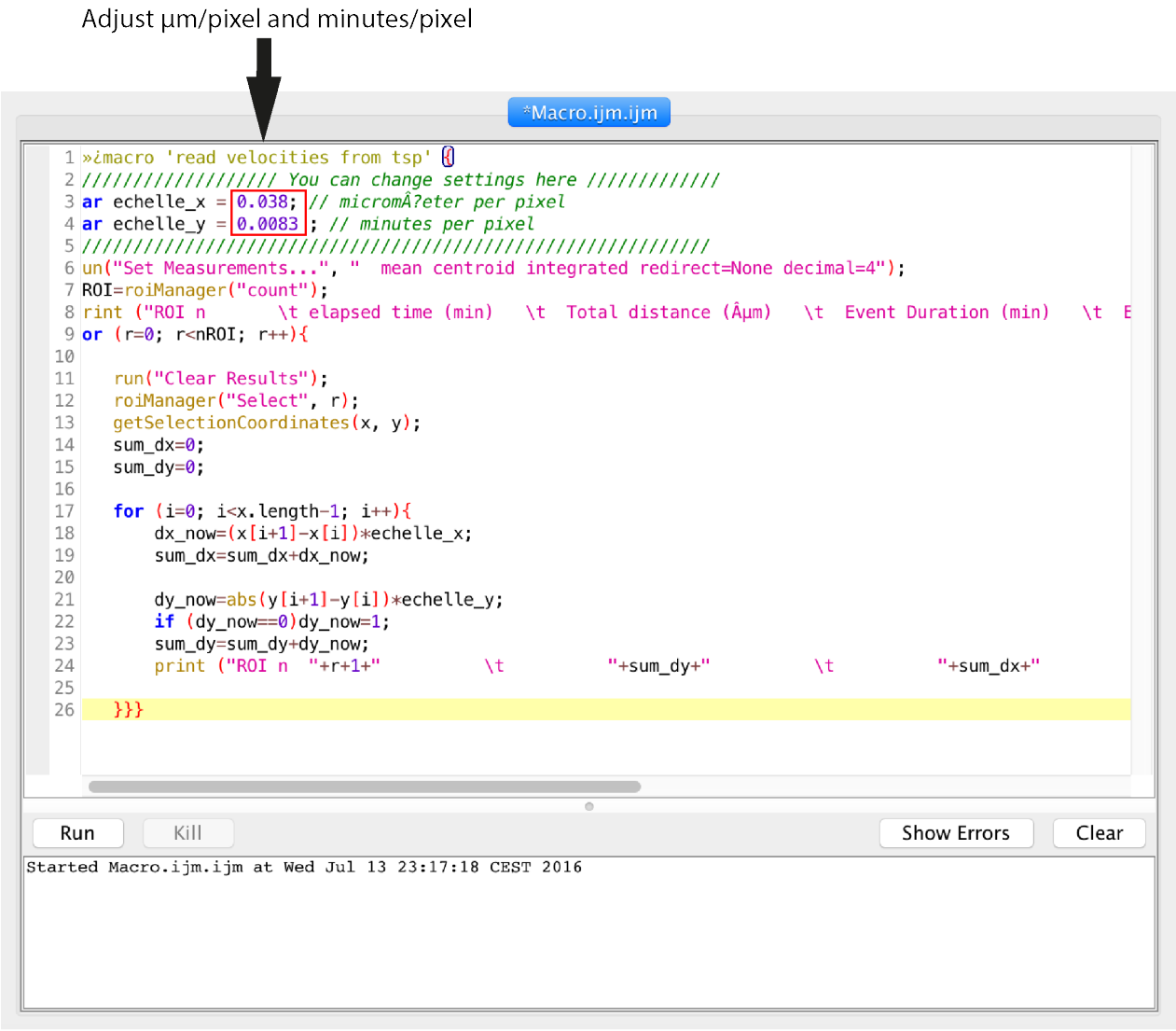

Figure 3-3 Macro for Axonal Transport Analysis.

3.14.1 Live-Cell Imaging

Images of unstressed neurons and those exposed to oxidative stress were taken with the Axiovert 200M microscope by Zeiss using a 63x objective. Live-cell imaging of neurons was performed by taking images every 3 seconds with a total of 200 frames (frame/3 seconds). Recordings of starving neurons were carried out with the TCS SP5 microscope using a 100x objective. Here, images were taken every 0.5 second with a total of 200 frames (frame/0.5

second). Both microscopes were enclosed by an incubator, which allowed to culture cells during the imaging process at 37 °C and 5 % CO_2.

3.14.2 Kymograph Generation

Kymographs graphically represent the spatial position of vesicles in the axoplasm over the time allowing the tracking of single trajectories. To create kymographs, various plug-ins provided by *ImageJ* were implemented. The following instruction supports the generation of kymographs of video recording:

1. Open video in *ImageJ*.
2. Create a MAX projection of the video (Image → Stacks → Z-Projection… → Projection type: Max Intensity → OK)
3. Using the 'segmented line' tool trace the axon with an appropriate line width covering the entire axonal width beginning from the soma. This is important as it allows the discrimination of anterograde and retrograde movement.
4. Import the drawn line to the original video (Edit → Selection → Add to Manager → activate window containing the video → chose appropriate coordinate in the 'ROI manager' window).
5. Generate kymograph (Analyze → Multi Kymograph → Multi Kymograph). Invert color, if necessary (shift + ctrl + I).
6. Using 'segmented line' tool with line width of '1' trace vesicle trajectories always from top to bottom. After each trajectory, save coordinates using the ROI manager (Edit → Selection → Add to Manager). Display all trajectories in the kymograph by ticking 'Show all' and 'Labels'.
7. Open 'New Macro' (Plugins → New → Macro).
8. Enter macro for analysing coordinates obtained from trajectories (see Figure 3-3).
9. Copy data to Excel for evaluation.

3.14.3 Kymograph Analysis

Evaluation of the data obtained from the kymographs allows the analysis of the distribution of anterograde and retrograde movement and static vesicles, the velocity and the pausing time. Figure 3-4 shows the extraction of an exemplary analysis. Each ROI depicts the trajectory of a

single vesicle tracked previously (yellow background). Calculation of the mean of the actual speed gives the average speed of each trajectory allowing its directional classification. Positive speed represents anterograde movement, whereas negative speed indicates retrograde movement. By sorting the average speed of each vesicle into anterograde and retrograde movement reveals the percentage distribution. Static vesicles can be recognized on the kymographs *per se* showing a vertical movement and have been marked in the data sheet.

For calculation of the pausing time, first total event duration needs to be determined by summation. Second, a cut-off for a pausing vesicle has to be defined. Here, we set it to 5 µm/min. Hence, the time of duration event of single sections of a trajectory exhibiting an actual speed below 5 µm/min has been added together. Subsequently, calculating the percentage distribution of the time a vesicle pauses of the total event duration gives the pausing time of the respective vesicle over its total movement. By averaging the pausing time of every single trajectory finally gives the pausing time exbited by vesicles moving along one axon.

	A	B	C	D	E	F	G	H	I
1	ROI n	elapsed time (min)	Total distance (µm)	Event Duration (min)	Event length (µm)	actual speed (µm/min)	Mean (actual speed)		Pausing time
2	ROI n 1	0,3	-32,1	0,3	-32,1	-107	-73,64285		0
3	ROI n 1	0,65	-46,2	0,35	-14,1	-40,2857			
4	ROI n 2	0,15	1,5	0,15	1,5	10	5,8857125		
5	ROI n 2	0,45	1,5	0,3	0	0		2,15	0,46511628
6	ROI n 2	0,6	0,3	0,15	-1,2	-8		1	
7	ROI n 2	0,85	2,4	0,25	2,1	8,4			
8	ROI n 2	1,2	3,6	0,35	1,2	3,4286			
9	ROI n 2	1,55	3,9	0,35	0,3	0,8571			
10	ROI n 2	1,8	6	0,25	2,1	8,4			
11	ROI n 2	2,15	14,4	0,35	8,4	24			
12	ROI n 3	0,05	4,8	0,05	4,8	96	61,2		0
13	ROI n 3	0,3	11,4	0,25	6,6	26,4			
14	ROI n 4	0,15	1,8	0,15	1,8	12	18,74286667		0
15	ROI n 4	0,4	4,5	0,25	2,7	10,8			
16	ROI n 4	0,75	16,2	0,35	11,7	33,4286			
17	ROI n 5	0,25	12	0,25	12	48	60		0
18	ROI n 5	0,3	24,9	0,05	12,9				
19	ROI n 5	0,4	32,1	0,1	7,2	72			
20	ROI n 6	0,05	-2,1	0,05	-2,1	-42	-61		0
21	ROI n 6	0,35	-26,1	0,3	-24	-80			
22	ROI n 7	0,2	-19,2	0,2	-19,2	-96	-96		0
23	ROI n 8	0,1	2,4	0,1	2,4	24	29,66666667		0
24	ROI n 8	0,2	5,7	0,1	3,3	33		1	0,6
25	ROI n 8	0,75	11,4	0,55	5,7	4,7		0,6	
26	ROI n 8	0,85	13,5	0,1	2,1	21			0
27	ROI n 8	0,9	17,7	0,05	4,2	2,3			
28	ROI n 8	1	27	0,1	9,3	93			
29									0,10651163

Figure 3-4 Example of analysing the axonal transport of single vesicles.

4 Results

4.1 Characterization of Isolated O4$^+$-Oligodendrocytes by Magnetic-activated Cell Sorting (MACS)

Exosomes are released by all neural cells in the brain executing different functions. Functional analysis of cell-specific exosomes therefore requires high purity of cultured cells to exclude functional interference of exosomes derived from other cell types. Here, we characterize oligodendroglial cultures obtained from postnatal mice based on the isolation by magnetic-activated cell sorting (MACS) via antibodies coupled to magnetic beads. This method allows cell purification from brain tissues within one day at a high purity (see section 3.4.1). Using anti-O4 antibodies coupled to magnetic beads, we isolated oligodendrocytes (OL) from P7 mice. O4 antibody is a specific marker of galactosylceramide expressed by premyelinating OL on their surface (Sommer and Schachner, 1981).

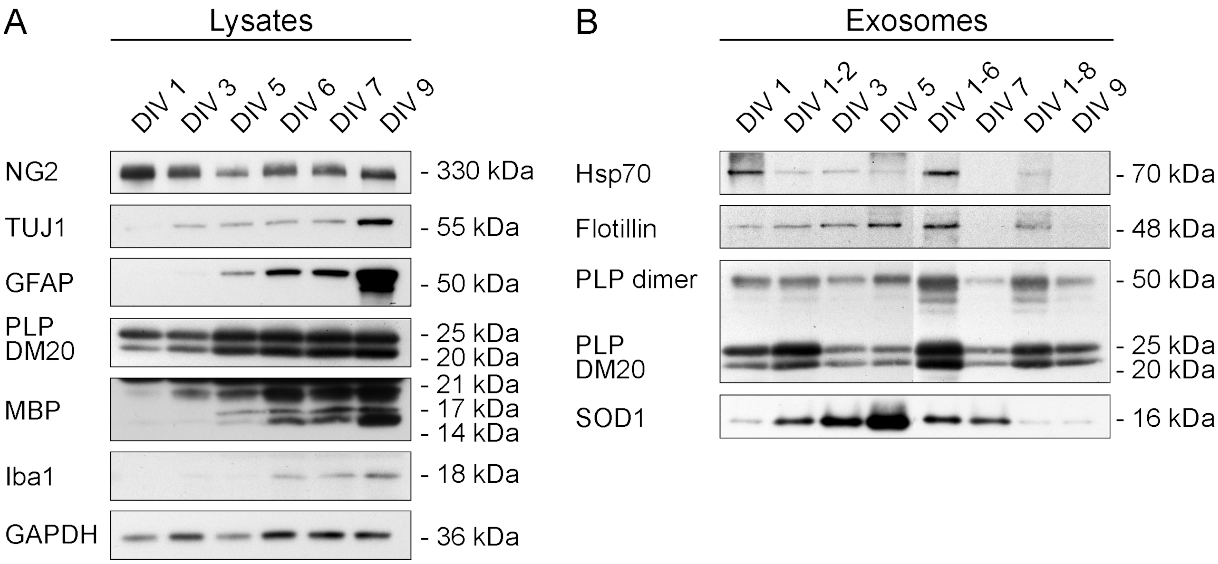

Figure 4-1 Characterization of O4$^+$-oligodendrocyte cultures. OL were isolated from P7 mice using anti-O4 antibodies coupled to magnetic beads and cultured for 1, 3, 5, 6, 7, and 9 DIV, respectively. (A) Cultures were analysed by western blotting using oligodendroglial- (PLP/DM20, MBP), neuron- (TUJ1), and microglia-specific (Iba1) markers. NG2 is a marker for OPCs. GAPDH served as loading control. (B) Exosomes derived from O4$^+$ OL were isolated after different DIV and collection periods, respectively. DIV 1, 3, 5, 7, and 9 represent exosome fractions collected over 24 h at the respective DIV. DIV 1 – 2, 1 – 6, and 1 – 8 depict the collection periods beginning at 1 DIV.

O4$^+$ OL were cultured for 1, 3, 5, 6, 7, and 9 days *in vitro* (DIV), respectively, and analysed by western blotting (Figure 4-1 A). Immunocytochemical analysis was performed of 1, 3, and 5 DIV

cultures (Figure 4-2). The differentiation state of the cells is depicted by the presence of PLP and MBP that are continuously upregulated. While PLP plays a role in early OL differentiation and is critical for continued differentiation, MBP is a marker for differentiated OL (Knapp et al., 1988; Pfeiffer et al., 1993; Trapp et al., 1997). Immunocytochemical analysis depicts $O4^+$ OL with characteristically arborized processes (Figure 4-2).

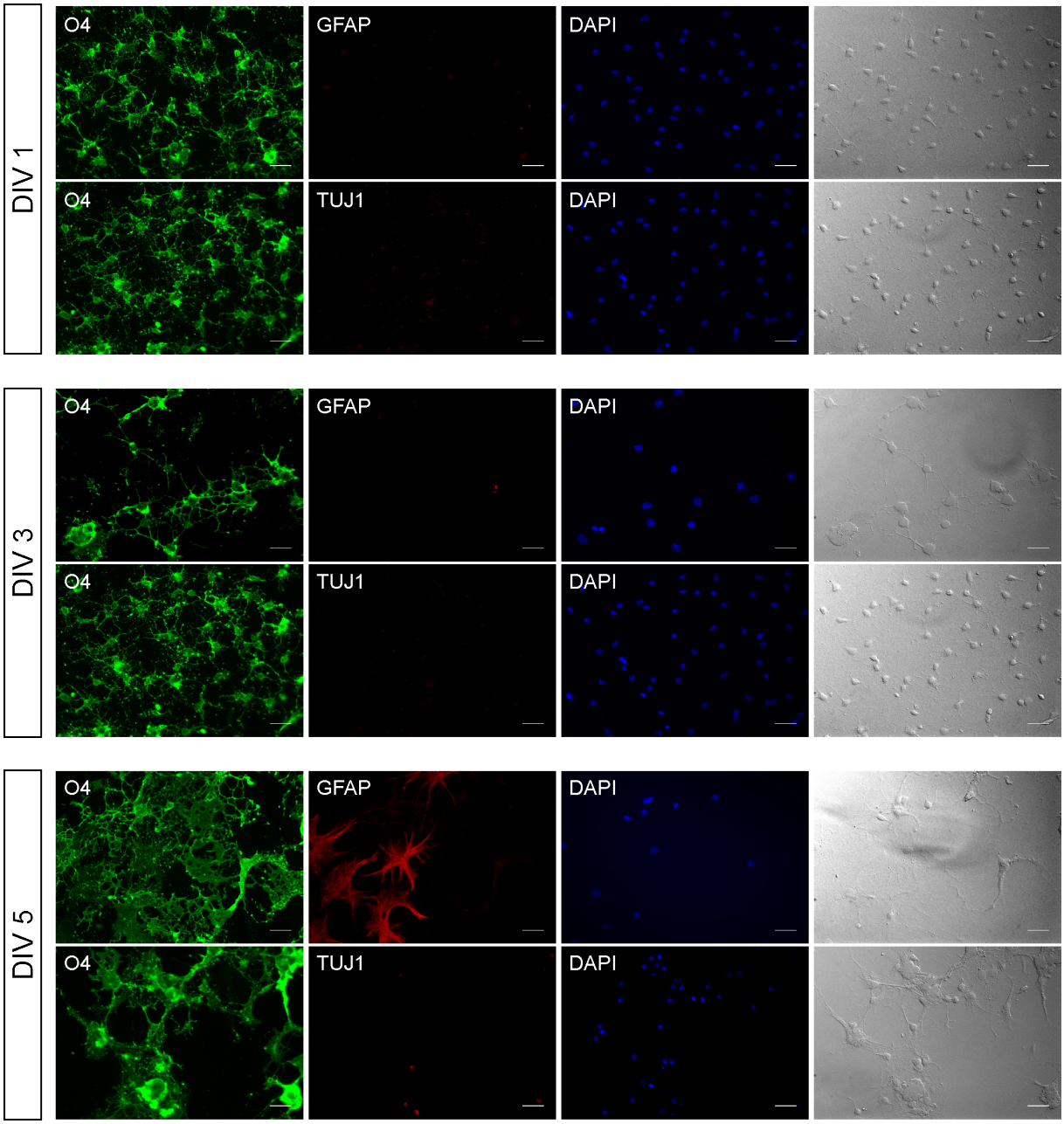

Figure 4-2 Immunocytochemical analysis of $O4^+$-oligodendrocyte cultures. $O4^+$ OL were cultured for 1, 3, and 5 DIV, respectively. Cultures were analysed by immuno-staining using antibodies directed against GFAP as astrocytic and TUJ1 as neuronal marker. DAPI stains cell nuclei. Scale bars, 20 µm.

GFAP, a marker for astrocytes, occurs first at 5 DIV in immuno-stainings, which could also be confirmed by western blotting. Neuronal contamination of oligodendroglial cultures could not be detected by immuno-staining using anti-TUJ1 antibody in 1, 3 and 5 DIV cultures. Anti-TUJ1 antibody labels ß III-tubulin of differentiated neurons and is only marginal present from 3 DIV as shown by western blotting. The emergence of astrocytes and neurons might be due to the presence of $NG2^+$ OPCs in the cell cultures, which have been suggested to give rise to neurons and astrocytes (Nishiyama et al., 2009; Zhu et al., 2008).

Exosomes derived from $O4^+$ OL were collected for different periods from the culture supernatants and analysed by western blotting after differential centrifugation (Figure 4-1 B). DIV 1, 3, 5, 6, 7, and 9 exosomes were isolated after 24 h from the respective OL cultures. DIV 1 – 2, 1 – 6, and 1 – 8 represent different collection periods beginning at 1 DIV. The presence of exosomes could be confirmed by the exosome markers Hsp70, flotillin, and PLP. SOD1 has been reported to be sorted into exosomes in astrocytes (Basso et al., 2013).

Based on these results, we decided to collect exosomes from $O4^+$ OL during 3 – 5 DIV for neuronal treatment in the following functional experiments.

4.2 Stress-Relevant Proteins are Shipped to Neurons via Oligodendroglial Exosomes

Proteomic analysis of the exosomal content revealed a list of putative stress-protective biomolecules (Krämer-Albers et al., 2007). Based on this data, we investigated the horizontal, exosome-mediated transfer of proteins with potential neuroprotective function using Boyden chambers, a transwell system allowing contact-free co-culture of cells. Previously, we have shown the exosome-dependent transfer of Hsc70 and catalase to neurons (Frohlich et al., 2014). Another vital protein coupled to antioxidant defense is SOD1. Here, we examined its presence in oligodendroglial exosomes and its potential to be horizontally transferred to target neurons. Exosome isolation and analysis via western blotting confirmed the presence of SOD1 in Alix/Hsp70-containing exosomes derived from transfected Oli-*neu* cells transiently expressing hSOD1-EGFP (Figure 4-3 A). hSOD1-EGFP or EGFP transfected Oli-*neu* cells were co-cultured with primary cortical neurons (DIV 5) in Boyden chambers for 48 h (**Figure 4-4** A). This contact-free co-culture system allows a constant supply for neurons with oligodendrocyte-derived factors including exosomes. Analysis of neuronal lysates confirmed the transfer of hSOD1-EGFP from Oli-*neu* cells to neurons (**Figure 4-3** B). Remarkably, EGFP itself could not be

found in exosomes and therefore could not be transported to neurons. Whether this is due to low EGFP-expression or an indication of specific protein sorting into exosomes remains elusive.

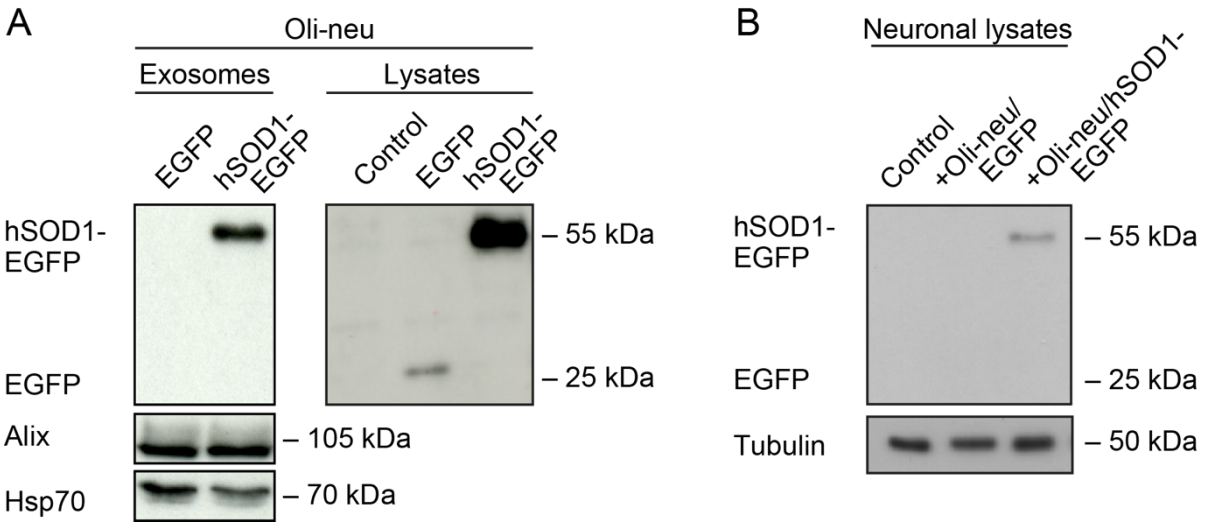

Figure 4-3 SOD1 is shuttled from oligodendrocytes to neurons via exosomes. (A) hSOD1-EGFP-expressing Oli-*neu* cells release hSOD1-EGFP in association with exosomes as shown by the presence of the exosome markers Alix and Hsp70. (B) Internalization of hSOD1-EGFP upon co-culture with Oli-*neu* cells transfected with hSOD1-EGFP or EGFP, respectively.

4.3 Oligodendroglial Exosomes Facilitate Neuroprotection under Cellular Stress

Various proteins involved in stress protection are horizontally transported from OL to neurons (section 4.2) via exosomes suggesting a potentially neuroprotective role of exosomes (Frohlich et al., 2014). To address the question whether exosome support neuronal metabolism, we performed viability assays using the yellow tetrazolium MTT (3-(4,5-dimethylthiazol-2-yl)-2,5-diphenyltetrazoliumbromid). MTT is reduced by metabolically active cells, partly by the action of dehydrogenase enzymes generating reducing equivalents, such as NADH and NADPH and thus reflects the number of viable cells by their mitochondrial activity (see section 3.11). Cortical neurons were exposed to oligodendroglial exosomes under optimized as well as cellular stress conditions such as oxidative stress, starvation stress, and oxygen-glucose deprivation.

4.3.1 Oxidative Stress

Primary OL (5 - 7 DIV) and primary cortical neurons (5 - 6 DIV) were co-cultured in Boyden chambers for 48 h as shown in Figure 4-4 A. Control neurons were cultured in the absence of OL but in OL-conditioned medium depleted from exosomes to exclude effects mediated by

soluble factors. Subsequently, neuronal metabolic activity was measured by MTT assay. Neurons grown under optimal conditions did not exhibit a significant improvement when exposed to exosomes (Figure 4-4 B, unstressed). Challenging neurons with 25 µM or 50 µM H_2O_2 for 1 h prior to co-culture reduces cell viability by 61.2 ± 8.8 % and 68.5 ± 9.1 %, respectively, without any significant, exosome-mediated amelioration (Figure 4-4 B). Intriguingly, when neurons were subjected to oxidative stress after exosome treatment for 48 h, their metabolic activity was significantly increased by 23.6 ± 7.4 % (25 µM H_2O_2) and 18.2 ± 12.3 % (50 µM H_2O_2) (Figure 4-4 C). Since oxidative stress was not alleviated when neurons were subjected to stress prior to co-culture (Figure 4-4, B), we assume that exosome supply is protective but is insufficient to rescue damaged neurons. *MitoCapture ™* staining of neurons confirmed the neuroprotective effect of exosomes (Figure 4-4 D). *MitoCapture ™* is a cationic dye, which aggregates in healthy cells due to mitochondrial transmembrane potential resulting in red fluorescent staining. In dead cells, it stays in its monomeric form and emits in green. Figure 4-4 D demonstrates that co-culture with OL prevents the breakdown of the mitochondrial membrane potential.

In order to prove that the neuroprotective effect can to be traced back to oligodendroglial exosomes, we incubated neurons with exosome-containing OL-conditioned culture supernatant for 12-14 h prior to oxidative stress exposure and determined their metabolic activity compared to neurons treated with OL-conditioned, exosome-deprived medium. Unexpectedly, application of exosomes did not exhibit a higher tolerance towards stress compared to control cells (Figure 4-4 E). In contrast, a single administration of exosomes isolated by differential centrifugation 12 - 14 h prior to oxidative stress exposure resulted in a significant increase of neuronal metabolic activity by 25.4 ± 9.5 % (Figure 4-4 F, OL). However, this was not the case when neurons received exosomes from Oli-neu or HEK293T cells, nor artificial liposomes indicating a cell-specific effect mediated only by primary oligodendroglial exosomes (Figure 4-4 F).

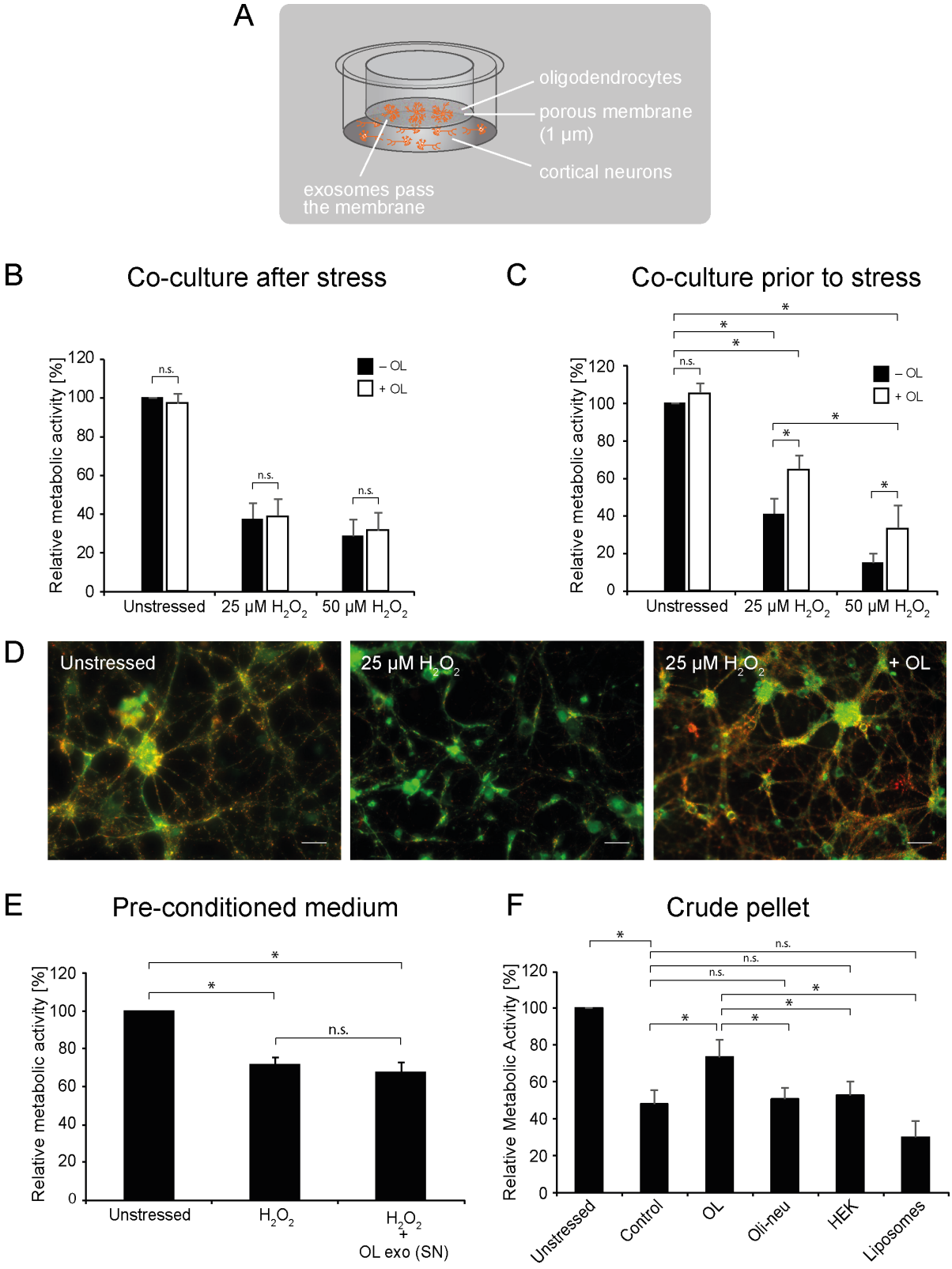
A
oligodendrocytes
porous membrane
(1 µm)
cortical neurons
exosomes pass
the membrane
B
Co-culture after stress
Relative metabolic activity [%]
– OL
+ OL
n.s.
Unstressed
25 µM H2O2
50 µM H2O2
C
Co-culture prior to stress
D
Unstressed
25 µM H2O2
25 µM H2O2
+ OL
E
Pre-conditioned medium
Unstressed
H2O2
H2O2
+
OL exo (SN)
F
Crude pellet
Relative Metabolic Activity [%]
Unstressed
Control
OL
Oli-neu
HEK
Liposomes

Figure 4-4 Oligodendroglial exosomes protect neurons from oxidative stress. (A - D) Cortical neurons and OL were co-cultured in Boyden chambers for 48 h allowing constant supply with exosomes, while control neurons were cultured in OL-conditioned culture medium depleted of exosomes. Subsequent MTT assay determined neuronal viability (B, C, E, F). (B) Neurons exposed to 25 µM and 50 µM H_2O_2 for 1 h before co-culture with OL compared to unstressed neurons. (C) Co-culture of neurons and OL prior to oxidative stress induction by 25 µM and 50 µM H_2O_2 for 1 h (n = 5). (D) *MitoCapture ™* staining of unstressed neurons, neurons exposed to 25 µM H_2O_2, and neurons co-cultured with OL prior to oxidative stress exposure (1 h, 25µM H_2O_2). Scale bar, 20 µm. (E) Incubation of neurons with OL-conditioned medium containing or deprived of exosomes (n = 8), and (F) single application of isolated exosomes derived from primary OL (OL), Oli-*neu*, and HEK293T cells as well as artificial liposomes followed by oxidative stress challenge (1h, 25 µM H_2O_2) after 15 h treatment (n = 5). Error bars, SEM (n.s., not significant; *p < 0.05; Wilcoxon-Test).

4.3.2 Nutrient Deprivation

To further validate the neuroprotective role of oligodendroglial exosomes, starvation stress was applied to neurons by withdrawing the serum-free B27-supplement from the culture medium. B27 contains optimized components including growth factors to facilitate neuronal longevity under *in vitro* culture conditions and B27 depletion causes a significantly lower viability compared to B27-supplied neuronal cultures (Brewer, 1995; Brewer et al., 1993). Thus, both primary cortical neurons (5 - 7 DIV) and primary OL (6 - 7 DIV) co-cultured in Boyden chambers suffered from starvation for 48 h due to B27-supplement depletion (ND + pOL). Neurons cultured in the absence of OL received pre-conditioned oligodendroglial medium depleted from exosomes (ND). Culture medium of unstressed cells contained B27-supplement. *MitoCapture ™* staining illustrates the mitochondrial membrane potential of neurons cultured under unstressed, OL-conditioned starvation medium excluding (ND), or including exosomes (ND + OL) (Figure 4-5 A). Accordingly, oligodendroglial exosomes impeded the collapse of the mitochondrial membrane potential in stressed neurons. Subsequent MTT assay revealed a significantly higher viability of neurons (31.2 ± 7 %) when co-cultured with OL (Figure 4-5 B) affirming the beneficial effect of oligodendroglial exosomes on neuronal metabolic activity.

As performed in the previous paradigm (**Figure 4-4**), we also applied purified exosomes to neurons to ensure the observed effect is indeed evoked by exosomes. Interestingly, a single administration of isolated exosomes for 12 – 14 h had no supportive effect on the metabolic activity of starving neurons (Figure 4-5 C). In order to use a more gentle isolation method, exosomes were pelleted at 100.000 x g on a sucrose cushion to avoid any negative influence on the exosomal bioactivity caused by centrifugal forces. Again, exosomes did not facilitate neuronal stress tolerance (**Figure 4-5** D). Since sucrose might influence the exosomal bioactivity due to its osmotic characteristics, we used iodixanol solution (Opti-prep) instead, a density gradient medium without osmotic properties suitable for the isolation of cells and cell

organelles. Also iodixanol preparations of exosomes failed to effectively support starving neurons (**Figure 4-5** E). Next, we abstained from ultracentrifugation and supplied neurons with OL-conditioned medium containing exosomes or, as a control, depleted from exosomes for 12 – 14 h. Intriguingly, this approach resulted in a significant elevation of neuronal viability by 13.8 ± 3.1 % (**Figure 4-5** F) leading to the assumption that in terms of starvation stress, exosome-mediated support is accompanied by other unknown factors present in OL-conditioned medium. We therefore combined previously described experiments by incubating neurons in OL-conditioned medium lacking exosomes but separately added purified exosomes (**Figure 4-5** G, ND + OL SN + exo). However, this combined treatment had only a minor supportive effect compared to untreated starving neurons (**Figure 4-5** G, ND).

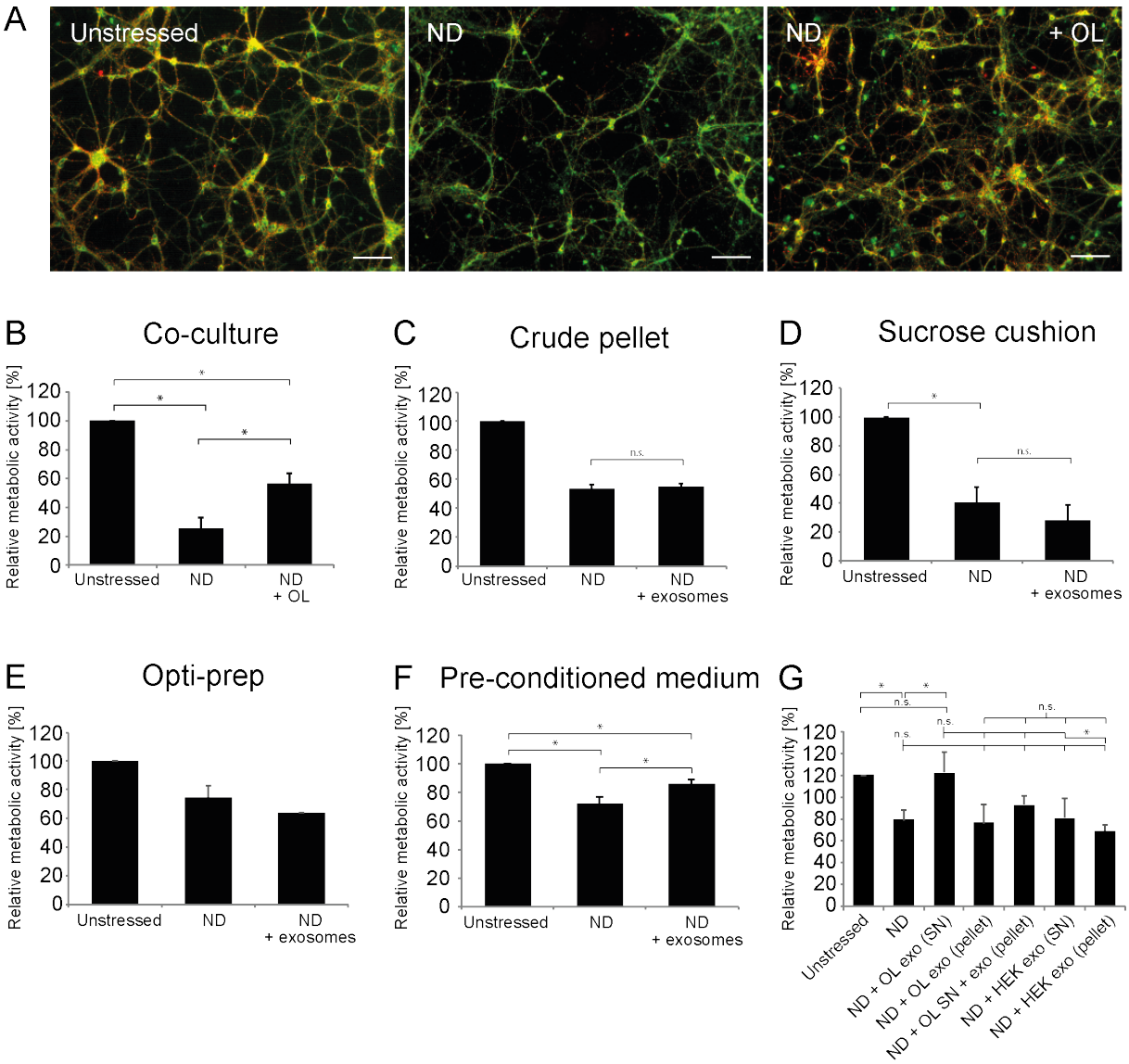

Figure 4-5 Oligodendroglial exosomes protect neurons from starvation stress. (A - G) Starvation stress in cortical neurons (ND, nutrient deprivation) caused by the depletion of B27-supplement was exerted for 12 – 48 h in the presence or absence of exosomes, whereas exosome-untreated neurons were supplied with pre-conditioned oligodendroglial (OL) starvation medium lacking exosomes. Control neurons received full culture medium (unstressed). Subsequently, neurons were subjected to MTT assay for viability determination (B – G). (A) *Mitocapture ™* staining of neurons co-cultured with OL for 15 h. Scale bar, 100 µm. (B) Neurons were co-cultured with OL in Boyden chambers under starvation conditions over 48 h (n = 5). Exosome-treatment of starving neurons was performed by a single administration of exosomes crudely isolated by ultracentrifugation (C, n = 8), ultracentrifuged on a sucrose cushion (D, n = 4), or on an Opti-prep cushion (E, n =2) followed by incubation over 15 h. (F) Neurons were cultured in OL-conditioned starvation medium ± exosomes (n = 5). (G) Neurons were cultured in conditioned starvation medium (SN) or treated with isolated exosomes (pellet) derived from OL or HEK293T cells for 15 h, respectively. Furthermore, neurons were cultured in OL-conditioned but exosome-depleted starvation medium rearmed with additional isolated exosomes (OL SN + exo (pellet)) (n = 5). Error bars, SEM (n.s., not significant; *p < 0.05; Wilcoxon-Test).

Assuming that lactate might be one of these associated components, we co-treated neurons with isolated exosomes and lactate, which also failed to alleviate stress (data not shown). Finally, to elucidate the functional specificity of oligodendroglial exosomes, starved neurons were exposed to HEK293T-derived exosomes by incubation in conditioned medium containing exosomes (ND + HEK exo (SN)) or by single exosome administration (ND + HEK exo (pellet)). Notably, both implementations did not arbitrate cell survival of starving neurons (Figure 4-5 G). Hence, exosome-mediated neuroprotection from starvation is restricted to oligodendroglial exosomes and may dependent on additional secreted factors.

4.3.3 Oxygen-Glucose Deprivation

The previous stress paradigms revealed that oligodendroglial exosomes possess neurosupportive characteristics by protecting recipient neurons from oxidative stress as well as starvation (Figure 4-4, Figure 4-5). To investigate the supportive effects of oligodendroglial exosomes on a disease background, we exposed neurons to oxygen-glucose deprivation (OGD). OGD is a widely accepted *in vitro* model for stroke, showing analogies with *in vivo* models of brain ischemia, which results in apoptotic and necrotic cell death (Tasca et al., 2015). Primary cortical neurons (10 DIV) and primary OL (7 DIV) were co-cultured in Boyden chambers for 48 h under optimal culture conditions. In order to mimic the interruption of oxygen and nutrient supply to the brain occurring during an ischemic event, the neuron-glia co-culture was subjected to glucose-free medium and cultured under a deoxygenated atmosphere for 2 h. Exosomes were provided to neurons by OL during the entire OGD period. Control neurons were cultured without OL, but in the presence of OL-conditioned medium depleted of exosomes to exclude effects mediated by soluble factors. Subsequently, co-cultures were transferred back to normal glucose-containing culture conditions under oxygenated atmosphere allowing cells

to recover for 1 h. Neuronal viability was assessed in relation to corresponding normoxic cultures by MTT assay. Intriguingly, neurons exposed to oligodendroglial exosomes during hypoxia revealed a significantly higher metabolic activity (21.5 ± 7.6 %) compared to control cells (Figure 4-6 A).

In a second approach, we supplied neurons with a single administration of purified exosomes for 12 – 14 h followed by glucose and oxygen-deprived but exosome-containing culture conditions for 2 h. After a 1 h recovery phase, neuronal metabolic activity was determined by MTT assay. Comparison of neurons supplied with oligodendroglial exosomes and control cells treated with PBS did not reveal an alleviated stress effect (Figure 4-6 B). Moreover, treatment of recipient neurons with exosomes derived from Oli-*neu* cells and HEK293T or liposomes before and during OGD exposure emerged to be ineffective as well (Figure 4-6 B).

Taken together, neurons cultured in the presence of exosome-secreting OL are significantly desensitized towards OGD. However, treatment with isolated exosomes did not exert stress alleviation.

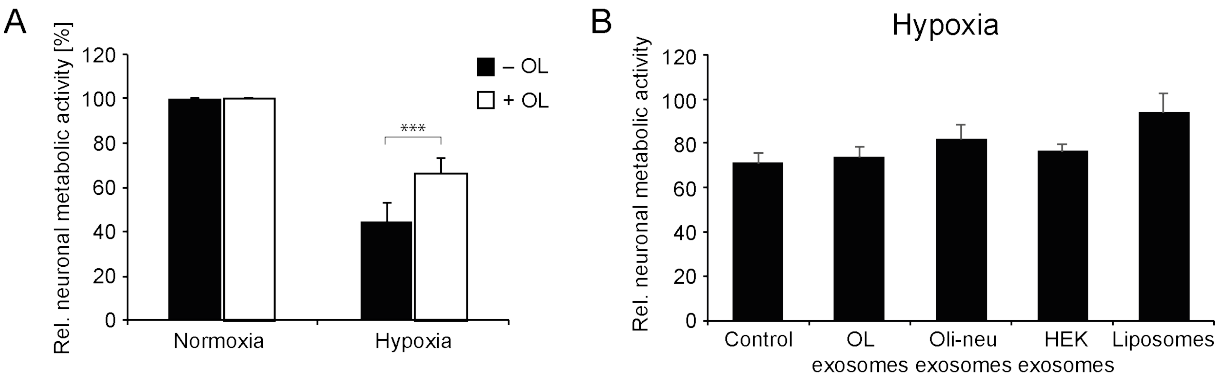

Figure 4-6 Oligodendroglial exosomes protect neurons during OGD. (A) Neurons and OL were co-cultured in Boyden chambers for 48 h. Subsequently, cells were subjected to OGD for 2 h followed by 1 h reoxygenation (n = 5). (B) Neurons were exposed to isolated exosomes derived from OL, Oli-neu cells or HEK cells, respectively, as well as liposomes for 12 h before being subjected to OGD for 2 h followed by 1 h reoxygenation (n = 4). Neuronal metabolic activity was determined by MTT assay. The relative metabolic activity correlates OGD neurons to respective neurons grown under normoxic conditions. Error bars, SEM (n.s., not significant; ***p < 0.001; Student's t-test).

4.4 Activation of Pro-Survival Signaling Pathways in Neurons by Oligodendroglial Exosomes

We have provided evidence that oligodendroglial exosomes protect recipient neurons under various cellular stress conditions. Cells respond to stress by activating signalling pathways to promote either cell survival or cell death. Thus, we performed a kinase screen of neurons treated with oligodendroglial exosomes to further elucidate the underlying mechanisms of exosome-mediated neuroprotection. To identify kinases phosphorylated in neurons due to exosome treatment, we used the Phospho-MAPK (Mitogen Activated Protein Kinases) Array. Primary cortical neurons (5 – 7 DIV) were cultured under optimal conditions and exposed to isolated exosomes by a single administration. Cells were lysed after 1 h and levels of protein phosphorylation were assessed using phospho-specific antibodies and chemiluminiscence detection (**Figure 4-7** A). Except from Akt3, p70 S6 kinase and TOR showing a marginally altered phosphorylated level, all remaining proteins seem unaffected compared to PBS-treated neurons (Figure 4-7 A, control, dashed line).

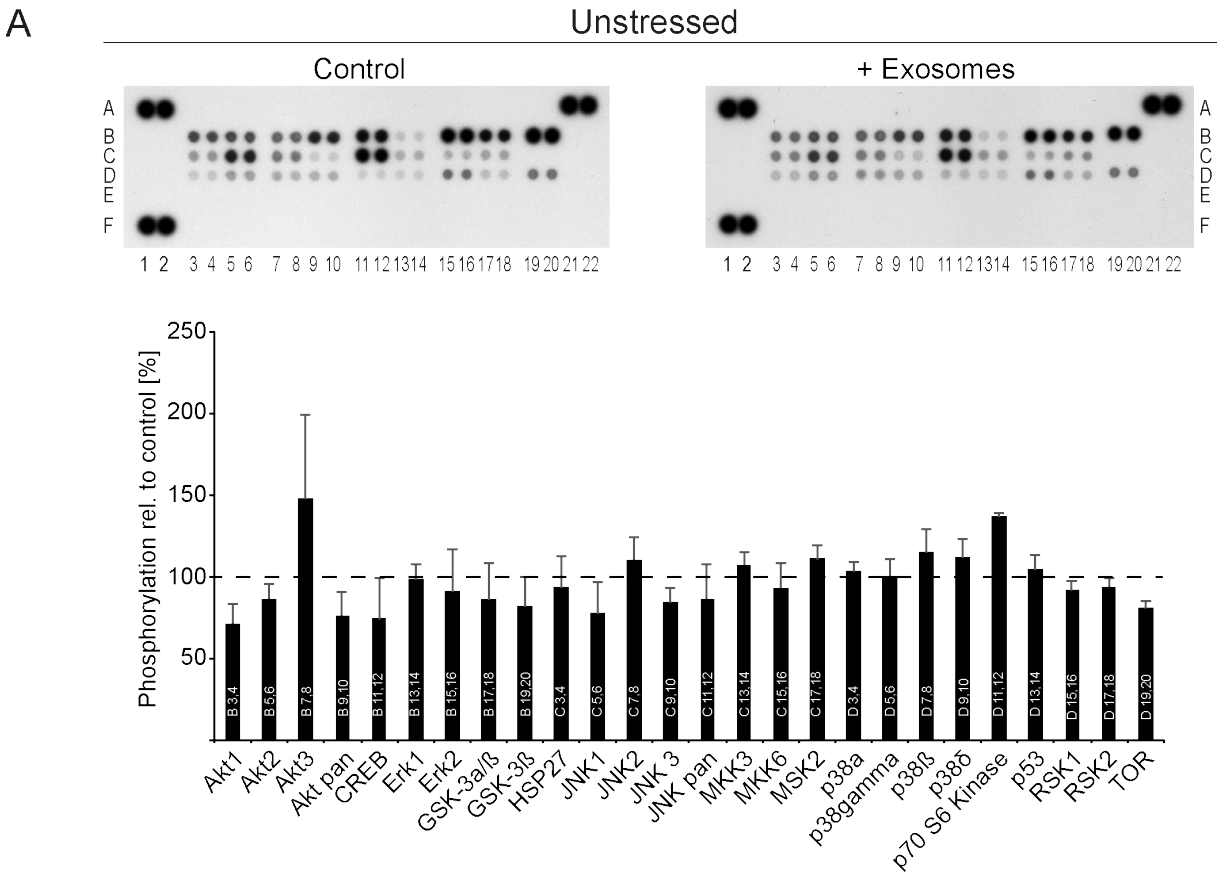

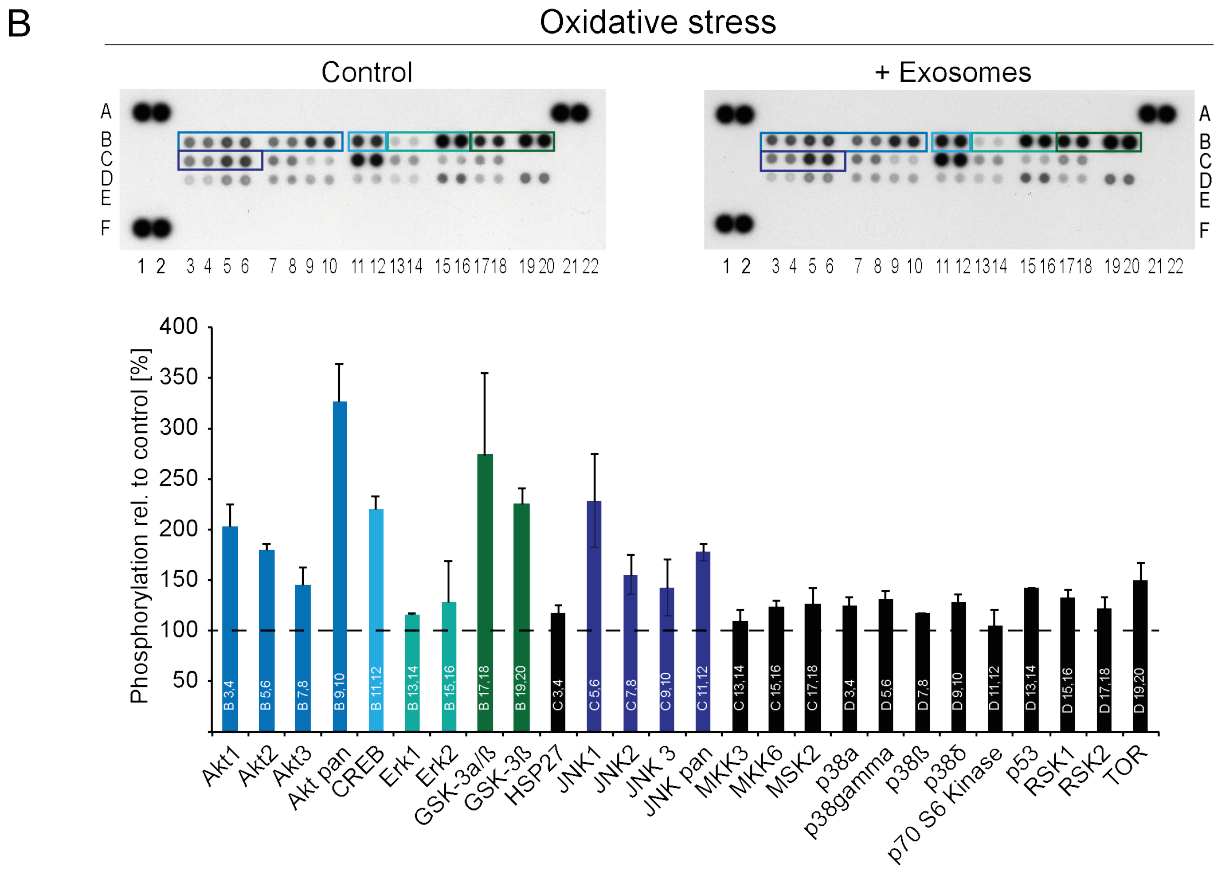

Figure 4-7 Kinase Screen of exosome-treated neurons. Phospho-MAPK Array allowed the detection of phosphorylated proteins in neuronal lysates. Bars are labelled with corresponding coordinates of each protein. (A) Purified oligodendroglial exosomes were applied to cortical neurons for 1 h before cells were lysed (n = 3). Control neurons were treated with PBS. Abundance of phosphorylated proteins was quantified by densitometry and compared to PBS-treated neurons (dashed line). (B) Neurons were exposed to purified oligodendroglial exosomes or PBS (control) for 12 h before being challenged with oxidative stress (25 µM H_2O_2) for 1 h (n = 4). Phosphorylation state of proteins was determined by densitometry. Dashed line depicts PBS-treated neurons prior to oxidative stress exposure. Proteins showing a higher phosphorylation level compared to control are highlighted by coloured boxes. Error bars, SEM.

Since the neuroprotective property of oligodendroglial exosomes was only observed after stress insult (**Figure 4-4** – **Figure 4-6**), we introduced cell stress in the follow-up experiment. Neurons were pre-incubated with isolated exosomes for 15 h and subjected to oxidative stress (25 µM H_2O_2) for 1 h before analysis.

The assay revealed an exosome-dependent increase in the phosphorylation state of Akt, CREB, GSK-3α/β, GSK-3β, and JNK, while ERK did not exhibit robust activation under these conditions (Figure 4-7 B). These results suggest that upon internalization of oligodendroglial exosomes distinct signalling pathways are activated by phosphorylation in the recipient neurons.

We next examined the activation of Akt and Erk1/2 pathways after exosome addition for different time periods (Figure 4-8). Subsequent analysis by western blotting did not reveal a

notable activation pattern, which is consistent with the kinase screen obtained from exosome-treated neurons under optimal culture conditions (Figure 4-7 A).

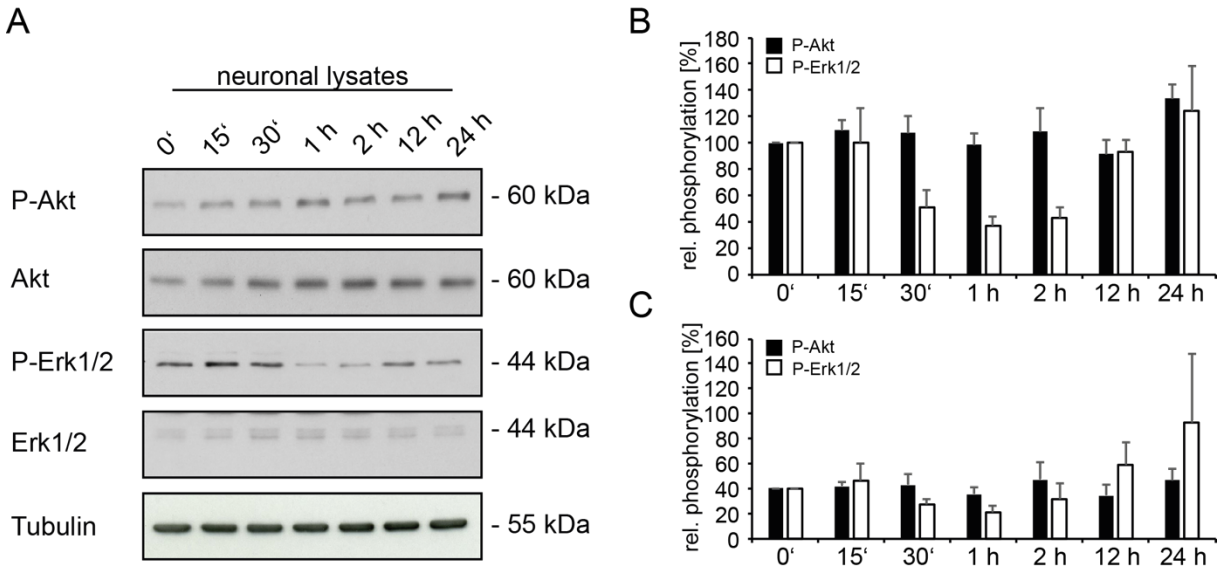

Figure 4-8 Exosome-dependent activation of Akt and Erk1/2. (A) Purified oligodendroglial exosomes were applied to primary cortical neurons for 0 min, 15 min, 30 min, 1 h, 2 h, 15 h and 24 h (n = 5). (B) P-Akt and P-Erk1/2 levels determined by western blotting were normalized to total Akt or Erk and expressed in relation to untreated neurons at timepoint 0 min. (C) Expression level of phosphorylated Akt and Erk were additionally normalized to tubulin. Error bars, SEM.

To test the activation of both pathways under stress, we analysed the phosphorylation levels in neurons after co-culture with OL in Boyden chambers (Figure 4-9). Neurons were either exposed to oxidative stress (25 µM H_2O_2 for 1 h) after or to starvation stress during co-culture.

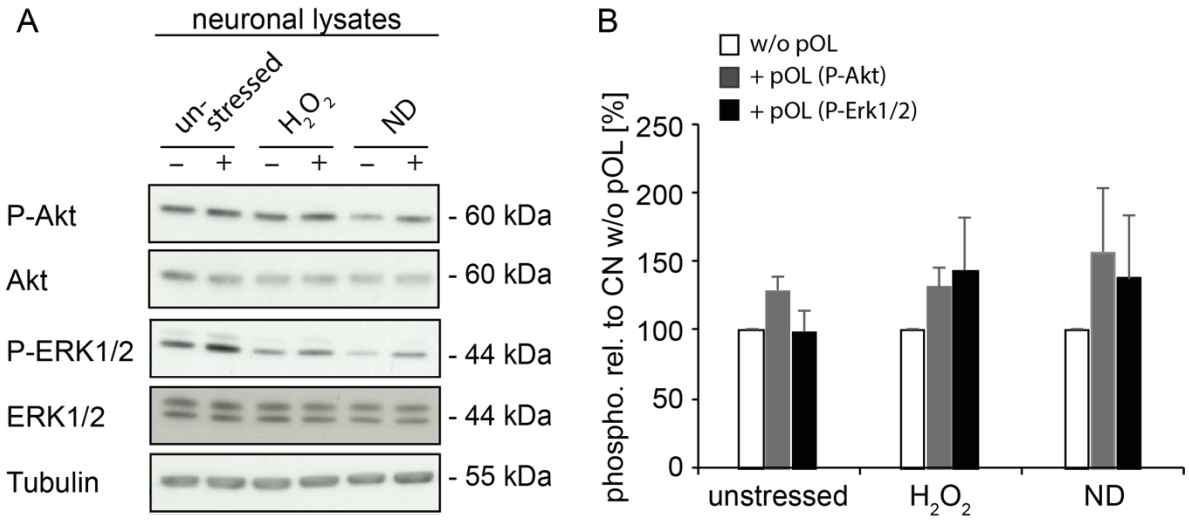

Figure 4-9 Exosome signalling in recipient neurons under stress conditions. Cortical neurons co-cultured in Boyden chambers with (+) or without (–) oligodendrocytes for 48 h were subjected to oxidative stress (25µM H2O2 for 1 h before lysis) or nutrient deprivation (ND, depletion of B27 supplement during co-culture) followed by Western blot analysis compared to unstressed cells. (B) Relative P-Akt and P-Erk1/2 levels in neurons are expressed in relation to control cells (–) of each condition to selectively visualize exosome-dependent kinase-activation (n = 5). Error bars, SEM.

Control neurons were cultured in the absence of OL, but in OL-conditioned culture supernatant depleted of exosomes. Neurons challenged with either stress exhibit a tendential activation of Akt and Erk1/2, which could not be statistically confirmed (Figure 4-9B). These results may suggest that stimulation of Akt and Erk signalling pathways might play a role in exosome-dependent neuroprotection.

4.5 Oligodendroglial Exosomes Facilitate Axonal Transport under Oxidative Stress and Starvation Stress

Axonal maintenance depends on axonal transport and a hallmark of neurodegenerative diseases is an impaired axonal transport (Morfini et al., 2009). Initial experiments clearly showed a beneficial impact of oligodendroglial exosomes on neuronal physiology (Frohlich et al., 2014; Fruhbeis et al., 2013a). Hence, we next investigated the effect of oligodendroglial exosomes on axonal transport. Microtubule tracks within an axon possess a specific polarity orientation in the axoplasm for a given direction of transport (Heidemann et al., 1981). The fast-growing distal (plus) end points toward the synapse, while the slow-growing proximal (minus) end points toward the cell body (Figure 4-10 A). The motor engines that power axonal transport on microtubules are proteins belonging to the kinesin and cytoplasmic dynein superfamilies. Kinesins are generally plus-end-directed motor proteins that transport cargoes anterogradely towards the synapse and cytoplasmic dyneins are minus-end-directed motor proteins that transport cargoes retrogradely towards the cell body. Here, we examined the axonal transport of vesicles positive for brain-derived neurotrophic factor (BDNF), which displays the characteristic features of a fast axonal transport (FAT)-dependent cargo and retains BDNF functions (Kwinter et al., 2009). Vesicular dynamics in primary hippocampal neurons (DIV 2-3) expressing BDNF-mCherry were recorded on videomicroscopy dishes (Figure 4-10 B). Images were taken every 3 seconds with a total of 200 frames (frame/3 seconds). Transport of BDNF-positive vesicles was analysed by generating kymographs from the video recordings (Figure 4-10 C). Kymographs graphically represent the spatial position of BDNF-mCherry-positive vesicles in the axoplasm over the time allowing the tracking of single trajectories. Neurons were exposed to exosomes for 30 min before video microscopy. Exosomes were previously collected from primary OL secreted over 48 h and purified by ultracentrifugation at 100000 x g. Control neurons were treated with PBS.

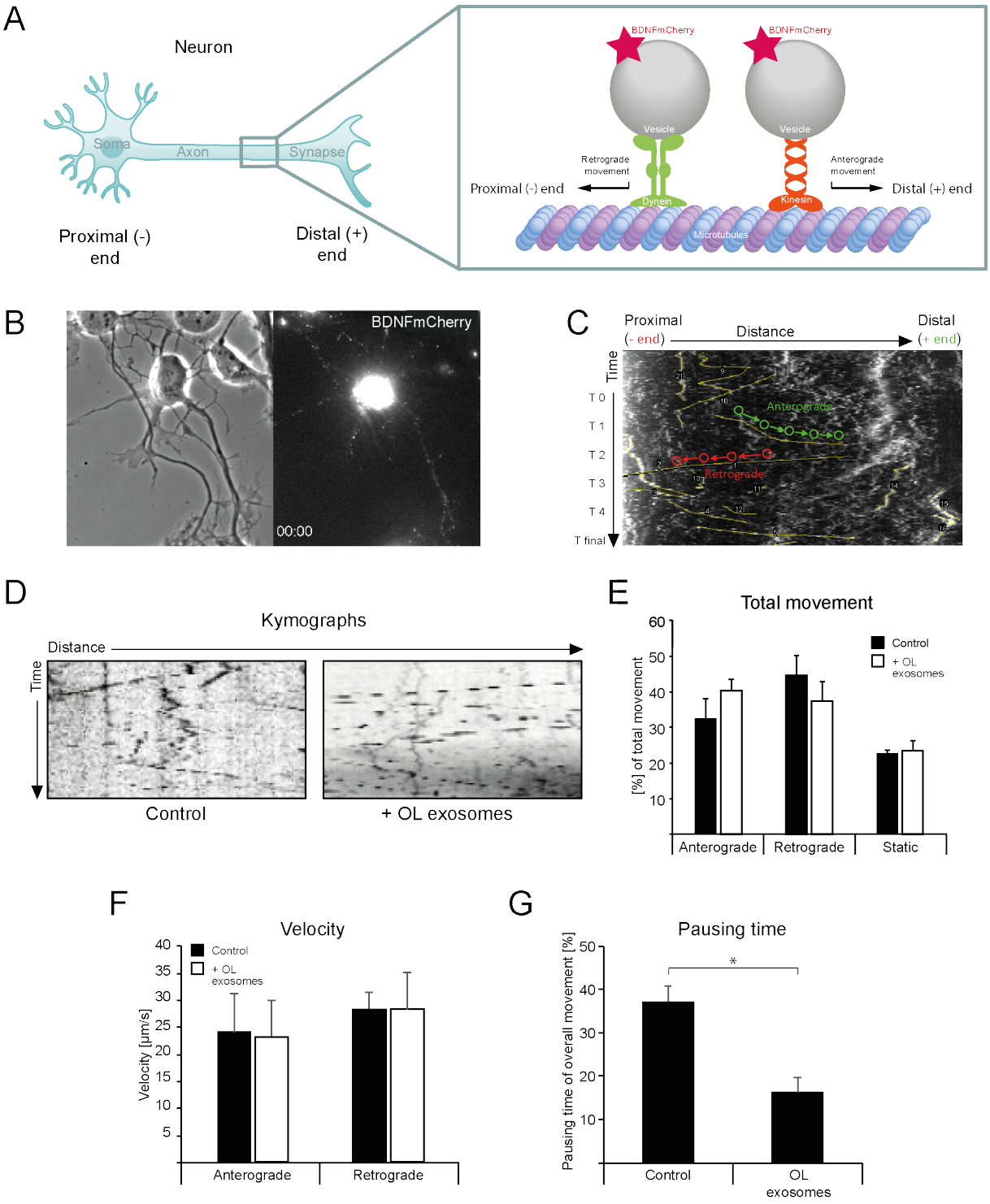

Figure 4-10 Impact of oligodendroglial exosomes on axonal transport. (A) Schematic illustration of vesicular BDNFmCherry transport along microtubules in axons. Retrograde transport towards the proximal (-) end (soma) is driven by dynein, anterograde transport towards the distal (+) end (synapse) is driven by kinesin. (B) Time-lapse imaging of BDNFmCherry-expressing hippocampal neurons. (C) Kymograph graphically representing the spatial position of BDNFmCherry-positive vesicles in axons over time. (D) Representative kymographs generated from neurons exposed to purified oligodendroglial exosomes (OL exosomes) for 30 min or PBS (control), respectively, before imaging (n = 21; n represents single neurons). (E-G) Kymograph-analysis of the total movement, velocity, and pausing time of BDNFmCherry-positive vesicles. Error bars depict SEM based on 3 independent experiments (*$p < 0.05$; Student's t-test with Bonferroni post-test).

Subsequently, we analysed BDNF vesicle dynamics by means of kymographs generated from control and exosome-treated neurons (**Figure 4-10** D) for total movement, velocity, and pausing time (Figure 4-10 E, F, G). The total movement displaying the percentage of anterogradely and retrogradely moving vesicles, as well as static vesicles, exhibit similar distribution profiles in both conditions (**Figure 4-10** E). Analysis of vesicle dynamics revealed anterograde and retrograde movements at velocities similar to those previously reported (Colin et al., 2008) indicating no alterations upon exosome treatment (**Figure 4-10** F). Interestingly, incubation with oligodendroglial exosomes significantly decreased the pausing time by 9.3 ± 1.8 % (**Figure 4-10** G), which depicts the percentage of pauses exhibited by every single vesicle during its total trajectory. Taken together, exosomes promoted axonal transport by reducing vesicle pausing time, without changing anterograde or retrograde movement or the pool of static vesicles.

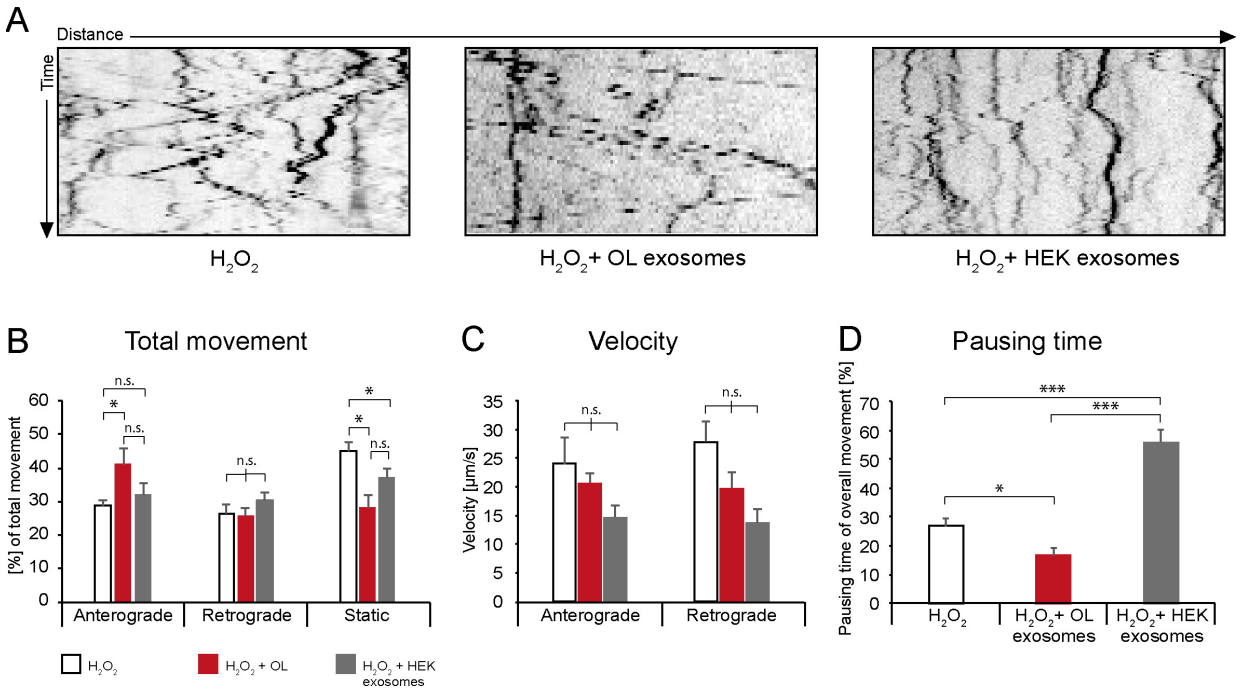

Figure 4-11 Oligodendroglial exosomes facilitate axonal transport under oxidative stress. (A) Representative kymographs generated from BDNFmCherry-expressing hippocampal neurons treated with PBS, exosomes derived from OL or HEK cells for 12 h before oxidative stress exposure (15 µM H_2O_2, 1 h). (B-D) Analysis of kymographs in (A) (n = 18; n represents single neurons). Error bars depict SEM based on 3 independent experiments (*p < 0.05; ***p < 0.001; Student's t-test with Bonferroni post-test).

We further studied axonal transport under stress conditions. Primary hippocampal neurons (DIV 2-3) transiently expressing BDNF-mCherry were incubated with exosomes isolated from

conditioned oligodendroglial culture supernatant by ultracentrifugation or PBS (control) for 12 h. In addition, one experimental group of neurons has been treated with HEK293T-derived exosomes assessing cell type specificity. Subsequently, neurons were challenged by oxidative stress via the application of 15 µM H_2O_2 for 1 h prior to video microscopy recordings. Analysis of kymographs (**Figure 4-11** A) revealed a significant increase of anterograde movement upon treatment with oligodendroglial exosomes by 12.6 ± 4.5 % and 9.2 ± 3.5 % compared to control and HEK293T-exosome-treated neurons, respectively (Figure 4-11 B). Concomitantly, we recorded a significant reduction of static vesicles compared to control and HEK293T-exosome-treated neurons by 17.1 ± 4.1 % and 9.3 ± 4.1 %, respectively. While the analysis of velocity exhibited only minor alterations, we observed a clear decline of the pausing time upon oligodendroglial exosome treatment to 15.2 ± 3.1 % (Figure 4-11 D). Next, we examined the vesicle dynamics in the axoplasm under nutrient deprivation by culturing neurons in culture medium depleted of B27-supplement. Primary hippocampal neurons (2 – 3 DIV) were either grown in full culture medium containing B27-supplement (unstressed), nutrient deprived culture medium (ND), or nutrient deprived medium containing oligodendroglial exosomes for 3 h prior video microscopy. Exosome-treated neurons were additionally pre-treated with OL-conditioned medium containing exosomes for 12 h before starvation stress exposure. According to the analysis of the kymographs (**Figure 4-12** A), a significant shift to anterograde movement of 18 ± 0.04 % as well as a decreased number of static vesicles by 30.9 ± 0.07 % was detected upon exosome treatment compared to untreated starving neurons (**Figure 4-12** B). While the velocity was unaffected, exosomes significantly decreased the pausing periods in starving neurons by 30 ± 0.09 % compared to control neurons (**Figure 4-12** D).

In summary, oligodendroglial exosomes affect BDNF vesicle dynamics under oxidative stress and starvation conditions by shifting total vesicle movement anterogradely and decreasing the pausing period during vesicle movement.

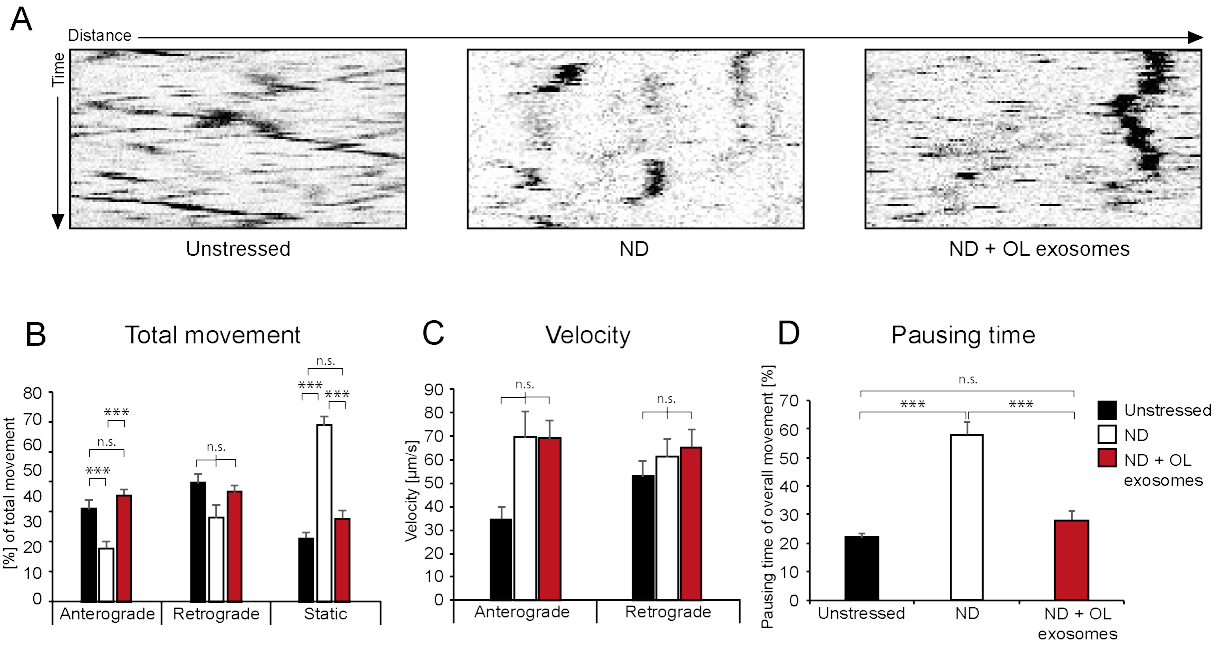

Figure 4-12 Oligodendroglial exosomes facilitate axonal transport under starvation stress. (A) Representative kymographs generated from BDNFmCherry-expressing hippocampal neurons exposed to starvation stress for 3 h before imaging. Neurons were either grown in complete medium (unstressed), nutrient-deprived OL-conditioned medium excluding exosomes (ND) or including exosomes (ND + OL exosomes). (B-D) Analysis of kymographs in (A) (n = 21; n represents single neurons). Error bars depict SEM based on 3 independent experiments (*p < 0.05; **p < 0.01; ***p < 0.001; Student's t-test with Bonferroni post-test).

4.6 Mutant Oligodendrocytes do not Mediate Neuroprotection

Proteomics data from oligodendroglial exosomes revealed a list of candidates with neurotrophic potential as well as the major myelin proteins PLP and CNP (Krämer-Albers et al., 2007). A functional deletion of either protein in mice results in axonal degeneration suggesting an essential role of both proteins in brain function (Griffiths et al., 1998; Lappe-Siefke et al., 2003). Initial investigations demonstrate that exosome levels in PLP^{null}- and CNP^{null} oligodendrocytes are significantly reduced compared to wildtype (WT) oligodendrocytes. Furthermore, proteomic analysis clearly shows an altered protein composition in PLP^{null}- and CNP^{null} oligodendrocytes compared to WT-derived exosomes (data unpublished).

Here, we examined the functional role of exosomes derived from mutant oligodendrocytes on neuronal physiology and addressed the question whether these exosomes are capable of facilitating neuroprotection.

4.6.1 PLP^{null}- and CNP^{null}-Exosomes do not Support Neurons under Starvation Stress

In a first set of experiments, neurons co-cultured with OL in Boyden chambers were assessed (see sections 4.3.1 and 4.3.2). Briefly, primary cortical neurons (5-7 DIV) were co-cultured with primary OL (6 DIV) derived from WT, CNP^{null}, and PLP^{null} mice under optimized, oxidative stress, or starvation conditions. Subsequent subjection of neurons to MTT assay confirmed the previously reported neuroprotective effect of WT exosomes. However, results exhibited a high degree of variability (data not shown). To facilitate reproducibility of experimental conditions, supernatants from starving WT and mutant OL cultures were collected after 48 h and depleted from bigger particles but exosomes (10000 x g supernatant) before being applied to neuronal cultures. The amount of exosomes used was deduced from the same number of OL in each case. In another condition, cells received OL-conditioned medium depleted of exosomes. Neurons were exposed to starvation for 12 – 15 h before being subjected to MTT assay.

Compared to neurons grown in complete medium containing B27-supplement, starvation stress significantly reduced neuronal metabolic activity by 52 ± 2.3 %. As expected, this stress effect was abolished when neurons were concomitantly exposed to exosomes derived from WT OL confirming the neuroprotective feature of oligodendroglial exosomes. WT exosomes enhanced stress tolerance by 58.4 ± 10.6 % compared to stressed but untreated neurons. Consistently, starving neurons treated with OL-conditioned medium lacking exosomes did not receive stress support. Intriguingly, treatment with exosomes derived from CNP^{null}- and PLP^{null}-oligodendrocytes did not increase neuronal viability under starvation stress indicating that mutant exosomes have lost their stress protective properties (Figure 4-13).

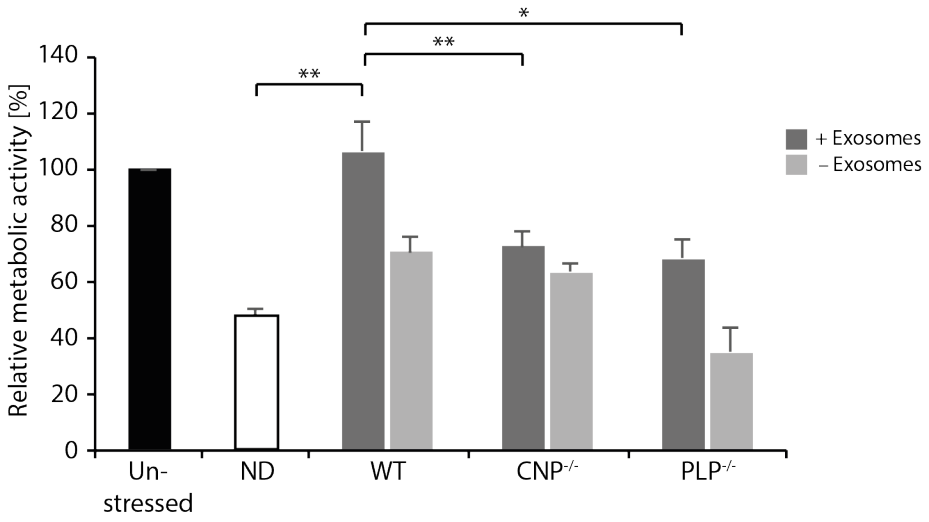

Figure 4-13 PLP$^{-/-}$ and CNP$^{-/-}$ exosomes do not protect neurons from starvation stress. Primary cortical neurons were cultured with conditioned starvation medium (10000 x g supernatant) derived from wildtype (WT), CNP knockout (CNP$^{-/-}$), and PLP knockout (PLP$^{-/-}$) oligodendrocytes, respectively, for 12 - 15 h (n = 5). Culture supernatant contained exosomes (n = 5) or was deprived of exosomes (n = 3). Metabolic activity was subsequently determined by MTT assay. Error bars, SEM (n.s., not significant; *p < 0.05; Wilcoxon-Test).

4.6.2 Neuroprotective Effect of Oligodendroglial Exosomes: A Matter of Quality or Quantity?

The finding that mutant exosomes fail to protect neurons from starvation stress, raises the question if diminished amount of secreted exosomes or the altered exosomal content causes the observed effects. Thus, is the deficiency in neuroprotection of mutant exosomes a matter of quantity or quality? To explore this question, we treated starving primary cortical neurons (0.35 x 10^6 neurons, DIV 5) with descending concentrations of exosomes derived from wildtype oligodendrocytes whereby 100 % is equivalent to the amount of exosomes contained in 1 ml of 10.000 x g supernatant secreted from 0.75 x 10^6 wildtype oligodendrocytes over 48 h. Figure 4-14 depicts the relative metabolic activity of starving neurons exposed to 100, 75, 50, 25, 10, and 0 % exosomes, respectively, whereas dilutions were prepared using oligodendrocyte-conditioned culture medium deprived from exosomes. Thus, 0 % exosomes implies oligodendrocyte-conditioned medium fully depleted of exosomes. Interestingly, the gradual reduction of exosomes did not result in a gradual decrease of neuronal metabolic activity.

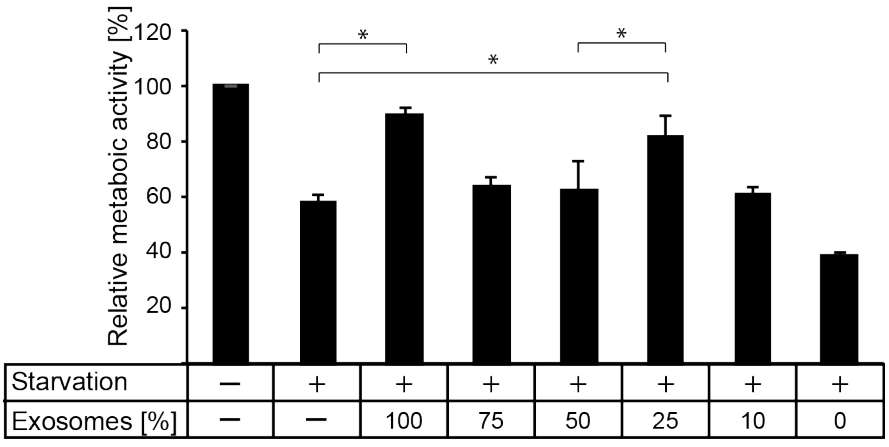

Figure 4-14 Dose-dependent effect of exosomes on neuronal metabolism. Primary cortical neurons were cultured in nutrient deprived medium supplied with different concentrations of oligodendroglial exosomes based on the amount of exosomes obtained from 0.75 x 10^6 oligodendrocytes (=100 %) (n = 6). Subsequent MTT assay determined neuronal metabolic activity. Error bars, SEM (*p < 0.05; ***p < 0.001; Student's t-Test).

Instead, we observe a diminished activity almost to the level of starving control neurons, which contradicts a quantitative effect. It might be reasonably assumed that the trophic effect of exosomes follows the principle of all-or-nothing. However, 25 % of exosomes was inexplicably sufficient to elicit a higher tolerance towards starvation stress, which was not the case when neurons received 75 % and 50 %. These results conclude that titration of exosomes by dilution does not reflect a dose response curve of exosome activity.

Next, we concentrated exosomes from oligodendrocyte-conditioned medium to a smaller volume by ultrafiltration. 10000 x g supernatant was transferred to an Amicon ultrafiltration tube containing a cellulose membrane that retains molecules bigger than 100 kDa including exosomes, while allowing smaller molecules and liquids to pass and accumulate in the flow-through. Exosomes were isolated from different starting volumes of culture supernatant containing exosomes (17.5 ml, 8.75 ml, 4.4 ml, and 2.2 ml), whereby 1 ml equates the amount of secreted exosomes by 0.75 x 10^6 oligodendrocytes (**Figure 4-15** A, B). Nanoparticle tracking analysis (NTA) and western blot analysis revealed the accumulation of isolated exosomes. A minimal concentration of exosomes was detected in the flow-through (FT). Subsequently, we performed a starvation stress experiment by treating primary cortical neurons (5 DIV) with differently concentrated exosomes (**Figure 4-15** C). The number of exosomes was adjusted by NTA, whereas the amount of exosomes present in 100 % exosomes refers to the amount contained in unprocessed 10000 x g culture supernatant derived from 0.75 x 10^6 primary oligodendrocytes. However, the degree of survival effect was lower than observed before upon incubation with oligodendrocyte-derived culture supernatant containing unprocessed exosomes not subjected to ultrafiltration. This effect did not rise by the treatment with doubled amount of exosomes, but has been exacerbated when neurons received the same amount of exosomes, which had been previously processed by ultrafiltration. Furthermore, conditioned medium obtained from ultrafiltration flow-through excluding exosomes dramatically shut down metabolic activity. Nevertheless, we used exosomes concentrated by this means for our next approach to allow titration of exosomes to wildtype levels. We exposed neurons to the same number of exosomes derived from each genotype under nutrient deprived conditions. The number of particles used was determined by NTA and normalized between wildtype and mutants (Figure 4-16 A). According to previous experiments, primary cortical neurons (DIV 5) were grown in starvation medium lacking B27 supplement and supplied with a defined number

of exosomes derived from wildtype, CNP^{null}, and PLP^{null} oligodendrocytes, respectively. Untreated starving neurons received medium depleted from exosomes. After 15 h of starvation stress, neurons were subjected to MTT assay to measure cell viability. Intriguingly, the application of an increased amount of mutant-derived exosomes compared to WT exosomes was not sufficient to ameliorate stress tolerance (Figure 4-16 B).

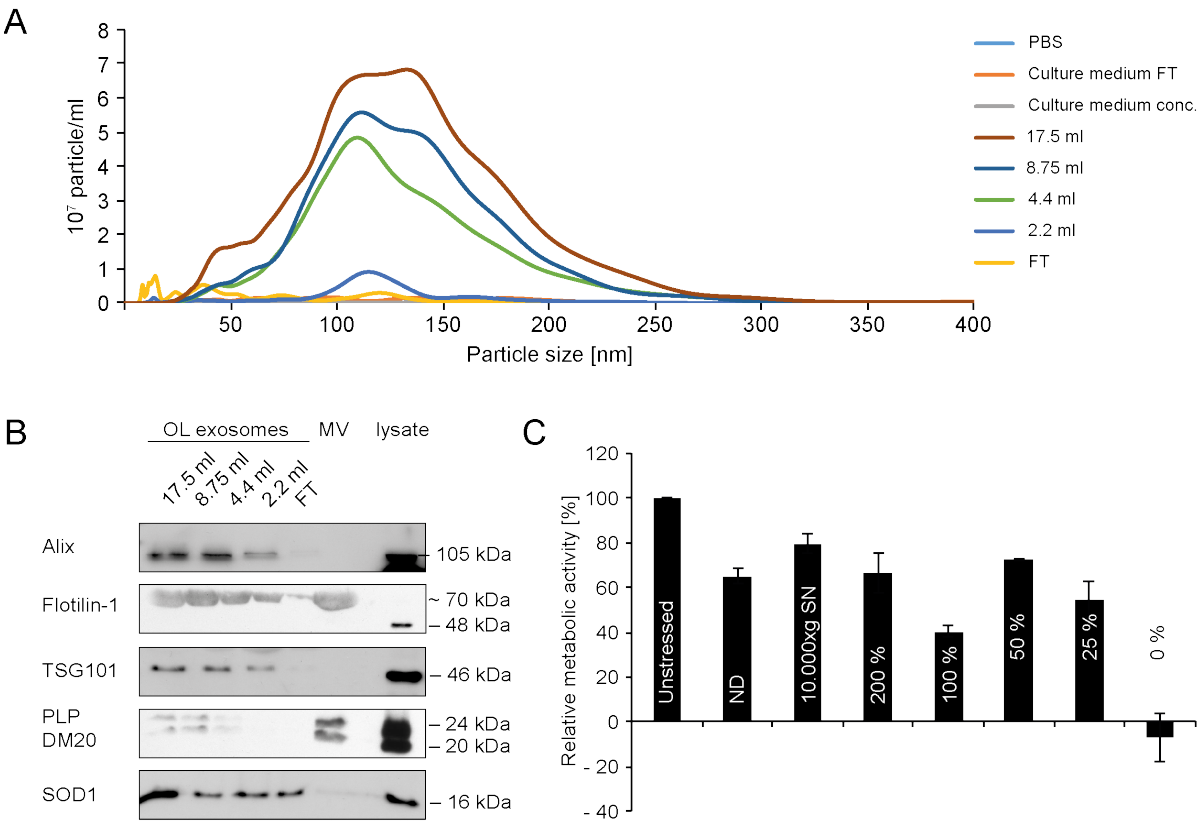

Figure 4-15 Characterization of exosomes purified by ultrafiltration. (A) Qualitative analysis of exosomes obtained from ultrafiltrated oligodendrocyte culture supernatant of different volumes (17.5 ml, 8.75 ml, 4.4 ml, and 2.2 ml). Measurements of the flown through medium (FT) as well as concentrated fresh culture medium show a very low particle background. (B) Western blot analysis of samples analysed in (A) confirming the presence of exosomes by characteristic exosome markers. (C) Starvation stress paradigm using ultrafiltrated exosomes of different concentration compared to unprocessed supernatant (10.000 x g SN) to treat cortical neurons (n = 3). 100 % corresponds to the amount of exosomes contained in the unprocessed culture supernatant released from 0.75 x 10^6 oligodendrocytes in 1 ml of culture supernatant during 48 h, whereas 0 % represents the flow-through obtained after ultrafiltration. Unstressed neurons were grown in full medium, whereas all other culture conditions lack B27 supplement. Neuronal metabolic activity was determined by MTT assay. Error bars, SEM.

In summary, these results indicate that the lack of support from mutant oligodendrocytes might not only arise from the reduced exosome secretion but rather from the altered exosomal content.

A

	Particle/ml [mean value]	Conc. factor [mean value]	Adjusted no. of particles	Particle/neuron
Wildtype	4.4 x 10^8	37 x	2.6 x 10^8	743
CNP$^{-/-}$	1.9 x 10^8	79 x		
PLP$^{-/-}$	2.1 x 10^8	60 x		

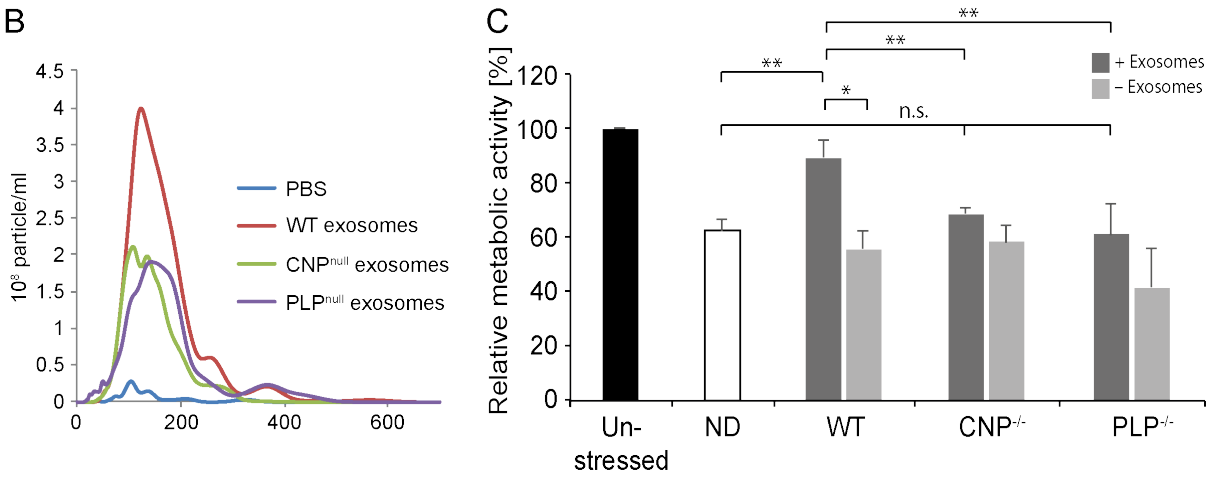

Figure 4-16 CNP^{null} and PLP^{null} exosomes do not mediate neuroprotection. (A, B) Quantitative evaluation of exosomes obtained from wildtype, CNP$^{-/-}$, and PLP$^{-/-}$ oligodendrocytes by NTA. (B) Neurons were supplied with same amounts of exosomes derived from wildtype, CNP$^{-/-}$, and PLP$^{-/-}$ oligodendrocytes during a 12 – 15 h starvation stress exposure (ND) compared to unstressed neurons (n= 6; n depicts biological independent neurons). MTT assay revealed neuronal viability. Error bars, SEM (n.s., not significant; *p < 0.05; **p < 0.01; Student's t-Test).

4.7 PLP^{null}- and CNP^{null}-Exosomes do not Facilitate Axonal Transport under Starvation Stress

We have provided evidence that WT-derived oligodendroglial exosomes influence axonal transport by promoting anterograde movement and simultaneously impeding the emergence of static vesicles. Reduction of the pausing time during vesicular trajectories might also facilitate axonal transport. Furthermore, we showed that exosomes derived from mutant OL do not share the neurosupportive features of WT exosomes. Both mutant genotypes exhibit perturbations in axonal transport resulting in the generation of axonal swellings (Edgar et al., 2004; Griffiths et al., 1998). We therefore addressed the question whether exosomes derived from CNP and PLP knockout OL influence axonal vesicle dynamics. In order to clarify these issues, we investigated the impact of exosomes derived from CNP^{null}- and PLP^{null}- OL on axonal transport. Considering cell specificity, we additionally examined the axoplasmic vesicle motion depending on exosomes derived from primary astrocytes.

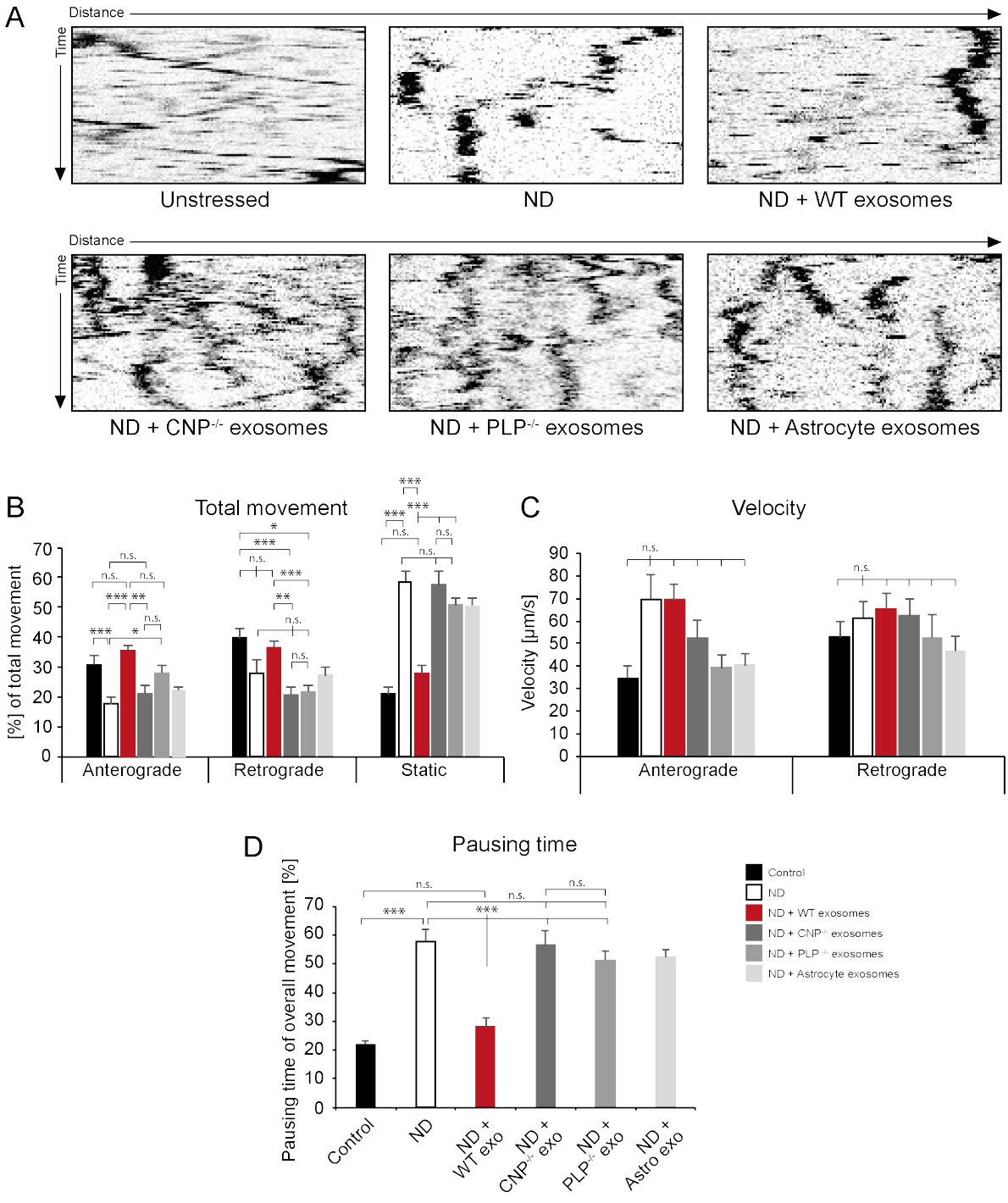

Figure 4-17 PLP^{null}- and CNP^{null}-derived exosomes do not affect axonal transport. (A) Kymographs generated from BDNFmCherry-expressing hippocampal neurons exposed to exosomes derived from WT (n = 21), CNP^{null} (n = 25), and PLP^{null} (n = 21) oligodendrocytes as well as astrocytes (n = 14) during starvation stress of 3 h. Exosome-treated neurons were pre-treated with respective conditioned full medium containing exosomes for 12 h. Control neurons (n = 21) were cultured in full medium unlike starving controls (ND, n = 20). Subsequently, neurons were subjected to time-lapse imaging for analysis. Evaluation of kymographs reveal the distribution of total movement (B), velocity (C), and pausing time (D) of BDNFmCherry positive vesicles transported along the axon. Error bars depict SEM based on 3 (control, ND, WT, CNP^{null}, and PLP^{null}) or 2 (astrocyte) independent experiments (n.s., not significant; *p < 0.05; **p < 0.01; ***p < 0.001; Student's t-Test with Bonferroni post-test).

Exosomes derived from WT-, CNP^{null}-, and PLP^{null}-OL as well as astrocytes were collected over 48 h in full medium or B27-supplement depleted medium. Exosome-treated neurons were pre-treated with OL-conditioned medium containing exosomes for 12 h before starvation stress exposure. The starvation stress was initiated by the exchange of full culture medium with conditioned nutrient deprived medium without B27-supplement for the duration of 3 h. Subsequently, BDNF vesicle motion was recorded by video microscopy. Figure 4-17 A depicts kymographs representing the trajectories of BDNFmCherry-positive vesicles in neurons grown under optimal conditions compared to starving neurons (ND), which received exosomes derived from the respective cell type. Evaluation of kymographs demonstrates a significant shift towards anterograde and retrograde movement upon treatment with WT exosomes whereas treatment with mutant or astrocytic exosomes had only minor effects (Figure 4-17 B). We observed a significant increase of anterogradely moving vesicles by 14.3 ± 0.03 % compared to neurons supplied with exosomes lacking CNP, but no significant difference compared to neurons exposed to PLP lacking exosomes. Retrograde movement was significantly increased by 16 ± 0.02 % and 15.1 ± 0.02 % in WT exosomes treated neurons compared to neurons treated with CNP- and PLP-knockout derived exosomes, respectively. Strikingly, WT exosomes compared to those derived from mutants or astrocytes significantly reduced the percentage of static vesicles to the level observed in unstressed neurons. While no significant differences in velocity could be reported, a significant reduction of the pausing time could be obtained upon treatment with WT exosome, but not with mutant exosomes (Figure 4-17 C, D). These results allow the conclusion that WT exosomes facilitate axonal transport almost to the level of unstressed neurons, while there were no significant alterations upon treatment with mutant or astrocytic exosomes providing further evidence that oligodendroglia exosomes contribute to the trophic support for neurons.

5 Discussion

The intimate cell-cell interaction between axon and glial cells is an evolutionary conserved mechanism of trophic support for neurons. Our group has recently provided the evidence for the functional transfer of exosomal cargo from oligodendrocytes to neurons (Fruhbeis et al., 2013a). We suggest that this mechanism represents an "on demand" support as exosome release is linked to neuronal electrical activity. The present study investigates the functional impact of oligodendroglial exosomes on neuronal physiology. Exosomes support neurons to combat different stress conditions as shown by co-culture experiments and direct exosome treatment possibly due to the transfer of stress protective proteins. This neuroprotective effect is accompanied by the activation of kinases, which are involved in pro-survival signalling pathways. Moreover, oligodendroglial exosomes promoted axonal transport indicating a role in axonal maintenance. Intriguingly, the boosting effect appears to be cell-specific as exosomes derived from other cell types or genotypes, such as HEK293T cells and astrocytes or CNP^{null} and PLP^{null} oligodendrocytes, malfunctioned.

This study adds a new component to the present model of metabolic support (delivery of energy rich metabolites such as lactate) involving the transfer of stress-protective molecules via exosomes and an alteration of neuronal signalling pathways.

5.1 Characterization of High-purity OL Cultures to Study OL Exosomes

Analysis of cell-type specific exosomal functions is highly dependent on the purity of the secreting cultures. To study the role of exosomes derived from mature oligodendrocytes, we utilized a novel isolation method based on magnetic bead separation to achieve a higher purity of oligodendrocytes. Primary oligodendrocytes were formerly obtained from embryonic brains (E14 – 15) followed by a cultivating period of 14 days and removal of neurons by immunocytolysis finally mechanical dissociation from mixed neural cultures (Trotter and Schachner, 1989). Although enriched in oligodendrocytes, primary cultures also contained contaminating cell types due to the mechanical impact. Consequently, functional analysis may not be unique to oligodendroglial exsosomes, since exosomes derived from other neural cells may differently impact neuronal physiology (Fruhbeis et al., 2013b). The isolation of

oligodendrocytes using O4 antibodies coupled to magnetic beads allowed a specific and gentle pull-down of mature oligodendrocytes from total brain suspension of postnatal mice (P7) with only a minor fraction of contaminating cells. Compared to the previously used isolation technique, oligodendrocytes obtained from the magnetic bead-based purification can be used for experimental purposes after a few hours. The presence of the myelin proteins PLP/DM20 and MBP indicates a proper differentiation state of the cells and contamination of neurons, astrocytes and microglia could be reduced to a minimum. Furthermore, magnetic bead-based cell sorting provides a more homogenous cell population that secretes exosomes with reproducible characteristics and properties. Profile of secreted exosomes contain characteristic marker proteins such as PLP, flotillin, and Hsp70, allowing their usage for the analysis of oligodendrocyte-specific influences on neuronal physiology.

5.2 Exosomes Ameliorate Cellular Stress Tolerance in Neurons

Glial support of neuronal cells is a conserved feature of vertebrate and invertebrate nervous systems. Neuronal support by oligodendrocytes has been discovered in mice deficient in the myelin proteins PLP and CNP. A common characteristic of these mice is a secondary axonal degeneration phenotype despite the presence of morphologically normal myelin (Griffiths et al., 1998; Lappe-Siefke et al., 2003). Also subsequent investigations provided evidence of neuronal support by oligodendroglial lactate, but linkage of this lactate supply to the lack of PLP and CNP in these mutant mice remains elusive (Fünfschilling et al., 2012). Mitochondrial disorders generate axonal transport defects reminiscent to those in PLP null mice suggesting that oligodendrocytes require PLP to support the axonal energy metabolism (Edgar et al., 2004; Ferreirinha et al., 2004; Saab et al., 2013; Tarrade et al., 2006). Oligodendroglial exosomes carry both, PLP and CNP, as well as a range of beneficial enzymes, potentially supporting myelinated axons. Coupling of exosome transfer to axonal electrical activity would link this “on demand” process to neuronal needs (Fruhbeis et al., 2013a). Indeed, oligodendroglial exosomes support the neuronal metabolism and increase neuronal viability under conditions of oxidative stress and starvation by about 30 %. However, oligodendroglial exosomes are not sufficient to rescue damaged neurons.

Bioactivity of exosomes seems to be influenced by the isolation method used *per se*, since the osmotic characteristic of sucrose diminishes the neuroprotective feature of exosomes during oxidative stress. Furthermore, ultracentrifugation provokes exosomal alterations that influence their protective properties at least needed by starving neurons. Exosomal alterations probably imply exosome aggregation impeding effective internalization by neurons but may still be able to activate signalling via surface receptor binding as neurons exposed to 'crude' exosomes prior to oxidative stress exhibit increased viability. Alleviation of stress tolerance towards starvation may require a combination of both exosomes and co-factors as conditioned medium depleted from exosomes was ineffective. Readdition of isolated exosomes was also ineffective, which might be explained by the inactivating impact of the isolation method *per se*.

Further evidence for the beneficial function of oligodendroglial exosomes on neuronal cells was examined during OGD, a well-established *in vitro* model of cerebral ischaemia (Goldberg and Choi, 1993). Neuronal cell death during brain ischemia is accompanied by elevated levels of extracellular glutamate (De Cristobal et al., 2002; Goldberg and Choi, 1993).Given that exosome secretion in mature oligodendrocytes is triggered by glutamate (Fruhbeis et al., 2013a), this might represent a protective mechanism to prevent neuronal cell death during stroke, mitigating the ischaemic insult. Same has recently been described for astrocyte-derived exosomes (Guitart et al., 2016). Astrocytes exposed to oxidative and ischemic stress shuttle exosomes with an enhanced level of PrP and neuroprotective factors to neurons mediating neuroprotection. Compositional alterations of exosomal cargo may also occur upon stress in oligodendrocytes and could explain the ineffectiveness of treating OGD-exposed neurons with exosomes derived from oligodendrocytes cultured under normoxic conditions. However, this again might also be due to the isolation method. Repetition of this experiment using conditioned medium containing exosomes would provide clarification. Mast cells have also been described to comprise a different mRNA pattern upon oxidative stress resulting in increased stress tolerance in recipient cells (Eldh et al., 2010). Our observations fit into a general theme of exosomal support during cellular stress conditions.

5.3 Oligodendrocytes Shuttle Stress-protective Cargo to Neurons via Exosomes

Oxidative stress is putatively involved in many neurodegenerative disorders demonstrating that neurons are particularly vulnerable to increased levels of reactive oxygen species (ROS), which

might be explained by their reduced capacity to detoxify ROS (Dringen et al., 2005). Oligodendroglial exosomes carry multiple enzymes with functions in metabolism or oxidative stress relieve suggesting the potential contribution of several components in supporting neurons (Krämer-Albers et al., 2007). Putative candidates present in oligodendroglial exosomes comprise Hsc/Hsp70 as well as SOD1 and catalase (Figure 5-1) (Frohlich et al., 2014; Fruhbeis et al., 2013a). Hsc70 is a chaperone of the Hsp family that is essentially involved in cellular processes such as proofreading and the repair of misfolded conformers (Mayer and Bukau, 2005). Due to its protective function, proteins of the Hsp70 family are indispensable for cell viability. Transfer of Hsps has been observed between various cell types including neuron-glia in squid, indicating an evolutionary conserved mode of protection (Tytell et al., 1986; Tytell et al., 2016). Furthermore, astrocytes also release exosomes in association with Hsp70 as well as the wild-type and mutant form of SOD1 (Basso et al., 2013; Gomes et al., 2007; Taylor et al., 2007). SOD1 binds copper and zinc ion and destroys harmful free superoxide radicals by converting them to oxygen and hydrogen peroxide (Zelko et al., 2002). Uptake and increased expression of SOD1 has been shown to relieve starvation stress in neurons (Matthews et al., 2000; Saez et al., 1987). Catalase, another vital protein, protects cells against toxicity of ROS as it catalyzes the decomposition of hydrogen peroxide to less reactive water and oxygen (Chelikani et al., 2004). Similarly, vesicular transfer of supportive cargo to axons has also been demonstrated for Schwann cells in the PNS facilitating regeneration of axons after injury (Lopez-Verrilli and Court, 2012; Lopez-Verrilli et al., 2013).

Oligodendroglial exosomes might also benefit neuronal survival by reprogramming neuronal gene expression via the transfer of functional miRNAs or mRNAs (Montecalvo et al., 2012; Umezu et al., 2013; Valadi et al., 2007). For example, exosomes derived from breast cancer cells contain miR-122, which inhibits glycolysis in target non-cancerous cells to meet their own needs of glucose consumption known as the Warburg effect (Brahimi-Horn et al., 2007; Fong et al., 2015; Gatenby and Gillies, 2004). We have found miR-122 in oligodendroglial exosomes (data unpublished), which would support the model of axon-oligodendrocyte metabolic coupling suggesting a metabolic switch of oligodendrocytes to supply neurons with lactate derived from glycolysis (Fünfschilling et al., 2012; Lee et al., 2012b). Simultanously, exosomes may complement the energy supply by delivering neurosupportive molecules to neurons.

In summary, the exosomal cargo of oligodendrocytes comprises stress-protective proteins as well as mRNAs and miRNAs, which could potentially intervene neuronal physiology on different levels to support neuroprotection.

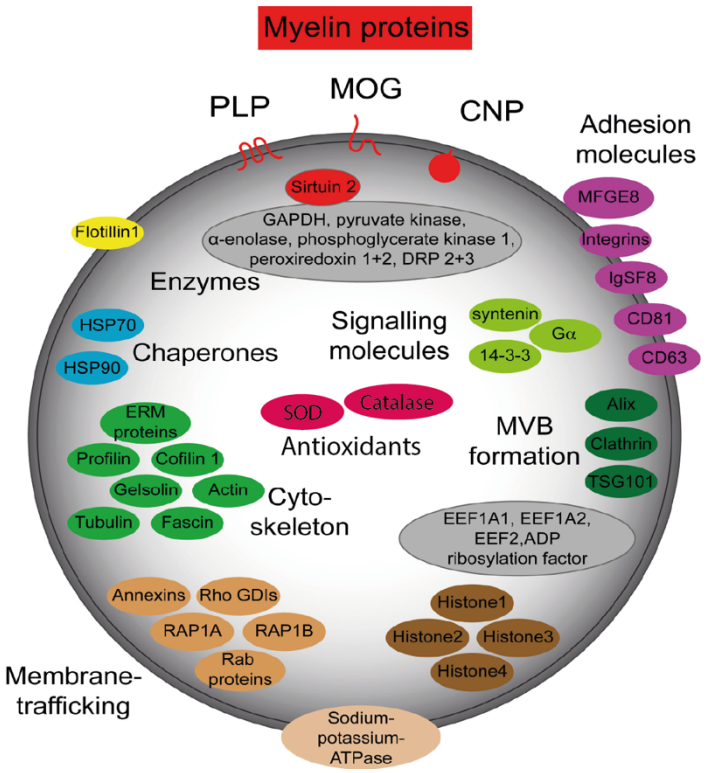

Figure 5-1 Composition of oligodendroglial exosomes. Modified from (Frühbeis et al., 2012).

5.4 Exosomes Activate Pro-Survival Signalling Pathways in Neurons

To examine the underlying pro-survival signalling pathways of the neuroprotective oligodendroglial exosomes, we performed a kinase screen in the target neurons upon treatment with oligodendroglial exosomes under normal as well as stress conditions. While unstressed neurons showed only minor changes, oligodendroglial exosomes induced the activation of Akt and Erk1/2 upon the exposure of oxidative stress. Both kinases have generally been implicated in promoting survival in various cellular systems (Atwal et al., 2000; Dudek et al., 1997; Jin et al., 2002; Kennedy et al., 1997). In a similar approach it has been shown that MSC-derived exosomes enhance cardiac function after myocardial injury via Akt phosphorylation (Arslan et al., 2013).

Furthermore, CREB, GSK3-α/ß, GSK-3ß and JNK were phosphorylated in response to oligodendroglial exosomes. The transcription factor CREB is ubiquitously expressed in the CNS promoting cell survival in addition to controlling neuronal plasticity and memory formation

(Kandel, 2012; Sakamoto et al., 2011; Walton and Dragunow, 2000). Noteworthy, the Akt pathway activates CREB and downstream targets of CREB include the transcripts of BDNF and VGF, which have been identified to be regulated in neurons exposed to oligodendroglial exosomes (Du and Montminy, 1998; Frohlich et al., 2014; Lonze and Ginty, 2002; Riccio et al., 2006; Tao et al., 1998). Akt inhibits GSK3-α/ß and GSK-3ß by phosphorylation, which may further support the neuroprotective effect of oligodendroglial exosomes (Beitner-Johnson et al., 2001; Chin et al., 2005; Doble and Woodgett, 2003; Rockenstein et al., 2007).

JNKs (c-Jun N-terminal kinases) are activated upon cellular stress and execute various functions, such as axon formation, neuronal pathfinding, migration and axodendritic architecture, but are also involved in pro-apoptotic pathways (Coffey, 2014; Dhanasekaran and Reddy, 2008; Leppa and Bohmann, 1999; Oliva et al., 2006). JNK targets the transcription factor ATF-2, a member of the ATF/CREB family, which has also been suggested to be involved in neuronal survival (Kreutz et al., 1999; Oliva et al., 2006; Robinson, 1996).

Our data obtained from the kinase screen in cortical neurons revealed a potential contribution of several pathways to the neurotrophic function of oligodendroglial exosomes under stress conditions. However, insights into the cellular mechanism remains to be elucidated. Signalling pathway activation could be triggered by cell surface binding of exosomes or the delivery of bioactive molecules after endocytosis (Raposo and Stoorvogel, 2013).

5.5 Axonal Transport Dynamics are Changed in Response to Oligodendroglial Exosomes

Axonal transport is a fundamental mechanism to supply distal synapses with newly synthesized proteins and lipids and clearance of damaged or misfolded proteins. A pathological hallmark of many human neurodegenerative diseases is the aberrant accumulation of organelles and other proteins along the axon, which is responsible for subsequent axonal degeneration (De Vos et al., 2008). Many studies have linked accurate myelination to axonal transport dynamics (Edgar et al., 2004; Monsma et al., 2014; Morfini et al., 2009; Nave and Trapp, 2008). Demyelinating diseases, such as leukodystrophies, display secondary axonal degenerations emphasizing the necessity of oligodendrocytes for axonal integrity (Morfini et al., 2009; Nave, 2010a).

We have found that oligodendroglial exosomes facilitate axonal transport dynamics under stress conditions by increasing anterograde movement and decreasing the proportion of static

vesicles as well as the pausing time of vesicular BDNF transportation. BDNF is packed to Golgi-derived vesicles and subsequently transported along MTs (Thomas and Davies, 2005). Axonal transport is regulated by various signalling pathways (Pigino et al., 2009). For example, JNKs mediate kinesin-driven anterograde transport in neurons by the phosphorylation of the cargo adaptor protein JIP1 (JNK-interacting protein 1) (Bowman et al., 2000; Fu and Holzbaur, 2013; Verhey et al., 2001). Therefore, activated JNK in response to oligodendroglial exosome treatment may facilitate anterograde movement observed in exosome-treated neurons. This is further supported by the exosome-dependent inhibition of GSK-3ß. In disease, elevation of ROS levels disrupts axonal transport by inhibiting mitochondrial ATP production and activating GSK-3ß, which leads to the detachment of kinesin light chains from transported cargoes (Andersen, 2004; Morfini et al., 2004; Morfini et al., 2002). Furthermore, it has been reported that kinesin is more susceptible to oxidative stress, while dynein remains unaffected (Fang et al., 2012; Hua et al., 1997; Marino et al., 2007). CREB, another protein related to axonal transport, is also phosphorylated upon exosome treatment. Interestingly, phosphorylated CREB derives from axonally translated CREB and its retrograde transport to the cell body, a mechanism required for neuronal survival (Cox et al., 2008). Generally, local translation is critical for synaptic plasticity and axon guidance allowing distal ends of axons to respond autonomously to important stimuli (Lin and Holt, 2007; Lin and Holt, 2008; Sutton and Schuman, 2005). Hence, exosome-dependent phosphorylation of CREB might also link oligodendroglial exosomes to the activation of local translation of mRNAs in the axon. Intriguingly, oligodendroglial exosomes tendentially increase retrograde movement of vesicular transport during starvation stress, which may support the idea of exosome-mediated local translation in the axon. However, exosomes derived from mutant oligodendrocytes as well as astrocytes did not facilitate retrograde movement indicating a cell-specific effect of wildtype oligodendroglial exosomes.

Axonal transport also depends on a constant ATP supply, which is predominantly required by the motor proteins to transport cargo. Recently, identification of GAPDH coupled to the surface of axonally transported vesicles suggests an ‘on-board’ energy supply, such as ATP, for fast axonal transport (Zala et al., 2013). Mitochondria serve as a local energy source by providing ATP and their trafficking along axonal MTs is crucial for neuronal survival (Schwarz, 2013). Transport of mitochondria itself requires ATP as it depends on MT-based motors (De Vos et al., 2008; Sheng, 2014). In myelinated axons, mitochondrial transport within internodes occurs at higher velocities and slows down as they traverse to nodal regions indicating a dissimilar

distribution of metabolites along the axon (Misgeld et al., 2007). Supply of energy metabolites by glycolytic oligodendrocytes might explain this phenomenon (Fünfschilling et al., 2012; Lee et al., 2012b). Recent studies have reported that urinary exosomes are capable to aerobically synthesize ATP and microglial exosomes carry lactate, both metabolites required for neuronal survival (Bruschi et al., 2016; Potolicchio et al., 2005). It is therefore tempting to speculate that oligodendroglial exosomes may support axonal transport by supplying ATP and lactate to neurons.

Analysis of axonal transport also revealed diminished pausing frequencies of moving cargoes and the suppression of static vesicles under stress conditions indicating constant moving rather than faster moving vesicles as the velocity was unaffected in response to exosome treatment. Transient pauses occur more frequently when moving cargoes cross stationary organelles, such as mitochondria (Che et al., 2016). Together with our finding, this suggests that oligodendroglial exosomes reduce the pausing time of moving vesicles probably by preventing the emergence of stationary organelles, since non-treated neurons exhibit an increased pausing time as well as a higher number of static vesicles.

Here, we provide evidence that oligodendroglial exosomes beneficially influence axonal transport dynamics. However, due to the regulatory effect of oligodendroglial exosomes downregulating BDNF expression in neurons and with regard to BDNF secretion, we cannot specify the direct effect mediated by exosomes (Dieni et al., 2012; Frohlich et al., 2014).

Therefore, evaluation of other transported organelles might be further informative. Since neurons are highly dependent on mitochondrial trafficking for their survival, analysis of mitochondrial transport may give further insight into the role of oligodendroglial exosomes in promoting neuronal integrity.

5.6 Comparison of Wildtype and Mutant Exosomes: Indications of Physiological Relevance?

Myelination of axonal segments bases on the expansion of oligodendroglial processes at the inner tongue (Snaidero et al., 2014). Newly-synthesized membrane is transported from the oligodendrocyte soma to the growing tip via cytoplasmic channels. The majority of these channels close as myelination progresses, but some of the radial cytoplasmic channels retain as functional connections most probably for the distribution of glial metabolites and vesicular

trafficking to the axonal compartment to provide long-term trophic support (Simons and Nave, 2015). However, PLP^{null} and CNP^{null} mutant mice generate a secondary axonal degeneration depite morphologically normal myelin. PLP has been suggested to support axonal energy metabolism, while CNP prevents premature myelin compaction accompanied by the closure of cytoplasmic channels (Edgar et al., 2004; Ferreirinha et al., 2004; Simons and Nave, 2015). The pathology of PLP and CNP knockout mice might be explained by perturbed energy support for neurons together with the abnormal closure of cytoplasmic channels (Simons and Nave, 2015). Since these cytoplasmic channels represent a transport route for metabolites and potentially also for MVBs containing exosomes carrying PLP and CNP to neurons, we examined the impact of exosomes derived from both mutant mice. Our data reveal disturbed exosome biogenesis patterns resulting in reduced secretion and compositional alterations of exosomes (data unpublished). Quantitative as well as qualitative changes may be attributed to sorting defects and perturbed fusion of MVBs with the plasma membrane, contributing to a loss of function of oligodendroglial exosomes with regard to their ability to protect neurons from starvation. However, the ineffectiveness of exosomes derived from PLP and CNP knockout oligodendrocytes is not due to the reduced exosome secretion but to the altered exosomal cargo of mutant oligodendrocytes. Treatment of neurons with the same amount of mutant exosomes as obtained from wildtype oligodendrocytes did not facilitate stress tolerance. Proteomics data of exosomes derived from CNP^{null} and PLP^{null} revealed reduced levels of protective biomolecules such as Hsp70 (data unpublished), which might provide a possible explanation for the observed effects. The qualitative effect of exosomes might also include alterations in the exosomal RNA cargo at least in CNP^{null} mice since CNP is a RNA-binding protein (Gravel et al., 2009). Levels of Rab35 mediating exosome release are unaltered (data unpublished), which suggests for the *in vivo* situation in CNP mutant mice the retention of MVBs within the myelin due to the absence of cytoplasmic channels.

A common characteristic of both mutant mice is the onset of secondary axonal swellings due to disturbances in axonal transport (Edgar et al., 2004; Griffiths et al., 1998; Lappe-Siefke et al., 2003). Analysis of axonal transport upon treatment with mutant exosomes exhibit a vesicular movement pattern similar to that of untreated neurons. In sharp contrast to wildtype exosome treated neurons, these observations may hint at malfunctions of kinesin and dynein. Targeted disruption of both kinesin and dynein or regulatory pathways modulating intracellular transport is already sufficient to induce neurodegeneration (Hirokawa et al., 2009; Perlson et al., 2010).

The proximal cause of neuronal cell death might be subsequent defects in localization or the delivery of essential cargoes. Psychosine is a toxic spingolipid accumulated in a leukodystrophy known as Krabbe disease and inhibits axonal transport through the activation of GSK-3ß (Cantuti Castelvetri et al., 2013). Mouse models of Krabbe disease suffer from axonal degeneration due to GSK-3ß-mediated impairment of axonal transport. We have shown that exosomes derived from wildtype oligodendrocytes induce GSK-3ß phosphorylation and thus its inactivation. It would be intriguing to examine whether PLP^{null}- and CNP^{null}- exosomes activate GSK-3ß as it is in Krabbe disease. This may partially explain the impaired axonal transport. A kinase screen may decipher the causative mechanism of neuronal vulnerability upon the exposure to mutant exosomes.

In summary, exosomes derived from PLP and CNP knockout oligodendrocytes do not mediate neuroprotection nor facilitate axonal transport probably to due to their loss of function. This may partially explain why oligodendrocytes derived from PLP and CNP knockout mice are not capable to maintain axonal integrity.

5.7 In vivo evidence of exosome-mediated axon-myelin communication

In line with our *in vitro* findings recent studies of *ex vivo* optic nerve axons suggest an activity-dependent glutamate-mediated signalling from axons to myelin *in vivo* (Micu et al., 2016). Accordingly, glutamate is released from axons in response to electrical stimulation and binds to myelinic NMDA and AMPA receptors. AMPA receptors operate on both, the axonal and myelinic site by promoting the release of Ca^{2+} from axoplasmic stores and together with NMDA receptors the increase of Ca^{2+} level in myelin, respectively. The authors also discovered “omega-like” fusion profiles of synapses between the axon and its myelin reminiscent to fusion profiles of MVBs. The appearance of these so-called axo-myelinic synapses seem to correlate with Ca^{2+} concentration in myelin and may modulate axon-glia signalling for trophic support of the axon. This model corresponds in every respect to our hypothesis, whereas the axo-myelinic synapse may represent MVBs. Thus, the study by Micu et al. may provide *in vivo* evidence of the activity-dependent neuron-glia communication via exosomes (Micu et al., 2006; Micu et al., 2016). Intriguingly, knockout of glutamate receptor subunits in mice inhibits Ca^{2+} entry in myelin (Micu et al., 2016). Recently, Saab et al. have shown that mice lacking NMDA receptors develop late-onset axonopathy and neuroinflammation, which may support the idea of

exosomal contribution to axonal integrity (Saab et al., 2016). Optic nerve axons may also represent an appropriate system to investigate the neuroprotective impact of oligodendroglial exosomes *in vivo*.

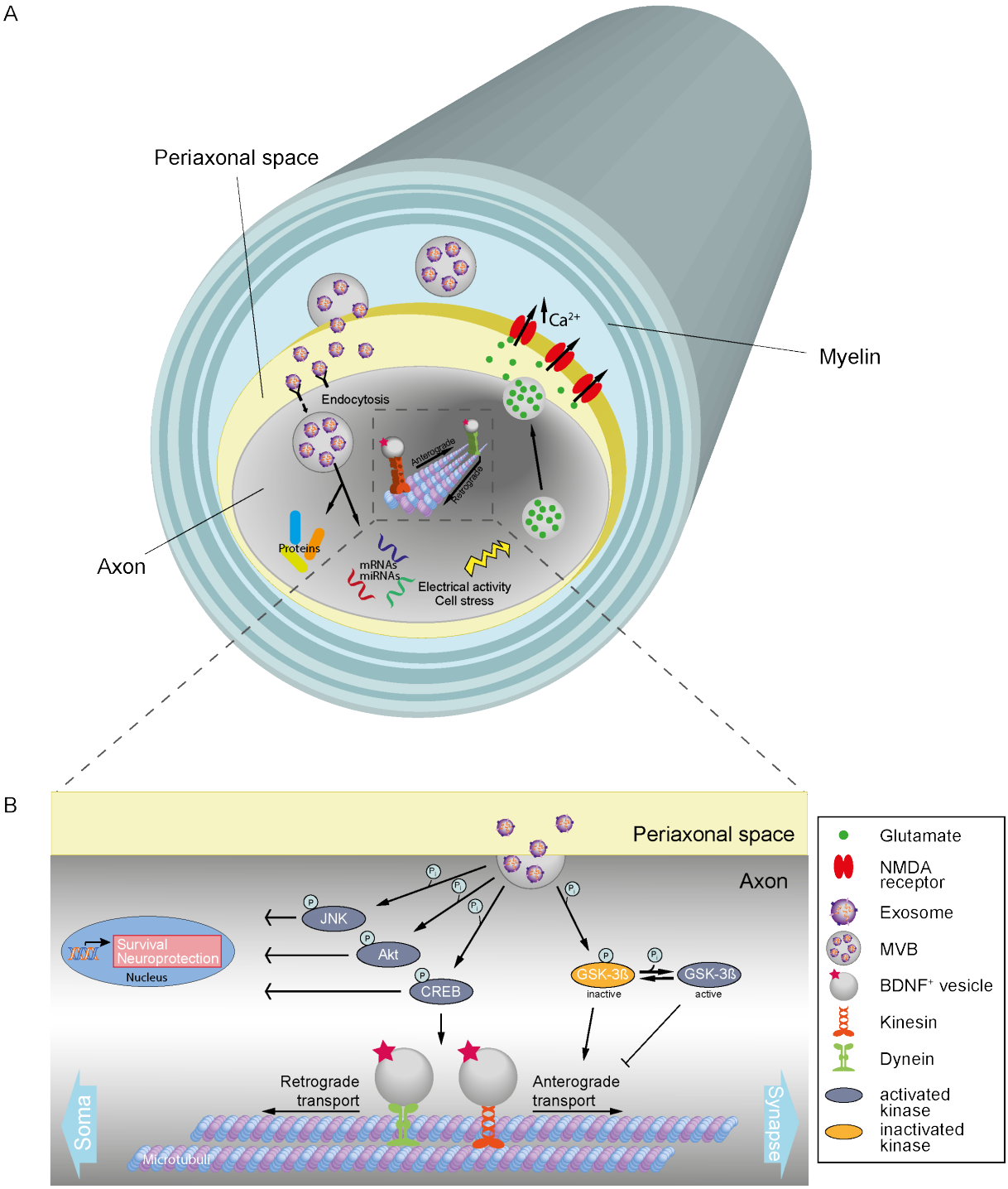

Figure 5-2 Schematic illustration of exosome-mediated neuroprotection. (A) Electrical active axons release glutamate that activates NMDA receptors on oligodendrocytes mediating Ca^{2+}-entry. Elevated levels of Ca^{2+} trigger fusion of MVBs with plasma membrane resulting in the release of exosomes into the periaxonal space. Exosomes are internalized by neurons via endocytosis and their protein and RNA cargo is functionally retrieved. Modified from (Fruhbeis et al., 2013a) (B) Under cellular stress conditions, oligodendroglial exosomes mediate neuroprotection and facilitate axonal transport by the activation of kinases involved in pro-survival signalling pathways and axonal transport. Phosphorylation of GSK-3ß by oligodendroglial exosomes prevent downstream inhibition of anterograde movement.

The implications of oligodendroglial exosomes in neuroprotection represent a promising approach for therapeutic strategies to mitigate axonal degeneration. Furthermore, exosomes are able to cross the BBB and may function as vehicles to deliver therapeutic agents into the diseased brain to mediate neuroprotection (Alvarez-Erviti et al., 2011; Lakhal and Wood, 2011).

5.8 Outlook

The concept of glial support by the horizontal transfer of energy-rich substrates from oligodendrocytes to neurons may be complemented by oligodendroglial exosomes carrying beneficial biomolecules, such as Hsp70, SOD1, and catalase, which are indispensable for the maintenance of homeostasis (Frohlich et al., 2014; Fruhbeis et al., 2013a; Fünfschilling et al., 2012; Lee et al., 2012b). The present study provides evidence that oligodendroglial exosomes beneficially influence neuronal physiology *in vitro* on different levels with neuroprotective properties (Figure 5-2) (Frohlich et al., 2014; Fruhbeis et al., 2013a).

To unravel the precise mechanisms, further studies are needed to specify the molecular determinants. Potential roles of OL exosomes involve the transfer of miRNAs, metabolites and proteins associated with stress protection. Thus, a comprehensive screening of exosomes derived from unstressed and stressed, as well as from PLP^{null} and CNP^{null} oligodendrocytes using proteomics, metabolomics, or next generation sequencing may reveal interesting candidates mediating the supportive effect. Comparative analysis of exosomes and target neurons may allow the identification of pathways on protein and mRNA level.

The most intriguing but also challenging approach will be the validation of the neuroprotective effect of oligodendroglial exosomes *in vivo*. A conditional knockout specifically interfering with exosome secretion in oligodendrocytes may be conclusive. However, better knowledge of the cell-type specific exosomal secretion apparatus is a prerequisite to design reliable mouse models. Candidates identified up to now, e.g. Rab35 and Rab27a/b, do not completely inhibit exosome secretion and may also mediate side effects (Hsu et al., 2010; Ostrowski et al., 2010). Considering that both PLP and CNP null mutant mice still secrete a basal level of exosomes, it

may be reasonable to generate a conditional Rab35 knockout in oligodendrocytes to study exosome-dependent axonal integrity. Thus, onset of axonal degeneration in these mice would allow the assessment of the physiological importance of oligodendroglial exosomes. Another valuable tool to investigate exosomal support is represented by the MOGi-Cre transgenic mouse model, which has been used to demonstrate horizontal exosome transfer *in vivo* (Fruhbeis et al., 2013a; Locatelli et al., 2012). Exposure of these mice to brain ischemia may elicit an increased number of recombined neurons as a result of elevated glutamate concentration, which in turn stimulates exosome secretion in oligodendrocytes. This experiment would provide evidence for the glutamate-triggered transfer of exosomes under stress conditions.

Our hypothesis of the neuroprotective function of oligodendroglial exosomes harbours a great potential not only in helping to unravel the mechanism of axonal integrity, but also to develop novel therapeutical strategies in clinical applications.

6 References

Abels, E.R., and X.O. Breakefield. 2016. Introduction to Extracellular Vesicles: Biogenesis, RNA Cargo Selection, Content, Release, and Uptake. *Cell Mol Neurobiol*. 36:301-312.

Allen, N.J., and B.A. Barres. 2009. Neuroscience: Glia - more than just brain glue. *Nature*. 457:675-677.

Alvarez-Erviti, L., Y. Seow, H. Yin, C. Betts, S. Lakhal, and M.J. Wood. 2011. Delivery of siRNA to the mouse brain by systemic injection of targeted exosomes. *Nature biotechnology*. 29:341-345.

Andersen, J.K. 2004. Oxidative stress in neurodegeneration: cause or consequence? *Nat Med*. 10 Suppl:S18-25.

Antonucci, F., E. Turola, L. Riganti, M. Caleo, M. Gabrielli, C. Perrotta, L. Novellino, E. Clementi, P. Giussani, P. Viani, M. Matteoli, and C. Verderio. 2012. Microvesicles released from microglia stimulate synaptic activity via enhanced sphingolipid metabolism. *EMBO J*. 31:1231-1240.

Arslan, F., R.C. Lai, M.B. Smeets, L. Akeroyd, A. Choo, E.N. Aguor, L. Timmers, H.V. van Rijen, P.A. Doevendans, G. Pasterkamp, S.K. Lim, and D.P. de Kleijn. 2013. Mesenchymal stem cell-derived exosomes increase ATP levels, decrease oxidative stress and activate PI3K/Akt pathway to enhance myocardial viability and prevent adverse remodeling after myocardial ischemia/reperfusion injury. *Stem Cell Res*. 10:301-312.

Asai, H., S. Ikezu, S. Tsunoda, M. Medalla, J. Luebke, T. Haydar, B. Wolozin, O. Butovsky, S. Kugler, and T. Ikezu. 2015. Depletion of microglia and inhibition of exosome synthesis halt tau propagation. *Nat Neurosci*. 18:1584-1593.

Attwell, D., and S.B. Laughlin. 2001. An energy budget for signaling in the grey matter of the brain. *Journal of cerebral blood flow and metabolism : official journal of the International Society of Cerebral Blood Flow and Metabolism*. 21:1133-1145.

Atwal, J.K., B. Massie, F.D. Miller, and D.R. Kaplan. 2000. The TrkB-Shc site signals neuronal survival and local axon growth via MEK and P13-kinase. *Neuron*. 27:265-277.

Bahrini, I., J.H. Song, D. Diez, and R. Hanayama. 2015. Neuronal exosomes facilitate synaptic pruning by up-regulating complement factors in microglia. *Sci Rep*. 5:7989.

Baietti, M.F., Z. Zhang, E. Mortier, A. Melchior, G. Degeest, A. Geeraerts, Y. Ivarsson, F. Depoortere, C. Coomans, E. Vermeiren, P. Zimmermann, and G. David. 2012. Syndecan-syntenin-ALIX regulates the biogenesis of exosomes. *Nat Cell Biol*. 14:677-685.

Bakhti, M., C. Winter, and M. Simons. 2011. Inhibition of myelin membrane sheath formation by oligodendrocyte-derived exosome-like vesicles. *J Biol Chem*. 286:787-796.

Barile, L., V. Lionetti, E. Cervio, M. Matteucci, M. Gherghiceanu, L.M. Popescu, T. Torre, F. Siclari, T. Moccetti, and G. Vassalli. 2014. Extracellular vesicles from human cardiac progenitor cells inhibit cardiomyocyte apoptosis and improve cardiac function after myocardial infarction. *Cardiovasc Res*. 103:530-541.

Basso, M., S. Pozzi, M. Tortarolo, F. Fiordaliso, C. Bisighini, L. Pasetto, G. Spaltro, D. Lidonnici, F. Gensano, E. Battaglia, C. Bendotti, and V. Bonetto. 2013. Mutant copper-zinc superoxide dismutase (SOD1) induces protein secretion pathway alterations and exosome release in astrocytes: implications for disease spreading and motor neuron pathology in amyotrophic lateral sclerosis. *J Biol Chem*. 288:15699-15711.

Baumann, N., and D. Pham-Dinh. 2001. Biology of oligodendrocyte and myelin in the mammalian central nervous system. *Physiol Rev*. 81:871-927.

Bechler, M.E., L. Byrne, and C. Ffrench-Constant. 2015. CNS Myelin Sheath Lengths Are an Intrinsic Property of Oligodendrocytes. *Current biology : CB*. 25:2411-2416.

Beirowski, B. 2013. Concepts for regulation of axon integrity by enwrapping glia. *Front Cell Neurosci*. 7:256.

Beirowski, B., E. Babetto, J.P. Golden, Y.J. Chen, K. Yang, R.W. Gross, G.J. Patti, and J. Milbrandt. 2014. Metabolic regulator LKB1 is crucial for Schwann cell-mediated axon maintenance. *Nat Neurosci*. 17:1351-1361.

Beitner-Johnson, D., R.T. Rust, T.C. Hsieh, and D.E. Millhorn. 2001. Hypoxia activates Akt and induces phosphorylation of GSK-3 in PC12 cells. *Cellular signalling*. 13:23-27.

Bercury, K.K., and W.B. Macklin. 2015. Dynamics and mechanisms of CNS myelination. *Dev Cell*. 32:447-458.

Bery, A., A. Cardona, P. Martinez, and V. Hartenstein. 2010. Structure of the central nervous system of a juvenile acoel, Symsagittifera roscoffensis. *Dev Genes Evol*. 220:61-76.

Bianco, F., E. Pravettoni, A. Colombo, U. Schenk, T. Moller, M. Matteoli, and C. Verderio. 2005. Astrocyte-derived ATP induces vesicle shedding and IL-1 beta release from microglia. *J Immunol*. 174:7268-7277.

Bifulco, M., C. Laezza, S. Stingo, and J. Wolff. 2002. 2',3'-Cyclic nucleotide 3'-phosphodiesterase: a membrane-bound, microtubule-associated protein and membrane anchor for tubulin. *Proc Natl Acad Sci U S A*. 99:1807-1812.

Bobrie, A., M. Colombo, S. Krumeich, G. Raposo, and C. Thery. 2012a. Diverse subpopulations of vesicles secreted by different intracellular mechanisms are present in exosome preparations obtained by differential ultracentrifugation. *Journal of extracellular vesicles*. 1.

Bobrie, A., M. Colombo, G. Raposo, and C. Thery. 2011. Exosome secretion: molecular mechanisms and roles in immune responses. *Traffic*. 12:1659-1668.

Bobrie, A., S. Krumeich, F. Reyal, C. Recchi, L.F. Moita, M.C. Seabra, M. Ostrowski, and C. Thery. 2012b. Rab27a supports exosome-dependent and -independent mechanisms that modify the tumor microenvironment and can promote tumor progression. *Cancer research*. 72:4920-4930.

Boelens, M.C., T.J. Wu, B.Y. Nabet, B. Xu, Y. Qiu, T. Yoon, D.J. Azzam, C. Twyman-Saint Victor, B.Z. Wiemann, H. Ishwaran, P.J. Ter Brugge, J. Jonkers, J. Slingerland, and A.J. Minn. 2014. Exosome transfer from stromal to breast cancer cells regulates therapy resistance pathways. *Cell*. 159:499-513.

Bowman, A.B., A. Kamal, B.W. Ritchings, A.V. Philp, M. McGrail, J.G. Gindhart, and L.S. Goldstein. 2000. Kinesin-dependent axonal transport is mediated by the sunday driver (SYD) protein. *Cell*. 103:583-594.

Brahimi-Horn, M.C., J. Chiche, and J. Pouyssegur. 2007. Hypoxia signalling controls metabolic demand. *Curr Opin Cell Biol*. 19:223-229.

Brewer, G.J. 1995. Serum-free B27/neurobasal medium supports differentiated growth of neurons from the striatum, substantia nigra, septum, cerebral cortex, cerebellum, and dentate gyrus. *J Neurosci Res*. 42:674-683.

Brewer, G.J., J.R. Torricelli, E.K. Evege, and P.J. Price. 1993. Optimized survival of hippocampal neurons in B27-supplemented Neurobasal, a new serum-free medium combination. *J Neurosci Res*. 35:567-576.

Brouwers, J.F., M. Aalberts, J.W. Jansen, G. van Niel, M.H. Wauben, T.A. Stout, J.B. Helms, and W. Stoorvogel. 2013. Distinct lipid compositions of two types of human prostasomes. *Proteomics*. 13:1660-1666.

Bruschi, M., L. Santucci, S. Ravera, G. Candiano, M. Bartolucci, D. Calzia, C. Lavarello, E. Inglese, L.A. Ramenghi, A. Petretto, G.M. Ghiggeri, and I. Panfoli. 2016. Human urinary exosome proteome unveils its aerobic respiratory ability. *Journal of proteomics*. 136:25-34.

Budnik, V., C. Ruiz-Canada, and F. Wendler. 2016. Extracellular vesicles round off communication in the nervous system. *Nat Rev Neurosci*. 17:160-172.

Cantuti Castelvetri, L., M.I. Givogri, A. Hebert, B. Smith, Y. Song, A. Kaminska, A. Lopez-Rosas, G. Morfini, G. Pigino, M. Sands, S.T. Brady, and E.R. Bongarzone. 2013. The sphingolipid psychosine inhibits fast axonal transport in Krabbe disease by activation of GSK3beta and deregulation of molecular motors. *J Neurosci*. 33:10048-10056.

Che, D.L., P.D. Chowdary, and B. Cui. 2016. A close look at axonal transport: Cargos slow down when crossing stationary organelles. *Neurosci Lett*. 610:110-116.

Chelikani, P., I. Fita, and P.C. Loewen. 2004. Diversity of structures and properties among catalases. *Cell Mol Life Sci*. 61:192-208.

Chen, S., C. Rio, R.R. Ji, P. Dikkes, R.E. Coggeshall, C.J. Woolf, and G. Corfas. 2003. Disruption of ErbB receptor signaling in adult non-myelinating Schwann cells causes progressive sensory loss. *Nat Neurosci*. 6:1186-1193.

Chin, P.C., N. Majdzadeh, and S.R. D'Mello. 2005. Inhibition of GSK3beta is a common event in neuroprotection by different survival factors. *Brain research. Molecular brain research*. 137:193-201.

Chivet, M., F. Hemming, K. Pernet-Gallay, S. Fraboulet, and R. Sadoul. 2012. Emerging role of neuronal exosomes in the central nervous system. *Front Physiol*. 3:145.

Chivet, M., C. Javalet, F. Hemming, K. Pernet-Gallay, K. Laulagnier, S. Fraboulet, and R. Sadoul. 2013. Exosomes as a novel way of interneuronal communication. *Biochemical Society transactions*. 41:241-244.

Chivet, M., C. Javalet, K. Laulagnier, B. Blot, F.J. Hemming, and R. Sadoul. 2014. Exosomes secreted by cortical neurons upon glutamatergic synapse activation specifically interact with neurons. *Journal of extracellular vesicles*. 3:24722.

Cirrito, J.R., B.M. Disabato, J.L. Restivo, D.K. Verges, W.D. Goebel, A. Sathyan, D. Hayreh, G. D'Angelo, T. Benzinger, H. Yoon, J. Kim, J.C. Morris, M.A. Mintun, and Y.I. Sheline. 2011. Serotonin signaling is associated with lower amyloid-beta levels and plaques in transgenic mice and humans. *Proc Natl Acad Sci U S A*. 108:14968-14973.

Clavaguera, F., T. Bolmont, R.A. Crowther, D. Abramowski, S. Frank, A. Probst, G. Fraser, A.K. Stalder, M. Beibel, M. Staufenbiel, M. Jucker, M. Goedert, and M. Tolnay. 2009. Transmission and spreading of tauopathy in transgenic mouse brain. *Nat Cell Biol*. 11:909-913.

Cocucci, E., G. Racchetti, and J. Meldolesi. 2009. Shedding microvesicles: artefacts no more. *Trends Cell Biol*. 19:43-51.

Coffey, E.T. 2014. Nuclear and cytosolic JNK signalling in neurons. *Nat Rev Neurosci*. 15:285-299.

Coleman, B.M., and A.F. Hill. 2015. Extracellular vesicles--Their role in the packaging and spread of misfolded proteins associated with neurodegenerative diseases. *Semin Cell Dev Biol*. 40:89-96.

Colin, E., D. Zala, G. Liot, H. Rangone, M. Borrell-Pages, X.J. Li, F. Saudou, and S. Humbert. 2008. Huntingtin phosphorylation acts as a molecular switch for anterograde/retrograde transport in neurons. *EMBO J*. 27:2124-2134.

Colombo, E., B. Borgiani, C. Verderio, and R. Furlan. 2012. Microvesicles: novel biomarkers for neurological disorders. *Front Physiol*. 3:63.

Colombo, M., G. Raposo, and C. Thery. 2014. Biogenesis, secretion, and intercellular interactions of exosomes and other extracellular vesicles. *Annu Rev Cell Dev Biol*. 30:255-289.

Corrotte, M., A.P. Nyguyen, M.L. Harlay, N. Vitale, M.F. Bader, and N.J. Grant. 2010. Ral isoforms are implicated in Fc gamma R-mediated phagocytosis: activation of phospholipase D by RalA. *J Immunol*. 185:2942-2950.

Cossetti, C., N. Iraci, T.R. Mercer, T. Leonardi, E. Alpi, D. Drago, C. Alfaro-Cervello, H.K. Saini, M.P. Davis, J. Schaeffer, B. Vega, M. Stefanini, C. Zhao, W. Muller, J.M. Garcia-Verdugo, S. Mathivanan, A. Bachi, A.J. Enright, J.S. Mattick, and S. Pluchino. 2014. Extracellular vesicles from neural stem cells transfer IFN-gamma via Ifngr1 to activate Stat1 signaling in target cells. *Mol Cell*. 56:193-204.

Costa-Silva, B., N.M. Aiello, A.J. Ocean, S. Singh, H. Zhang, B.K. Thakur, A. Becker, A. Hoshino, M.T. Mark, H. Molina, J. Xiang, T. Zhang, T.M. Theilen, G. Garcia-Santos, C. Williams, Y. Ararso, Y. Huang, G. Rodrigues, T.L. Shen, K.J. Labori, I.M. Lothe, E.H. Kure, J. Hernandez, A. Doussot, S.H. Ebbesen, P.M. Grandgenett, M.A. Hollingsworth, M. Jain, K. Mallya, S.K. Batra, W.R. Jarnagin, R.E. Schwartz, I. Matei, H. Peinado, B.Z. Stanger, J. Bromberg, and

D. Lyden. 2015. Pancreatic cancer exosomes initiate pre-metastatic niche formation in the liver. *Nat Cell Biol*. 17:816-826.

Cox, L.J., U. Hengst, N.G. Gurskaya, K.A. Lukyanov, and S.R. Jaffrey. 2008. Intra-axonal translation and retrograde trafficking of CREB promotes neuronal survival. *Nat Cell Biol*. 10:149-159.

Czopka, T., C. Ffrench-Constant, and D.A. Lyons. 2013. Individual oligodendrocytes have only a few hours in which to generate new myelin sheaths in vivo. *Dev Cell*. 25:599-609.

Darios, F., C. Wasser, A. Shakirzyanova, A. Giniatullin, K. Goodman, J.L. Munoz-Bravo, J. Raingo, J. Jorgacevski, M. Kreft, R. Zorec, J.M. Rosa, L. Gandia, L.M. Gutierrez, T. Binz, R. Giniatullin, E.T. Kavalali, and B. Davletov. 2009. Sphingosine facilitates SNARE complex assembly and activates synaptic vesicle exocytosis. *Neuron*. 62:683-694.

Dawson, M.R., A. Polito, J.M. Levine, and R. Reynolds. 2003. NG2-expressing glial progenitor cells: an abundant and widespread population of cycling cells in the adult rat CNS. *Mol Cell Neurosci*. 24:476-488.

De Cristobal, J., A. Cardenas, I. Lizasoain, J.C. Leza, P. Fernandez-Tome, P. Lorenzo, and M.A. Moro. 2002. Inhibition of glutamate release via recovery of ATP levels accounts for a neuroprotective effect of aspirin in rat cortical neurons exposed to oxygen-glucose deprivation. *Stroke; a journal of cerebral circulation*. 33:261-267.

De Vos, K.J., A.J. Grierson, S. Ackerley, and C.C. Miller. 2008. Role of axonal transport in neurodegenerative diseases. *Annu Rev Neurosci*. 31:151-173.

de Waegh, S., and S.T. Brady. 1990. Altered slow axonal transport and regeneration in a myelin-deficient mutant mouse: the trembler as an in vivo model for Schwann cell-axon interactions. *J Neurosci*. 10:1855-1865.

Del Conde, I., C.N. Shrimpton, P. Thiagarajan, and J.A. Lopez. 2005. Tissue-factor-bearing microvesicles arise from lipid rafts and fuse with activated platelets to initiate coagulation. *Blood*. 106:1604-1611.

Deoni, S.C., J. O'Muircheartaigh, J.T. Elison, L. Walker, E. Doernberg, N. Waskiewicz, H. Dirks, I. Piryatinsky, D.C. Dean, 3rd, and N.L. Jumbe. 2016. White matter maturation profiles through early childhood predict general cognitive ability. *Brain Struct Funct*. 221:1189-1203.

Dhanasekaran, D.N., and E.P. Reddy. 2008. JNK signaling in apoptosis. *Oncogene*. 27:6245-6251.

Dieni, S., T. Matsumoto, M. Dekkers, S. Rauskolb, M.S. Ionescu, R. Deogracias, E.D. Gundelfinger, M. Kojima, S. Nestel, M. Frotscher, and Y.A. Barde. 2012. BDNF and its pro-peptide are stored in presynaptic dense core vesicles in brain neurons. *J Cell Biol*. 196:775-788.

Doble, B.W., and J.R. Woodgett. 2003. GSK-3: tricks of the trade for a multi-tasking kinase. *J Cell Sci*. 116:1175-1186.

Doeppner, T.R., J. Herz, A. Gorgens, J. Schlechter, A.K. Ludwig, S. Radtke, K. de Miroschedji, P.A. Horn, B. Giebel, and D.M. Hermann. 2015. Extracellular Vesicles Improve Post-Stroke Neuroregeneration and Prevent Postischemic Immunosuppression. *Stem Cells Transl Med*. 4:1131-1143.

Dringen, R., P.G. Pawlowski, and J. Hirrlinger. 2005. Peroxide detoxification by brain cells. *J Neurosci Res*. 79:157-165.

Du, K., and M. Montminy. 1998. CREB is a regulatory target for the protein kinase Akt/PKB. *J Biol Chem*. 273:32377-32379.

Dudek, H., S.R. Datta, T.F. Franke, M.J. Birnbaum, R. Yao, G.M. Cooper, R.A. Segal, D.R. Kaplan, and M.E. Greenberg. 1997. Regulation of neuronal survival by the serine-threonine protein kinase Akt. *Science*. 275:661-665.

Duncan, J.E., and L.S. Goldstein. 2006. The genetics of axonal transport and axonal transport disorders. *PLoS Genet*. 2:e124.

Edenfeld, G., T. Stork, and C. Klambt. 2005. Neuron-glia interaction in the insect nervous system. *Curr Opin Neurobiol*. 15:34-39.

Edgar, J.M., M. McLaughlin, H.B. Werner, M.C. McCulloch, J.A. Barrie, A. Brown, A.B. Faichney, N. Snaidero, K.A. Nave, and I.R. Griffiths. 2009. Early ultrastructural defects of axons and axon-glia junctions in mice lacking expression of Cnp1. *Glia*. 57:1815-1824.

Edgar, J.M., M. McLaughlin, D. Yool, S.C. Zhang, J.H. Fowler, P. Montague, J.A. Barrie, M.C. McCulloch, I.D. Duncan, J. Garbern, K.A. Nave, and I.R. Griffiths. 2004. Oligodendroglial modulation of fast axonal transport in a mouse model of hereditary spastic paraplegia. *J Cell Biol*. 166:121-131.

Edgar, J.M., and K.A. Nave. 2009. The role of CNS glia in preserving axon function. *Curr Opin Neurobiol*. 19:498-504.

Eldh, M., K. Ekstrom, H. Valadi, M. Sjostrand, B. Olsson, M. Jernas, and J. Lotvall. 2010. Exosomes communicate protective messages during oxidative stress; possible role of exosomal shuttle RNA. *PLoS One*. 5:e15353.

Emery, B. 2010. Regulation of oligodendrocyte differentiation and myelination. *Science*. 330:779-782.

Emmanouilidou, E., K. Melachroinou, T. Roumeliotis, S.D. Garbis, M. Ntzouni, L.H. Margaritis, L. Stefanis, and K. Vekrellis. 2010. Cell-produced alpha-synuclein is secreted in a calcium-dependent manner by exosomes and impacts neuronal survival. *J Neurosci*. 30:6838-6851.

Escudero, C.A., O.M. Lazo, C. Galleguillos, J.I. Parraguez, M.A. Lopez-Verrilli, C. Cabeza, L. Leon, U. Saeed, C. Retamal, A. Gonzalez, M.P. Marzolo, B.D. Carter, F.A. Court, and F.C. Bronfman. 2014. The p75 neurotrophin receptor evades the endolysosomal route in neuronal cells, favouring multivesicular bodies specialised for exosomal release. *J Cell Sci*. 127:1966-1979.

Fang, C., D. Bourdette, and G. Banker. 2012. Oxidative stress inhibits axonal transport: implications for neurodegenerative diseases. *Mol Neurodegener*. 7:29.

Faure, J., G. Lachenal, M. Court, J. Hirrlinger, C. Chatellard-Causse, B. Blot, J. Grange, G. Schoehn, Y. Goldberg, V. Boyer, F. Kirchhoff, G. Raposo, J. Garin, and R. Sadoul. 2006. Exosomes are released by cultured cortical neurones. *Mol Cell Neurosci*. 31:642-648.

Ferreirinha, F., A. Quattrini, M. Pirozzi, V. Valsecchi, G. Dina, V. Broccoli, A. Auricchio, F. Piemonte, G. Tozzi, L. Gaeta, G. Casari, A. Ballabio, and E.I. Rugarli. 2004. Axonal degeneration in paraplegin-deficient mice is associated with abnormal mitochondria and impairment of axonal transport. *The Journal of clinical investigation*. 113:231-242.

Fields, R.D. 2015. A new mechanism of nervous system plasticity: activity-dependent myelination. *Nat Rev Neurosci*. 16:756-767.

Fields, R.D., and B. Stevens-Graham. 2002. New insights into neuron-glia communication. *Science*. 298:556-562.

Fitzner, D., M. Schnaars, D. van Rossum, G. Krishnamoorthy, P. Dibaj, M. Bakhti, T. Regen, U.K. Hanisch, and M. Simons. 2011. Selective transfer of exosomes from oligodendrocytes to microglia by macropinocytosis. *J Cell Sci*. 124:447-458.

Fong, M.Y., W. Zhou, L. Liu, A.Y. Alontaga, M. Chandra, J. Ashby, A. Chow, S.T. O'Connor, S. Li, A.R. Chin, G. Somlo, M. Palomares, Z. Li, J.R. Tremblay, A. Tsuyada, G. Sun, M.A. Reid, X.

Wu, P. Swiderski, X. Ren, Y. Shi, M. Kong, W. Zhong, Y. Chen, and S.E. Wang. 2015. Breast-cancer-secreted miR-122 reprograms glucose metabolism in premetastatic niche to promote metastasis. *Nat Cell Biol*. 17:183-194.

Freeman, M.R., and J. Doherty. 2006. Glial cell biology in Drosophila and vertebrates. *Trends in neurosciences*. 29:82-90.

Freeman, M.R., and D.H. Rowitch. 2013. Evolving concepts of gliogenesis: a look way back and ahead to the next 25 years. *Neuron*. 80:613-623.

Frohlich, D., W.P. Kuo, C. Fruhbeis, J.J. Sun, C.M. Zehendner, H.J. Luhmann, S. Pinto, J. Toedling, J. Trotter, and E.M. Kramer-Albers. 2014. Multifaceted effects of oligodendroglial exosomes on neurons: impact on neuronal firing rate, signal transduction and gene regulation. *Philos Trans R Soc Lond B Biol Sci*. 369.

Frühbeis, C., D. Fröhlich, and E.M. Krämer-Albers. 2012. Emerging roles of exosomes in neuron-glia communication. *Front Physiol*. 3:119.

Fruhbeis, C., D. Frohlich, W.P. Kuo, J. Amphornrat, S. Thilemann, A.S. Saab, F. Kirchhoff, W. Mobius, S. Goebbels, K.A. Nave, A. Schneider, M. Simons, M. Klugmann, J. Trotter, and E.M. Kramer-Albers. 2013a. Neurotransmitter-triggered transfer of exosomes mediates oligodendrocyte-neuron communication. *PLoS Biol*. 11:e1001604.

Fruhbeis, C., D. Frohlich, W.P. Kuo, and E.M. Kramer-Albers. 2013b. Extracellular vesicles as mediators of neuron-glia communication. *Front Cell Neurosci*. 7:182.

Fu, M.M., and E.L. Holzbaur. 2013. JIP1 regulates the directionality of APP axonal transport by coordinating kinesin and dynein motors. *J Cell Biol*. 202:495-508.

Fünfschilling, U., L.M. Supplie, D. Mahad, S. Boretius, A.S. Saab, J. Edgar, B.G. Brinkmann, C.M. Kassmann, I.D. Tzvetanova, W. Mobius, F. Diaz, D. Meijer, U. Suter, B. Hamprecht, M.W. Sereda, C.T. Moraes, J. Frahm, S. Goebbels, and K.A. Nave. 2012. Glycolytic oligodendrocytes maintain myelin and long-term axonal integrity. *Nature*. 485:517-521.

Gabrielli, M., N. Battista, L. Riganti, I. Prada, F. Antonucci, L. Cantone, M. Matteoli, M. Maccarrone, and C. Verderio. 2015. Active endocannabinoids are secreted on extracellular membrane vesicles. *EMBO Rep*. 16:213-220.

Garcia, M.L., C.S. Lobsiger, S.B. Shah, T.J. Deerinck, J. Crum, D. Young, C.M. Ward, T.O. Crawford, T. Gotow, Y. Uchiyama, M.H. Ellisman, N.A. Calcutt, and D.W. Cleveland. 2003. NF-M is an essential target for the myelin-directed "outside-in" signaling cascade that mediates radial axonal growth. *J Cell Biol*. 163:1011-1020.

Gatenby, R.A., and R.J. Gillies. 2004. Why do cancers have high aerobic glycolysis? *Nat Rev Cancer*. 4:891-899.

Gatti, S., S. Bruno, M.C. Deregibus, A. Sordi, V. Cantaluppi, C. Tetta, and G. Camussi. 2011. Microvesicles derived from human adult mesenchymal stem cells protect against ischaemia-reperfusion-induced acute and chronic kidney injury. *Nephrol Dial Transplant*. 26:1474-1483.

Ghossoub, R., F. Lembo, A. Rubio, C.B. Gaillard, J. Bouchet, N. Vitale, J. Slavik, M. Machala, and P. Zimmermann. 2014. Syntenin-ALIX exosome biogenesis and budding into multivesicular bodies are controlled by ARF6 and PLD2. *Nat Commun*. 5:3477.

Gibson, E.M., D. Purger, C.W. Mount, A.K. Goldstein, G.L. Lin, L.S. Wood, I. Inema, S.E. Miller, G. Bieri, J.B. Zuchero, B.A. Barres, P.J. Woo, H. Vogel, and M. Monje. 2014. Neuronal activity promotes oligodendrogenesis and adaptive myelination in the mammalian brain. *Science*. 344:1252304.

Glebov, K., M. Lochner, R. Jabs, T. Lau, O. Merkel, P. Schloss, C. Steinhauser, and J. Walter. 2015. Serotonin stimulates secretion of exosomes from microglia cells. *Glia*. 63:626-634.

Goldberg, M.P., and D.W. Choi. 1993. Combined oxygen and glucose deprivation in cortical cell culture: calcium-dependent and calcium-independent mechanisms of neuronal injury. *J Neurosci*. 13:3510-3524.

Goldie, B.J., M.D. Dun, M. Lin, N.D. Smith, N.M. Verrills, C.V. Dayas, and M.J. Cairns. 2014. Activity-associated miRNA are packaged in Map1b-enriched exosomes released from depolarized neurons. *Nucleic Acids Res*. 42:9195-9208.

Gomes, C., S. Keller, P. Altevogt, and J. Costa. 2007. Evidence for secretion of Cu,Zn superoxide dismutase via exosomes from a cell model of amyotrophic lateral sclerosis. *Neurosci Lett*. 428:43-46.

Grad, L.I., S.M. Fernando, and N.R. Cashman. 2015. From molecule to molecule and cell to cell: prion-like mechanisms in amyotrophic lateral sclerosis. *Neurobiol Dis*. 77:257-265.

Grad, L.I., W.C. Guest, A. Yanai, E. Pokrishevsky, M.A. O'Neill, E. Gibbs, V. Semenchenko, M. Yousefi, D.S. Wishart, S.S. Plotkin, and N.R. Cashman. 2011. Intermolecular transmission of superoxide dismutase 1 misfolding in living cells. *Proc Natl Acad Sci U S A*. 108:16398-16403.

Gravel, M., F. Robert, V. Kottis, I.E. Gallouzi, J. Pelletier, and P.E. Braun. 2009. 2',3'-Cyclic nucleotide 3'-phosphodiesterase: a novel RNA-binding protein that inhibits protein synthesis. *J Neurosci Res*. 87:1069-1079.

Griffiths, I., M. Klugmann, T. Anderson, D. Yool, C. Thomson, M.H. Schwab, A. Schneider, F. Zimmermann, M. McCulloch, N. Nadon, and K.A. Nave. 1998. Axonal swellings and degeneration in mice lacking the major proteolipid of myelin. *Science*. 280:1610-1613.

Guitart, K., G. Loers, F. Buck, U. Bork, M. Schachner, and R. Kleene. 2016. Improvement of neuronal cell survival by astrocyte-derived exosomes under hypoxic and ischemic conditions depends on prion protein. *Glia*. 64:896-910.

Harding, C., J. Heuser, and P. Stahl. 1983. Receptor-mediated endocytosis of transferrin and recycling of the transferrin receptor in rat reticulocytes. *J Cell Biol*. 97:329-339.

Hawkins, A., and J. Olszewski. 1957. Glia/nerve cell index for cortex of the whale. *Science*. 126:76-77.

Heidemann, S.R., J.M. Landers, and M.A. Hamborg. 1981. Polarity orientation of axonal microtubules. *J Cell Biol*. 91:661-665.

Henne, W.M., H. Stenmark, and S.D. Emr. 2013. Molecular mechanisms of the membrane sculpting ESCRT pathway. *Cold Spring Harb Perspect Biol*. 5.

Herculano-Houzel, S. 2014. The glia/neuron ratio: how it varies uniformly across brain structures and species and what that means for brain physiology and evolution. *Glia*. 62:1377-1391.

Herculano-Houzel, S., D.J. Messeder, K. Fonseca-Azevedo, and N.A. Pantoja. 2015. When larger brains do not have more neurons: increased numbers of cells are compensated by decreased average cell size across mouse individuals. *Front Neuroanat*. 9:64.

Hergenreider, E., S. Heydt, K. Treguer, T. Boettger, A.J. Horrevoets, A.M. Zeiher, M.P. Scheffer, A.S. Frangakis, X. Yin, M. Mayr, T. Braun, C. Urbich, R.A. Boon, and S. Dimmeler. 2012. Atheroprotective communication between endothelial cells and smooth muscle cells through miRNAs. *Nat Cell Biol*. 14:249-256.

Heusermann, W., J. Hean, D. Trojer, E. Steib, S. von Bueren, A. Graff-Meyer, C. Genoud, K. Martin, N. Pizzato, J. Voshol, D.V. Morrissey, S.E. Andaloussi, M.J. Wood, and N.C. Meisner-Kober. 2016. Exosomes surf on filopodia to enter cells at endocytic hot spots, traffic within endosomes, and are targeted to the ER. *J Cell Biol*. 213:173-184.

Hirokawa, N., R. Nitta, and Y. Okada. 2009. The mechanisms of kinesin motor motility: lessons from the monomeric motor KIF1A. *Nature reviews. Molecular cell biology*. 10:877-884.

Hoffman, P.N., J.W. Griffin, and D.L. Price. 1984. Control of axonal caliber by neurofilament transport. *J Cell Biol*. 99:705-714.

Hooper, C., R. Sainz-Fuertes, S. Lynham, A. Hye, R. Killick, A. Warley, C. Bolondi, J. Pocock, and S. Lovestone. 2012. Wnt3a induces exosome secretion from primary cultured rat microglia. *BMC neuroscience*. 13:144.

Hoshino, A., B. Costa-Silva, T.L. Shen, G. Rodrigues, A. Hashimoto, M. Tesic Mark, H. Molina, S. Kohsaka, A. Di Giannatale, S. Ceder, S. Singh, C. Williams, N. Soplop, K. Uryu, L. Pharmer, T. King, L. Bojmar, A.E. Davies, Y. Ararso, T. Zhang, H. Zhang, J. Hernandez, J.M. Weiss, V.D. Dumont-Cole, K. Kramer, L.H. Wexler, A. Narendran, G.K. Schwartz, J.H. Healey, P. Sandstrom, K.J. Labori, E.H. Kure, P.M. Grandgenett, M.A. Hollingsworth, M. de Sousa, S. Kaur, M. Jain, K. Mallya, S.K. Batra, W.R. Jarnagin, M.S. Brady, O. Fodstad, V. Muller, K. Pantel, A.J. Minn, M.J. Bissell, B.A. Garcia, Y. Kang, V.K. Rajasekhar, C.M. Ghajar, I. Matei, H. Peinado, J. Bromberg, and D. Lyden. 2015. Tumour exosome integrins determine organotropic metastasis. *Nature*. 527:329-335.

Hsu, C., Y. Morohashi, S. Yoshimura, N. Manrique-Hoyos, S. Jung, M.A. Lauterbach, M. Bakhti, M. Gronborg, W. Mobius, J. Rhee, F.A. Barr, and M. Simons. 2010. Regulation of exosome secretion by Rab35 and its GTPase-activating proteins TBC1D10A-C. *J Cell Biol*. 189:223-232.

Hu, G., H. Yao, A.D. Chaudhuri, M. Duan, S.V. Yelamanchili, H. Wen, P.D. Cheney, H.S. Fox, and S. Buch. 2012. Exosome-mediated shuttling of microRNA-29 regulates HIV Tat and morphine-mediated neuronal dysfunction. *Cell death & disease*. 3:e381.

Hua, W., E.C. Young, M.L. Fleming, and J. Gelles. 1997. Coupling of kinesin steps to ATP hydrolysis. *Nature*. 388:390-393.

Hughes, E.G., and B. Appel. 2016. The cell biology of CNS myelination. *Curr Opin Neurobiol*. 39:93-100.

Hurley, J.H. 2008. ESCRT complexes and the biogenesis of multivesicular bodies. *Curr Opin Cell Biol*. 20:4-11.

Hurley, J.H., E. Boura, L.A. Carlson, and B. Rozycki. 2010. Membrane budding. *Cell*. 143:875-887.

Hyenne, V., A. Apaydin, D. Rodriguez, C. Spiegelhalter, S. Hoff-Yoessle, M. Diem, S. Tak, O. Lefebvre, Y. Schwab, J.G. Goetz, and M. Labouesse. 2015. RAL-1 controls multivesicular body biogenesis and exosome secretion. *J Cell Biol*. 211:27-37.

Irion, U., and D. St Johnston. 2007. bicoid RNA localization requires specific binding of an endosomal sorting complex. *Nature*. 445:554-558.

Jin, K., X.O. Mao, Y. Zhu, and D.A. Greenberg. 2002. MEK and ERK protect hypoxic cortical neurons via phosphorylation of Bad. *J Neurochem*. 80:119-125.

Joshi, P., L. Benussi, R. Furlan, R. Ghidoni, and C. Verderio. 2015. Extracellular vesicles in Alzheimer's disease: friends or foes? Focus on abeta-vesicle interaction. *Int J Mol Sci*. 16:4800-4813.

Joshi, P., E. Turola, A. Ruiz, A. Bergami, D.D. Libera, L. Benussi, P. Giussani, G. Magnani, G. Comi, G. Legname, R. Ghidoni, R. Furlan, M. Matteoli, and C. Verderio. 2014. Microglia convert aggregated amyloid-beta into neurotoxic forms through the shedding of microvesicles. *Cell death and differentiation*. 21:582-593.

Jung, M., E. Kramer, M. Grzenkowski, K. Tang, W. Blakemore, A. Aguzzi, K. Khazaie, K. Chlichlia, G. von Blankenfeld, H. Kettenmann, and et al. 1995. Lines of murine oligodendroglial precursor cells immortalized by an activated neu tyrosine kinase show distinct degrees of interaction with axons in vitro and in vivo. *The European journal of neuroscience*. 7:1245-1265.

Kalra, H., R.J. Simpson, H. Ji, E. Aikawa, P. Altevogt, P. Askenase, V.C. Bond, F.E. Borras, X. Breakefield, V. Budnik, E. Buzas, G. Camussi, A. Clayton, E. Cocucci, J.M. Falcon-Perez, S. Gabrielsson, Y.S. Gho, D. Gupta, H.C. Harsha, A. Hendrix, A.F. Hill, J.M. Inal, G. Jenster, E.M. Kramer-Albers, S.K. Lim, A. Llorente, J. Lotvall, A. Marcilla, L. Mincheva-Nilsson, I. Nazarenko, R. Nieuwland, E.N. Nolte-'t Hoen, A. Pandey, T. Patel, M.G. Piper, S. Pluchino, T.S. Prasad, L. Rajendran, G. Raposo, M. Record, G.E. Reid, F. Sanchez-Madrid, R.M. Schiffelers, P. Siljander, A. Stensballe, W. Stoorvogel, D. Taylor, C. Thery, H. Valadi, B.W. van Balkom, J. Vazquez, M. Vidal, M.H. Wauben, M. Yanez-Mo, M. Zoeller, and S. Mathivanan. 2012. Vesiclepedia: a compendium for extracellular vesicles with continuous community annotation. *PLoS Biol*. 10:e1001450.

Kandel, E.R. 2012. The molecular biology of memory: cAMP, PKA, CRE, CREB-1, CREB-2, and CPEB. *Molecular brain*. 5:14.

Karadottir, R., and D. Attwell. 2007. Neurotransmitter receptors in the life and death of oligodendrocytes. *Neuroscience*. 145:1426-1438.

Kassmann, C.M., C. Lappe-Siefke, M. Baes, B. Brugger, A. Mildner, H.B. Werner, O. Natt, T. Michaelis, M. Prinz, J. Frahm, and K.A. Nave. 2007. Axonal loss and neuroinflammation caused by peroxisome-deficient oligodendrocytes. *Nat Genet*. 39:969-976.

Kassmann, C.M., S. Quintes, J. Rietdorf, W. Mobius, M.W. Sereda, T. Nientiedt, G. Saher, M. Baes, and K.A. Nave. 2011. A role for myelin-associated peroxisomes in maintaining paranodal loops and axonal integrity. *FEBS letters*. 585:2205-2211.

Katsuda, T., R. Tsuchiya, N. Kosaka, Y. Yoshioka, K. Takagaki, K. Oki, F. Takeshita, Y. Sakai, M. Kuroda, and T. Ochiya. 2013. Human adipose tissue-derived mesenchymal stem cells secrete functional neprilysin-bound exosomes. *Sci Rep*. 3:1197.

Katzmann, D.J., M. Babst, and S.D. Emr. 2001. Ubiquitin-dependent sorting into the multivesicular body pathway requires the function of a conserved endosomal protein sorting complex, ESCRT-I. *Cell*. 106:145-155.

Keller, S., C. Rupp, A. Stoeck, S. Runz, M. Fogel, S. Lugert, H.D. Hager, M.S. Abdel-Bakky, P. Gutwein, and P. Altevogt. 2007. CD24 is a marker of exosomes secreted into urine and amniotic fluid. *Kidney Int*. 72:1095-1102.

Kennedy, S.G., A.J. Wagner, S.D. Conzen, J. Jordan, A. Bellacosa, P.N. Tsichlis, and N. Hay. 1997. The PI 3-kinase/Akt signaling pathway delivers an anti-apoptotic signal. *Genes & development*. 11:701-713.

Kim, D.K., H. Nishida, S.Y. An, A.K. Shetty, T.J. Bartosh, and D.J. Prockop. 2016. Chromatographically isolated CD63+CD81+ extracellular vesicles from mesenchymal stromal cells rescue cognitive impairments after TBI. *Proc Natl Acad Sci U S A*. 113:170-175.

Knapp, P.E., R.P. Skoff, and T.J. Sprinkle. 1988. Differential expression of galactocerebroside, myelin basic protein, and 2',3'-cyclic nucleotide 3'-phosphohydrolase during development of oligodendrocytes in vitro. *J Neurosci Res*. 21:249-259.

Koles, K., J. Nunnari, C. Korkut, R. Barria, C. Brewer, Y. Li, J. Leszyk, B. Zhang, and V. Budnik. 2012. Mechanism of evenness interrupted (Evi)-exosome release at synaptic boutons. *J Biol Chem*. 287:16820-16834.

Kong, S.M., B.K. Chan, J.S. Park, K.J. Hill, J.B. Aitken, L. Cottle, H. Farghaian, A.R. Cole, P.A. Lay, C.M. Sue, and A.A. Cooper. 2014. Parkinson's disease-linked human PARK9/ATP13A2

maintains zinc homeostasis and promotes alpha-Synuclein externalization via exosomes. *Hum Mol Genet*. 23:2816-2833.

Korkut, C., B. Ataman, P. Ramachandran, J. Ashley, R. Barria, N. Gherbesi, and V. Budnik. 2009. Trans-synaptic transmission of vesicular Wnt signals through Evi/Wntless. *Cell*. 139:393-404.

Korkut, C., Y. Li, K. Koles, C. Brewer, J. Ashley, M. Yoshihara, and V. Budnik. 2013. Regulation of postsynaptic retrograde signaling by presynaptic exosome release. *Neuron*. 77:1039-1046.

Kowal, J., G. Arras, M. Colombo, M. Jouve, J.P. Morath, B. Primdal-Bengtson, F. Dingli, D. Loew, M. Tkach, and C. Thery. 2016. Proteomic comparison defines novel markers to characterize heterogeneous populations of extracellular vesicle subtypes. *Proc Natl Acad Sci U S A*. 113:E968-977.

Kowal, J., M. Tkach, and C. Thery. 2014. Biogenesis and secretion of exosomes. *Curr Opin Cell Biol*. 29:116-125.

Krämer-Albers, E.M., N. Bretz, S. Tenzer, C. Winterstein, W. Möbius, H. Berger, K.A. Nave, H. Schild, and J. Trotter. 2007. Oligodendrocytes secrete exosomes containing major myelin and stress-protective proteins: Trophic support for axons? *Proteomics Clin Appl*. 1:1446-1461.

Kramer-Albers, E.M., and A.F. Hill. 2016. Extracellular vesicles: interneural shuttles of complex messages. *Curr Opin Neurobiol*. 39:101-107.

Kramer-Albers, E.M., and W.P. Kuo-Elsner. 2016. Extracellular Vesicles: Goodies for the Brain? *Neuropsychopharmacology*. 41:371-372.

Kreutz, M.R., A. Bien, C.K. Vorwerk, T.M. Bockers, C.I. Seidenbecher, W. Tischmeyer, and B.A. Sabel. 1999. Co-expression of c-Jun and ATF-2 characterizes the surviving retinal ganglion cells which maintain axonal connections after partial optic nerve injury. *Brain research. Molecular brain research*. 69:232-241.

Kunadt, M., K. Eckermann, A. Stuendl, J. Gong, B. Russo, K. Strauss, S. Rai, S. Kugler, L. Falomir Lockhart, M. Schwalbe, P. Krumova, L.M. Oliveira, M. Bahr, W. Mobius, J. Levin, A. Giese, N. Kruse, B. Mollenhauer, R. Geiss-Friedlander, A.C. Ludolph, A. Freischmidt, M.S. Feiler, K.M. Danzer, M. Zweckstetter, T.M. Jovin, M. Simons, J.H. Weishaupt, and A. Schneider. 2015. Extracellular vesicle sorting of alpha-Synuclein is regulated by sumoylation. *Acta Neuropathol*. 129:695-713.

Kwinter, D.M., K. Lo, P. Mafi, and M.A. Silverman. 2009. Dynactin regulates bidirectional transport of dense-core vesicles in the axon and dendrites of cultured hippocampal neurons. *Neuroscience*. 162:1001-1010.

Lachenal, G., K. Pernet-Gallay, M. Chivet, F.J. Hemming, A. Belly, G. Bodon, B. Blot, G. Haase, Y. Goldberg, and R. Sadoul. 2011. Release of exosomes from differentiated neurons and its regulation by synaptic glutamatergic activity. *Mol Cell Neurosci*. 46:409-418.

Lakhal, S., and M.J. Wood. 2011. Intranasal exosomes for treatment of neuroinflammation? Prospects and limitations. *Molecular therapy : the journal of the American Society of Gene Therapy*. 19:1754-1756.

Laming, P.R., H. Kimelberg, S. Robinson, A. Salm, N. Hawrylak, C. Muller, B. Roots, and K. Ng. 2000. Neuronal-glial interactions and behaviour. *Neurosci Biobehav Rev*. 24:295-340.

Lappe-Siefke, C., S. Goebbels, M. Gravel, E. Nicksch, J. Lee, P.E. Braun, I.R. Griffiths, and K.A. Nave. 2003. Disruption of Cnp1 uncouples oligodendroglial functions in axonal support and myelination. *Nat Genet*. 33:366-374.

Lee, J., M. Gravel, R. Zhang, P. Thibault, and P.E. Braun. 2005. Process outgrowth in oligodendrocytes is mediated by CNP, a novel microtubule assembly myelin protein. *J Cell Biol*. 170:661-673.

Lee, S., M.K. Leach, S.A. Redmond, S.Y. Chong, S.H. Mellon, S.J. Tuck, Z.Q. Feng, J.M. Corey, and J.R. Chan. 2012a. A culture system to study oligodendrocyte myelination processes using engineered nanofibers. *Nat Methods*. 9:917-922.

Lee, Y., B.M. Morrison, Y. Li, S. Lengacher, M.H. Farah, P.N. Hoffman, Y. Liu, A. Tsingalia, L. Jin, P.W. Zhang, L. Pellerin, P.J. Magistretti, and J.D. Rothstein. 2012b. Oligodendroglia metabolically support axons and contribute to neurodegeneration. *Nature*. 487:443-448.

Leppa, S., and D. Bohmann. 1999. Diverse functions of JNK signaling and c-Jun in stress response and apoptosis. *Oncogene*. 18:6158-6162.

Limmer, S., and C. Klambt. 2014. Closing the gap between glia and neuroblast proliferation. *Dev Cell*. 30:249-250.

Lin, A.C., and C.E. Holt. 2007. Local translation and directional steering in axons. *EMBO J*. 26:3729-3736.

Lin, A.C., and C.E. Holt. 2008. Function and regulation of local axonal translation. *Curr Opin Neurobiol*. 18:60-68.

Llorente, A., T. Skotland, T. Sylvanne, D. Kauhanen, T. Rog, A. Orlowski, I. Vattulainen, K. Ekroos, and K. Sandvig. 2013. Molecular lipidomics of exosomes released by PC-3 prostate cancer cells. *Biochimica et biophysica acta*. 1831:1302-1309.

Lo Cicero, A., C. Delevoye, F. Gilles-Marsens, D. Loew, F. Dingli, C. Guere, N. Andre, K. Vie, G. van Niel, and G. Raposo. 2015a. Exosomes released by keratinocytes modulate melanocyte pigmentation. *Nat Commun*. 6:7506.

Lo Cicero, A., P.D. Stahl, and G. Raposo. 2015b. Extracellular vesicles shuffling intercellular messages: for good or for bad. *Curr Opin Cell Biol*. 35:69-77.

Locatelli, G., S. Wortge, T. Buch, B. Ingold, F. Frommer, B. Sobottka, M. Kruger, K. Karram, C. Buhlmann, I. Bechmann, F.L. Heppner, A. Waisman, and B. Becher. 2012. Primary oligodendrocyte death does not elicit anti-CNS immunity. *Nat Neurosci*. 15:543-550.

Lonze, B.E., and D.D. Ginty. 2002. Function and regulation of CREB family transcription factors in the nervous system. *Neuron*. 35:605-623.

Lopez-Verrilli, M.A., and F.A. Court. 2012. Transfer of vesicles from schwann cells to axons: a novel mechanism of communication in the peripheral nervous system. *Front Physiol*. 3:205.

Lopez-Verrilli, M.A., F. Picou, and F.A. Court. 2013. Schwann cell-derived exosomes enhance axonal regeneration in the peripheral nervous system. *Glia*.

Luk, K.C., V. Kehm, J. Carroll, B. Zhang, P. O'Brien, J.Q. Trojanowski, and V.M. Lee. 2012. Pathological alpha-synuclein transmission initiates Parkinson-like neurodegeneration in nontransgenic mice. *Science*. 338:949-953.

Maday, S., A.E. Twelvetrees, A.J. Moughamian, and E.L. Holzbaur. 2014. Axonal transport: cargo-specific mechanisms of motility and regulation. *Neuron*. 84:292-309.

Madison, R.D., C. McGee, R. Rawson, and G.A. Robinson. 2014. Extracellular vesicles from a muscle cell line (C2C12) enhance cell survival and neurite outgrowth of a motor neuron cell line (NSC-34). *Journal of extracellular vesicles*. 3.

Magistretti, P.J. 2006. Neuron-glia metabolic coupling and plasticity. *J Exp Biol*. 209:2304-2311.

Magistretti, P.J., and I. Allaman. 2015. A cellular perspective on brain energy metabolism and functional imaging. *Neuron*. 86:883-901.

Marcilla, A., L. Martin-Jaular, M. Trelis, A. de Menezes-Neto, A. Osuna, D. Bernal, C. Fernandez-Becerra, I.C. Almeida, and H.A. Del Portillo. 2014. Extracellular vesicles in parasitic diseases. *Journal of extracellular vesicles*. 3:25040.

Marino, S., L. Marani, C. Nazzaro, L. Beani, and A. Siniscalchi. 2007. Mechanisms of sodium azide-induced changes in intracellular calcium concentration in rat primary cortical neurons. *Neurotoxicology*. 28:622-629.

Matthews, C.C., D.M. Figueiredo, J.B. Wollack, N.F. Fairweather, G. Dougan, R.A. Hallewell, J.L. Cadet, and P.S. Fishman. 2000. Protective effect of supplemental superoxide dismutase on survival of neuronal cells during starvation. Requirement for cytosolic distribution. *J Mol Neurosci*. 14:155-166.

Mayer, M.P., and B. Bukau. 2005. Hsp70 chaperones: cellular functions and molecular mechanism. *Cell Mol Life Sci*. 62:670-684.

McKenzie, A.J., D. Hoshino, N.H. Hong, D.J. Cha, J.L. Franklin, R.J. Coffey, J.G. Patton, and A.M. Weaver. 2016. KRAS-MEK Signaling Controls Ago2 Sorting into Exosomes. *Cell Rep*. 15:978-987.

McKenzie, I.A., D. Ohayon, H. Li, J.P. de Faria, B. Emery, K. Tohyama, and W.D. Richardson. 2014. Motor skill learning requires active central myelination. *Science*. 346:318-322.

Menn, B., J.M. Garcia-Verdugo, C. Yaschine, O. Gonzalez-Perez, D. Rowitch, and A. Alvarez-Buylla. 2006. Origin of oligodendrocytes in the subventricular zone of the adult brain. *J Neurosci*. 26:7907-7918.

Mensch, S., M. Baraban, R. Almeida, T. Czopka, J. Ausborn, A. El Manira, and D.A. Lyons. 2015. Synaptic vesicle release regulates myelin sheath number of individual oligodendrocytes in vivo. *Nat Neurosci*. 18:628-630.

Micu, I., Q. Jiang, E. Coderre, A. Ridsdale, L. Zhang, J. Woulfe, X. Yin, B.D. Trapp, J.E. McRory, R. Rehak, G.W. Zamponi, W. Wang, and P.K. Stys. 2006. NMDA receptors mediate calcium accumulation in myelin during chemical ischaemia. *Nature*. 439:988-992.

Micu, I., J.R. Plemel, C. Lachance, J. Proft, A.J. Jansen, K. Cummins, J. van Minnen, and P.K. Stys. 2016. The molecular physiology of the axo-myelinic synapse. *Experimental neurology*. 276:41-50.

Minciacchi, V.R., M.R. Freeman, and D. Di Vizio. 2015. Extracellular vesicles in cancer: exosomes, microvesicles and the emerging role of large oncosomes. *Semin Cell Dev Biol*. 40:41-51.

Misgeld, T., M. Kerschensteiner, F.M. Bareyre, R.W. Burgess, and J.W. Lichtman. 2007. Imaging axonal transport of mitochondria in vivo. *Nat Methods*. 4:559-561.

Mitew, S., C.M. Hay, H. Peckham, J. Xiao, M. Koenning, and B. Emery. 2014. Mechanisms regulating the development of oligodendrocytes and central nervous system myelin. *Neuroscience*. 276:29-47.

Monsma, P.C., Y. Li, J.D. Fenn, P. Jung, and A. Brown. 2014. Local regulation of neurofilament transport by myelinating cells. *J Neurosci*. 34:2979-2988.

Montecalvo, A., A.T. Larregina, W.J. Shufesky, D.B. Stolz, M.L. Sullivan, J.M. Karlsson, C.J. Baty, G.A. Gibson, G. Erdos, Z. Wang, J. Milosevic, O.A. Tkacheva, S.J. Divito, R. Jordan, J. Lyons-Weiler, S.C. Watkins, and A.E. Morelli. 2012. Mechanism of transfer of functional microRNAs between mouse dendritic cells via exosomes. *Blood*. 119:756-766.

Morel, L., M. Regan, H. Higashimori, S.K. Ng, C. Esau, S. Vidensky, J. Rothstein, and Y. Yang. 2013. Neuronal exosomal miRNA-dependent translational regulation of astroglial glutamate transporter GLT1. *J Biol Chem*. 288:7105-7116.

Morfini, G., G. Szebenyi, H. Brown, H.C. Pant, G. Pigino, S. DeBoer, U. Beffert, and S.T. Brady. 2004. A novel CDK5-dependent pathway for regulating GSK3 activity and kinesin-driven motility in neurons. *EMBO J*. 23:2235-2245.

Morfini, G., G. Szebenyi, R. Elluru, N. Ratner, and S.T. Brady. 2002. Glycogen synthase kinase 3 phosphorylates kinesin light chains and negatively regulates kinesin-based motility. *EMBO J*. 21:281-293.

Morfini, G.A., M. Burns, L.I. Binder, N.M. Kanaan, N. LaPointe, D.A. Bosco, R.H. Brown, Jr., H. Brown, A. Tiwari, L. Hayward, J. Edgar, K.A. Nave, J. Garberrn, Y. Atagi, Y. Song, G. Pigino, and S.T. Brady. 2009. Axonal transport defects in neurodegenerative diseases. *J Neurosci*. 29:12776-12786.

Morrison, B.M., Y. Lee, and J.D. Rothstein. 2013a. Oligodendroglia metabolically support axons and maintain structural integrity. *Trends Cell Biol*.

Morrison, B.M., Y. Lee, and J.D. Rothstein. 2013b. Oligodendroglia: metabolic supporters of axons. *Trends Cell Biol*. 23:644-651.

Mota, B., and S. Herculano-Houzel. 2014. All brains are made of this: a fundamental building block of brain matter with matching neuronal and glial masses. *Front Neuroanat*. 8:127.

Mulcahy, L.A., R.C. Pink, and D.R. Carter. 2014. Routes and mechanisms of extracellular vesicle uptake. *Journal of extracellular vesicles*. 3.

Nave, K.A. 2010a. Myelination and support of axonal integrity by glia. *Nature*. 468:244-252.

Nave, K.A. 2010b. Myelination and the trophic support of long axons. *Nat Rev Neurosci*. 11:275-283.

Nave, K.A., and B.D. Trapp. 2008. Axon-glial signaling and the glial support of axon function. *Annu Rev Neurosci*. 31:535-561.

Nave, K.A., and H.B. Werner. 2014. Myelination of the nervous system: mechanisms and functions. *Annu Rev Cell Dev Biol*. 30:503-533.

Nawaz, S., P. Sanchez, S. Schmitt, N. Snaidero, M. Mitkovski, C. Velte, B.R. Bruckner, I. Alexopoulos, T. Czopka, S.Y. Jung, J.S. Rhee, A. Janshoff, W. Witke, I.A. Schaap, D.A. Lyons, and M. Simons. 2015. Actin filament turnover drives leading edge growth during myelin sheath formation in the central nervous system. *Dev Cell*. 34:139-151.

Nishiyama, A., M. Komitova, R. Suzuki, and X. Zhu. 2009. Polydendrocytes (NG2 cells): multifunctional cells with lineage plasticity. *Nat Rev Neurosci*. 10:9-22.

Oikonomou, G., and S. Shaham. 2011. The glia of Caenorhabditis elegans. *Glia*. 59:1253-1263.

Oliva, A.A., Jr., C.M. Atkins, L. Copenagle, and G.A. Banker. 2006. Activated c-Jun N-terminal kinase is required for axon formation. *J Neurosci*. 26:9462-9470.

Ostrowski, M., N.B. Carmo, S. Krumeich, I. Fanget, G. Raposo, A. Savina, C.F. Moita, K. Schauer, A.N. Hume, R.P. Freitas, B. Goud, P. Benaroch, N. Hacohen, M. Fukuda, C. Desnos, M.C. Seabra, F. Darchen, S. Amigorena, L.F. Moita, and C. Thery. 2010. Rab27a and Rab27b control different steps of the exosome secretion pathway. *Nat Cell Biol*. 12:19-30; sup pp 11-13.

Pan, B.T., R. Blostein, and R.M. Johnstone. 1983. Loss of the transferrin receptor during the maturation of sheep reticulocytes in vitro. An immunological approach. *Biochem J*. 210:37-47.

Pan, B.T., and R.M. Johnstone. 1983. Fate of the transferrin receptor during maturation of sheep reticulocytes in vitro: selective externalization of the receptor. *Cell*. 33:967-978.

Pan, B.T., K. Teng, C. Wu, M. Adam, and R.M. Johnstone. 1985. Electron microscopic evidence for externalization of the transferrin receptor in vesicular form in sheep reticulocytes. *J Cell Biol*. 101:942-948.

Peinado, H., M. Aleckovic, S. Lavotshkin, I. Matei, B. Costa-Silva, G. Moreno-Bueno, M. Hergueta-Redondo, C. Williams, G. Garcia-Santos, C. Ghajar, A. Nitadori-Hoshino, C. Hoffman, K. Badal, B.A. Garcia, M.K. Callahan, J. Yuan, V.R. Martins, J. Skog, R.N. Kaplan, M.S. Brady, J.D. Wolchok, P.B. Chapman, Y. Kang, J. Bromberg, and D. Lyden. 2012.

Melanoma exosomes educate bone marrow progenitor cells toward a pro-metastatic phenotype through MET. *Nat Med*. 18:883-891.

Pelvig, D.P., H. Pakkenberg, A.K. Stark, and B. Pakkenberg. 2008. Neocortical glial cell numbers in human brains. *Neurobiol Aging*. 29:1754-1762.

Perlson, E., S. Maday, M.M. Fu, A.J. Moughamian, and E.L. Holzbaur. 2010. Retrograde axonal transport: pathways to cell death? *Trends in neurosciences*. 33:335-344.

Pfeiffer, S.E., A.E. Warrington, and R. Bansal. 1993. The oligodendrocyte and its many cellular processes. *Trends Cell Biol*. 3:191-197.

Pigino, G., G. Morfini, Y. Atagi, A. Deshpande, C. Yu, L. Jungbauer, M. LaDu, J. Busciglio, and S. Brady. 2009. Disruption of fast axonal transport is a pathogenic mechanism for intraneuronal amyloid beta. *Proc Natl Acad Sci U S A*. 106:5907-5912.

Pisitkun, T., R.F. Shen, and M.A. Knepper. 2004. Identification and proteomic profiling of exosomes in human urine. *Proc Natl Acad Sci U S A*. 101:13368-13373.

Potolicchio, I., G.J. Carven, X. Xu, C. Stipp, R.J. Riese, L.J. Stern, and L. Santambrogio. 2005. Proteomic analysis of microglia-derived exosomes: metabolic role of the aminopeptidase CD13 in neuropeptide catabolism. *J Immunol*. 175:2237-2243.

Pusic, A.D., and R.P. Kraig. 2014. Youth and environmental enrichment generate serum exosomes containing miR-219 that promote CNS myelination. *Glia*. 62:284-299.

Pusic, A.D., K.M. Pusic, B.L. Clayton, and R.P. Kraig. 2014. IFNgamma-stimulated dendritic cell exosomes as a potential therapeutic for remyelination. *J Neuroimmunol*. 266:12-23.

Pusic, K.M., A.D. Pusic, and R.P. Kraig. 2016. Environmental Enrichment Stimulates Immune Cell Secretion of Exosomes that Promote CNS Myelination and May Regulate Inflammation. *Cell Mol Neurobiol*. 36:313-325.

Rana, S., S. Yue, D. Stadel, and M. Zoller. 2012. Toward tailored exosomes: the exosomal tetraspanin web contributes to target cell selection. *The international journal of biochemistry & cell biology*. 44:1574-1584.

Rana, S., and M. Zoller. 2011. Exosome target cell selection and the importance of exosomal tetraspanins: a hypothesis. *Biochemical Society transactions*. 39:559-562.

Rani, S., A.E. Ryan, M.D. Griffin, and T. Ritter. 2015. Mesenchymal Stem Cell-derived Extracellular Vesicles: Toward Cell-free Therapeutic Applications. *Molecular therapy : the journal of the American Society of Gene Therapy*. 23:812-823.

Raposo, G., H.W. Nijman, W. Stoorvogel, R. Liejendekker, C.V. Harding, C.J. Melief, and H.J. Geuze. 1996. B lymphocytes secrete antigen-presenting vesicles. *The Journal of experimental medicine*. 183:1161-1172.

Raposo, G., and W. Stoorvogel. 2013. Extracellular vesicles: exosomes, microvesicles, and friends. *J Cell Biol*. 200:373-383.

Ratajczak, J., K. Miekus, M. Kucia, J. Zhang, R. Reca, P. Dvorak, and M.Z. Ratajczak. 2006. Embryonic stem cell-derived microvesicles reprogram hematopoietic progenitors: evidence for horizontal transfer of mRNA and protein delivery. *Leukemia*. 20:847-856.

Regis, S., S. Grossi, F. Corsolini, R. Biancheri, and M. Filocamo. 2009. PLP1 gene duplication causes overexpression and alteration of the PLP/DM20 splicing balance in fibroblasts from Pelizaeus-Merzbacher disease patients. *Biochimica et biophysica acta*. 1792:548-554.

Riccio, A., R.S. Alvania, B.E. Lonze, N. Ramanan, T. Kim, Y. Huang, T.M. Dawson, S.H. Snyder, and D.D. Ginty. 2006. A nitric oxide signaling pathway controls CREB-mediated gene expression in neurons. *Mol Cell*. 21:283-294.

Ridder, K., S. Keller, M. Dams, A.K. Rupp, J. Schlaudraff, D. Del Turco, J. Starmann, J. Macas, D. Karpova, K. Devraj, C. Depboylu, B. Landfried, B. Arnold, K.H. Plate, G. Hoglinger, H. Sultmann, P. Altevogt, and S. Momma. 2014. Extracellular vesicle-mediated transfer of genetic information between the hematopoietic system and the brain in response to inflammation. *PLoS Biol*. 12:e1001874.

Rinholm, J.E., N.B. Hamilton, N. Kessaris, W.D. Richardson, L.H. Bergersen, and D. Attwell. 2011. Regulation of oligodendrocyte development and myelination by glucose and lactate. *J Neurosci*. 31:538-548.

Riss, T.L., R.A. Moravec, A.L. Niles, H.A. Benink, T.J. Worzella, and L. Minor. 2004. Cell Viability Assays. *In* Assay Guidance Manual. G.S. Sittampalam, N.P. Coussens, H. Nelson, M. Arkin, D. Auld, C. Austin, B. Bejcek, M. Glicksman, J. Inglese, P.W. Iversen, Z. Li, J. McGee, O. McManus, L. Minor, A. Napper, J.M. Peltier, T. Riss, O.J. Trask, Jr., and J. Weidner, editors, Bethesda (MD).

Robinson, G.A. 1996. Changes in the expression of transcription factors ATF-2 and Fra-2 after axotomy and during regeneration in rat retinal ganglion cells. *Brain research. Molecular brain research*. 41:57-64.

Rockenstein, E., M. Torrance, A. Adame, M. Mante, P. Bar-on, J.B. Rose, L. Crews, and E. Masliah. 2007. Neuroprotective effects of regulators of the glycogen synthase kinase-3beta signaling pathway in a transgenic model of Alzheimer's disease are associated with reduced amyloid precursor protein phosphorylation. *J Neurosci*. 27:1981-1991.

Rosenbluth, J., K.A. Nave, A. Mierzwa, and R. Schiff. 2006. Subtle myelin defects in PLP-null mice. *Glia*. 54:172-182.

Roucourt, B., S. Meeussen, J. Bao, P. Zimmermann, and G. David. 2015. Heparanase activates the syndecan-syntenin-ALIX exosome pathway. *Cell Res*. 25:412-428.

Rowitch, D.H., and A.R. Kriegstein. 2010. Developmental genetics of vertebrate glial-cell specification. *Nature*. 468:214-222.

Saab, A.S., I.D. Tzvetanova, and K.A. Nave. 2013. The role of myelin and oligodendrocytes in axonal energy metabolism. *Curr Opin Neurobiol*. 23:1065-1072.

Saab, A.S., I.D. Tzvetavona, A. Trevisiol, S. Baltan, P. Dibaj, K. Kusch, W. Mobius, B. Goetze, H.M. Jahn, W. Huang, H. Steffens, E.D. Schomburg, A. Perez-Samartin, F. Perez-Cerda, D. Bakhtiari, C. Matute, S. Lowel, C. Griesinger, J. Hirrlinger, F. Kirchhoff, and K.A. Nave. 2016. Oligodendroglial NMDA Receptors Regulate Glucose Import and Axonal Energy Metabolism. *Neuron*. 91:119-132.

Saez, J.C., J.A. Kessler, M.V. Bennett, and D.C. Spray. 1987. Superoxide dismutase protects cultured neurons against death by starvation. *Proc Natl Acad Sci U S A*. 84:3056-3059.

Sakamoto, K., K. Karelina, and K. Obrietan. 2011. CREB: a multifaceted regulator of neuronal plasticity and protection. *J Neurochem*. 116:1-9.

Sambrook, J., and D. Russell. 2001. Molecular Cloning - A Laboratory Manual. *Cold Spring Harbor Laboratory Press, New York, USA*.

Sanchez, I., L. Hassinger, R.K. Sihag, D.W. Cleveland, P. Mohan, and R.A. Nixon. 2000. Local control of neurofilament accumulation during radial growth of myelinating axons in vivo. Selective role of site-specific phosphorylation. *J Cell Biol*. 151:1013-1024.

Savina, A., C.M. Fader, M.T. Damiani, and M.I. Colombo. 2005. Rab11 promotes docking and fusion of multivesicular bodies in a calcium-dependent manner. *Traffic*. 6:131-143.

Schirmeier, S., T. Matzat, and C. Klambt. 2015. Axon ensheathment and metabolic supply by glial cells in Drosophila. *Brain research*.

Schneider, A., and M. Simons. 2016. Catching filopodia: Exosomes surf on fast highways to enter cells. *J Cell Biol*. 213:143-145.

Scholz, J., M.C. Klein, T.E. Behrens, and H. Johansen-Berg. 2009. Training induces changes in white-matter architecture. *Nat Neurosci*. 12:1370-1371.

Schwarz, T.L. 2013. Mitochondrial trafficking in neurons. *Cold Spring Harb Perspect Biol*. 5.

Shaham, S. 2006. Glia-neuron interactions in the nervous system of Caenorhabditis elegans. *Curr Opin Neurobiol*. 16:522-528.

Sheng, Z.H. 2014. Mitochondrial trafficking and anchoring in neurons: New insight and implications. *J Cell Biol*. 204:1087-1098.

Shimoda, M., S. Principe, H.W. Jackson, V. Luga, H. Fang, S.D. Molyneux, Y.W. Shao, A. Aiken, P.D. Waterhouse, C. Karamboulas, F.M. Hess, T. Ohtsuka, Y. Okada, L. Ailles, A. Ludwig, J.L. Wrana, T. Kislinger, and R. Khokha. 2014. Loss of the Timp gene family is sufficient for the acquisition of the CAF-like cell state. *Nat Cell Biol*. 16:889-901.

Simons, M., and K.A. Nave. 2015. Oligodendrocytes: Myelination and Axonal Support. *Cold Spring Harb Perspect Biol*. 8.

Simons, M., and G. Raposo. 2009. Exosomes--vesicular carriers for intercellular communication. *Curr Opin Cell Biol*. 21:575-581.

Simons, M., and K. Trajkovic. 2006. Neuron-glia communication in the control of oligodendrocyte function and myelin biogenesis. *J Cell Sci*. 119:4381-4389.

Skog, J., T. Wurdinger, S. van Rijn, D.H. Meijer, L. Gainche, M. Sena-Esteves, W.T. Curry, Jr., B.S. Carter, A.M. Krichevsky, and X.O. Breakefield. 2008. Glioblastoma microvesicles transport RNA and proteins that promote tumour growth and provide diagnostic biomarkers. *Nat Cell Biol*. 10:1470-1476.

Smith, Z.J., C. Lee, T. Rojalin, R.P. Carney, S. Hazari, A. Knudson, K. Lam, H. Saari, E.L. Ibanez, T. Viitala, T. Laaksonen, M. Yliperttula, and S. Wachsmann-Hogiu. 2015. Single exosome study reveals subpopulations distributed among cell lines with variability related to membrane content. *Journal of extracellular vesicles*. 4:28533.

Snaidero, N., W. Mobius, T. Czopka, L.H. Hekking, C. Mathisen, D. Verkleij, S. Goebbels, J. Edgar, D. Merkler, D.A. Lyons, K.A. Nave, and M. Simons. 2014. Myelin membrane wrapping of CNS axons by PI(3,4,5)P3-dependent polarized growth at the inner tongue. *Cell*. 156:277-290.

Snaidero, N., and M. Simons. 2014. Myelination at a glance. *J Cell Sci*. 127:2999-3004.

Sommer, I., and M. Schachner. 1981. Monoclonal antibodies (O1 to O4) to oligodendrocyte cell surfaces: an immunocytological study in the central nervous system. *Dev Biol*. 83:311-327.

Stegmayr, B., and G. Ronquist. 1982. Promotive effect on human sperm progressive motility by prostasomes. *Urol Res*. 10:253-257.

Stoorvogel, W., M.J. Kleijmeer, H.J. Geuze, and G. Raposo. 2002. The biogenesis and functions of exosomes. *Traffic*. 3:321-330.

Stork, T., R. Bernardos, and M.R. Freeman. 2012. Analysis of glial cell development and function in Drosophila. *Cold Spring Harb Protoc*. 2012:1-17.

Street, J.M., P.E. Barran, C.L. Mackay, S. Weidt, C. Balmforth, T.S. Walsh, R.T. Chalmers, D.J. Webb, and J.W. Dear. 2012. Identification and proteomic profiling of exosomes in human cerebrospinal fluid. *J Transl Med*. 10:5.

Subra, C., K. Laulagnier, B. Perret, and M. Record. 2007. Exosome lipidomics unravels lipid sorting at the level of multivesicular bodies. *Biochimie*. 89:205-212.

Sutton, M.A., and E.M. Schuman. 2005. Local translational control in dendrites and its role in long-term synaptic plasticity. *Journal of neurobiology*. 64:116-131.

Tadokoro, H., T. Umezu, K. Ohyashiki, T. Hirano, and J.H. Ohyashiki. 2013. Exosomes derived from hypoxic leukemia cells enhance tube formation in endothelial cells. *J Biol Chem*. 288:34343-34351.

Tao, X., S. Finkbeiner, D.B. Arnold, A.J. Shaywitz, and M.E. Greenberg. 1998. Ca2+ influx regulates BDNF transcription by a CREB family transcription factor-dependent mechanism. *Neuron*. 20:709-726.

Tarrade, A., C. Fassier, S. Courageot, D. Charvin, J. Vitte, L. Peris, A. Thorel, E. Mouisel, N. Fonknechten, N. Roblot, D. Seilhean, A. Dierich, J.J. Hauw, and J. Melki. 2006. A mutation of spastin is responsible for swellings and impairment of transport in a region of axon characterized by changes in microtubule composition. *Hum Mol Genet*. 15:3544-3558.

Tasca, C.I., T. Dal-Cim, and H. Cimarosti. 2015. In vitro oxygen-glucose deprivation to study ischemic cell death. *Methods Mol Biol*. 1254:197-210.

Taylor, A.R., M.B. Robinson, D.J. Gifondorwa, M. Tytell, and C.E. Milligan. 2007. Regulation of heat shock protein 70 release in astrocytes: role of signaling kinases. *Developmental neurobiology*. 67:1815-1829.

Tetta, C., E. Ghigo, L. Silengo, M.C. Deregibus, and G. Camussi. 2013. Extracellular vesicles as an emerging mechanism of cell-to-cell communication. *Endocrine*. 44:11-19.

Thery, C., S. Amigorena, G. Raposo, and A. Clayton. 2006. Isolation and characterization of exosomes from cell culture supernatants and biological fluids. *Current protocols in cell biology / editorial board, Juan S. Bonifacino ... [et al.]*. Chapter 3:Unit 3 22.

Thery, C., M. Ostrowski, and E. Segura. 2009. Membrane vesicles as conveyors of immune responses. *Nat Rev Immunol*. 9:581-593.

Thery, C., L. Zitvogel, and S. Amigorena. 2002. Exosomes: composition, biogenesis and function. *Nat Rev Immunol*. 2:569-579.

Thomas, K., and A. Davies. 2005. Neurotrophins: a ticket to ride for BDNF. *Current biology : CB*. 15:R262-264.

Tkach, M., and C. Thery. 2016. Communication by Extracellular Vesicles: Where We Are and Where We Need to Go. *Cell*. 164:1226-1232.

Tower, D.B. 1954. Structural and functional organization of mammalian cerebral cortex; the correlation of neurone density with brain size; cortical neurone density in the fin whale (Balaenoptera physalus L.) with a note on the cortical neurone density in the Indian elephant. *J Comp Neurol*. 101:19-51.

Trajkovic, K., C. Hsu, S. Chiantia, L. Rajendran, D. Wenzel, F. Wieland, P. Schwille, B. Brugger, and M. Simons. 2008. Ceramide triggers budding of exosome vesicles into multivesicular endosomes. *Science*. 319:1244-1247.

Trapp, B.D., A. Nishiyama, D. Cheng, and W. Macklin. 1997. Differentiation and death of premyelinating oligodendrocytes in developing rodent brain. *J Cell Biol*. 137:459-468.

Tress, O., M. Maglione, D. May, T. Pivneva, N. Richter, J. Seyfarth, S. Binder, A. Zlomuzica, G. Seifert, M. Theis, E. Dere, H. Kettenmann, and K. Willecke. 2012. Panglial gap junctional communication is essential for maintenance of myelin in the CNS. *J Neurosci*. 32:7499-7518.

Trevisiol, A., and K.A. Nave. 2015. Brain Energy Metabolism: Conserved Functions of Glycolytic Glial Cells. *Cell Metab*. 22:361-363.

Trotter, J., K. Karram, and A. Nishiyama. 2010. NG2 cells: Properties, progeny and origin. *Brain Res Rev*. 63:72-82.

Trotter, J., and M. Schachner. 1989. Cells positive for the O4 surface antigen isolated by cell sorting are able to differentiate into astrocytes or oligodendrocytes. *Brain Res Dev Brain Res*. 46:115-122.

Turola, E., R. Furlan, F. Bianco, M. Matteoli, and C. Verderio. 2012. Microglial microvesicle secretion and intercellular signaling. *Front Physiol*. 3:149.

Tytell, M., S.G. Greenberg, and R.J. Lasek. 1986. Heat shock-like protein is transferred from glia to axon. *Brain research*. 363:161-164.

Tytell, M., R.J. Lasek, and H. Gainer. 2016. Axonal maintenance, glia, exosomes, and heat shock proteins. *F1000Res*. 5.

Umezu, T., K. Ohyashiki, M. Kuroda, and J.H. Ohyashiki. 2013. Leukemia cell to endothelial cell communication via exosomal miRNAs. *Oncogene*. 32:2747-2755.

Valadi, H., K. Ekstrom, A. Bossios, M. Sjostrand, J.J. Lee, and J.O. Lotvall. 2007. Exosome-mediated transfer of mRNAs and microRNAs is a novel mechanism of genetic exchange between cells. *Nat Cell Biol*. 9:654-659.

van Balkom, B.W., O.G. de Jong, M. Smits, J. Brummelman, K. den Ouden, P.M. de Bree, M.A. van Eijndhoven, D.M. Pegtel, W. Stoorvogel, T. Wurdinger, and M.C. Verhaar. 2013. Endothelial cells require miR-214 to secrete exosomes that suppress senescence and induce angiogenesis in human and mouse endothelial cells. *Blood*. 121:3997-4006, S3991-3915.

Van Deun, J., P. Mestdagh, R. Sormunen, V. Cocquyt, K. Vermaelen, J. Vandesompele, M. Bracke, O. De Wever, and A. Hendrix. 2014. The impact of disparate isolation methods for extracellular vesicles on downstream RNA profiling. *Journal of extracellular vesicles*. 3.

Verhey, K.J., D. Meyer, R. Deehan, J. Blenis, B.J. Schnapp, T.A. Rapoport, and B. Margolis. 2001. Cargo of kinesin identified as JIP scaffolding proteins and associated signaling molecules. *J Cell Biol*. 152:959-970.

Villarroya-Beltri, C., C. Gutierrez-Vazquez, F. Sanchez-Cabo, D. Perez-Hernandez, J. Vazquez, N. Martin-Cofreces, D.J. Martinez-Herrera, A. Pascual-Montano, M. Mittelbrunn, and F. Sanchez-Madrid. 2013. Sumoylated hnRNPA2B1 controls the sorting of miRNAs into exosomes through binding to specific motifs. *Nat Commun*. 4:2980.

Vitale, N., J. Mawet, J. Camonis, R. Regazzi, M.F. Bader, and S. Chasserot-Golaz. 2005. The Small GTPase RalA controls exocytosis of large dense core secretory granules by interacting with ARF6-dependent phospholipase D1. *J Biol Chem*. 280:29921-29928.

Volkenhoff, A., A. Weiler, M. Letzel, M. Stehling, C. Klambt, and S. Schirmeier. 2015. Glial Glycolysis Is Essential for Neuronal Survival in Drosophila. *Cell Metab*. 22:437-447.

Wake, H., P.R. Lee, and R.D. Fields. 2011. Control of Local Protein Synthesis and Initial Events in Myelination by Action Potentials. *Science*.

Walton, M.R., and I. Dragunow. 2000. Is CREB a key to neuronal survival? *Trends in neurosciences*. 23:48-53.

Wang, J., R. Kaletsky, M. Silva, A. Williams, L.A. Haas, R.J. Androwski, J.N. Landis, C. Patrick, A. Rashid, D. Santiago-Martinez, M. Gravato-Nobre, J. Hodgkin, D.H. Hall, C.T. Murphy, and M.M. Barr. 2015. Cell-Specific Transcriptional Profiling of Ciliated Sensory Neurons Reveals Regulators of Behavior and Extracellular Vesicle Biogenesis. *Current biology : CB*. 25:3232-3238.

Wang, J., M. Silva, L.A. Haas, N.S. Morsci, K.C. Nguyen, D.H. Hall, and M.M. Barr. 2014. C. elegans ciliated sensory neurons release extracellular vesicles that function in animal communication. *Current biology : CB*. 24:519-525.

Wang, S., F. Cesca, G. Loers, M. Schweizer, F. Buck, F. Benfenati, M. Schachner, and R. Kleene. 2011. Synapsin I is an oligomannose-carrying glycoprotein, acts as an oligomannose-binding lectin, and promotes neurite outgrowth and neuronal survival when released via glia-derived exosomes. *J Neurosci*. 31:7275-7290.

Wei, X., X. Yang, Z.P. Han, F.F. Qu, L. Shao, and Y.F. Shi. 2013. Mesenchymal stem cells: a new trend for cell therapy. *Acta Pharmacol Sin*. 34:747-754.

White, R., C. Gonsior, E.M. Kramer-Albers, N. Stohr, S. Huttelmaier, and J. Trotter. 2008. Activation of oligodendroglial Fyn kinase enhances translation of mRNAs transported in hnRNP A2-dependent RNA granules. *J Cell Biol*. 181:579-586.

White, R., and E.M. Kramer-Albers. 2014. Axon-glia interaction and membrane traffic in myelin formation. *Front Cell Neurosci*. 7:284.

Willms, E., H.J. Johansson, I. Mager, Y. Lee, K.E. Blomberg, M. Sadik, A. Alaarg, C.I. Smith, J. Lehtio, S. El Andaloussi, M.J. Wood, and P. Vader. 2016. Cells release subpopulations of exosomes with distinct molecular and biological properties. *Sci Rep*. 6:22519.

Witan, H., A. Kern, I. Koziollek-Drechsler, R. Wade, C. Behl, and A.M. Clement. 2008. Heterodimer formation of wild-type and amyotrophic lateral sclerosis-causing mutant Cu/Zn-superoxide dismutase induces toxicity independent of protein aggregation. *Hum Mol Genet*. 17:1373-1385.

Witt, A., and S.T. Brady. 2000. Unwrapping new layers of complexity in axon/glial relationships. *Glia*. 29:112-117.

Witwer, K.W., E.I. Buzas, L.T. Bemis, A. Bora, C. Lasser, J. Lotvall, E.N. Nolte-'t Hoen, M.G. Piper, S. Sivaraman, J. Skog, C. Thery, M.H. Wauben, and F. Hochberg. 2013. Standardization of sample collection, isolation and analysis methods in extracellular vesicle research. *Journal of extracellular vesicles*. 2.

Xin, H., Y. Li, Y. Cui, J.J. Yang, Z.G. Zhang, and M. Chopp. 2013a. Systemic administration of exosomes released from mesenchymal stromal cells promote functional recovery and neurovascular plasticity after stroke in rats. *Journal of cerebral blood flow and metabolism : official journal of the International Society of Cerebral Blood Flow and Metabolism*. 33:1711-1715.

Xin, H., Y. Li, Z. Liu, X. Wang, X. Shang, Y. Cui, Z.G. Zhang, and M. Chopp. 2013b. MiR-133b promotes neural plasticity and functional recovery after treatment of stroke with multipotent mesenchymal stromal cells in rats via transfer of exosome-enriched extracellular particles. *Stem Cells*. 31:2737-2746.

Yanez-Mo, M., P.R. Siljander, Z. Andreu, A.B. Zavec, F.E. Borras, E.I. Buzas, K. Buzas, E. Casal, F. Cappello, J. Carvalho, E. Colas, A. Cordeiro-da Silva, S. Fais, J.M. Falcon-Perez, I.M. Ghobrial, B. Giebel, M. Gimona, M. Graner, I. Gursel, M. Gursel, N.H. Heegaard, A. Hendrix, P. Kierulf, K. Kokubun, M. Kosanovic, V. Kralj-Iglic, E.M. Kramer-Albers, S. Laitinen, C. Lasser, T. Lener, E. Ligeti, A. Line, G. Lipps, A. Llorente, J. Lotvall, M. Mancek-Keber, A. Marcilla, M. Mittelbrunn, I. Nazarenko, E.N. Nolte-'t Hoen, T.A. Nyman, L. O'Driscoll, M. Olivan, C. Oliveira, E. Pallinger, H.A. Del Portillo, J. Reventos, M. Rigau, E. Rohde, M. Sammar, F. Sanchez-Madrid, N. Santarem, K. Schallmoser, M.S. Ostenfeld, W. Stoorvogel, R. Stukelj, S.G. Van der Grein, M.H. Vasconcelos, M.H. Wauben, and O. De Wever. 2015. Biological properties of extracellular vesicles and their physiological functions. *Journal of extracellular vesicles*. 4:27066.

Yu, B., M. Gong, Y. Wang, R.W. Millard, Z. Pasha, Y. Yang, M. Ashraf, and M. Xu. 2013. Cardiomyocyte protection by GATA-4 gene engineered mesenchymal stem cells is partially mediated by translocation of miR-221 in microvesicles. *PLoS One*. 8:e73304.

Yu, X., S.L. Harris, and A.J. Levine. 2006. The regulation of exosome secretion: a novel function of the p53 protein. *Cancer research*. 66:4795-4801.

Yuan, A., E.L. Farber, A.L. Rapoport, D. Tejada, R. Deniskin, N.B. Akhmedov, and D.B. Farber. 2009. Transfer of microRNAs by embryonic stem cell microvesicles. *PLoS One*. 4:e4722.

Yuyama, K., H. Sun, S. Mitsutake, and Y. Igarashi. 2012. Sphingolipid-modulated exosome secretion promotes clearance of amyloid-beta by microglia. *J Biol Chem*. 287:10977-10989.

Yuyama, K., H. Sun, S. Usuki, S. Sakai, H. Hanamatsu, T. Mioka, N. Kimura, M. Okada, H. Tahara, J. Furukawa, N. Fujitani, Y. Shinohara, and Y. Igarashi. 2015. A potential function for neuronal exosomes: sequestering intracerebral amyloid-beta peptide. *FEBS letters*. 589:84-88.

Zala, D., M.V. Hinckelmann, H. Yu, M.M. Lyra da Cunha, G. Liot, F.P. Cordelieres, S. Marco, and F. Saudou. 2013. Vesicular glycolysis provides on-board energy for fast axonal transport. *Cell*. 152:479-491.

Zalc, B., D. Goujet, and D. Colman. 2008. The origin of the myelination program in vertebrates. *Current biology : CB*. 18:R511-512.

Zelko, I.N., T.J. Mariani, and R.J. Folz. 2002. Superoxide dismutase multigene family: a comparison of the CuZn-SOD (SOD1), Mn-SOD (SOD2), and EC-SOD (SOD3) gene structures, evolution, and expression. *Free Radic Biol Med*. 33:337-349.

Zhu, X., D.E. Bergles, and A. Nishiyama. 2008. NG2 cells generate both oligodendrocytes and gray matter astrocytes. *Development*. 135:145-157.

Zitvogel, L., A. Regnault, A. Lozier, J. Wolfers, C. Flament, D. Tenza, P. Ricciardi-Castagnoli, G. Raposo, and S. Amigorena. 1998. Eradication of established murine tumors using a novel cell-free vaccine: dendritic cell-derived exosomes. *Nat Med*. 4:594-600.

Zuchero, J.B., M.M. Fu, S.A. Sloan, A. Ibrahim, A. Olson, A. Zaremba, J.C. Dugas, S. Wienbar, A.V. Caprariello, C. Kantor, D. Leonoudakis, K. Lariosa-Willingham, G. Kronenberg, K. Gertz, S.H. Soderling, R.H. Miller, and B.A. Barres. 2015. CNS myelin wrapping is driven by actin disassembly. *Dev Cell*. 34:152-167.

7 Appendix

7.1 List of Abbreviations

Aß	Amyloid beta
AD	Alzheimer's disease
ADP	Adenosine-diphosphate
Ago2	Argonaut 2
Alix	ALG-2-interacting protein X
ALS	Amyotrophic lateral sclerosis
AMPA	α-Amino-3-hydroxyl-5-methyl-4-isoxazolepropionic acid
AMPAR	AMPA receptor
APP	Amyloid precursor protein
ARF6	ADP-ribosylation factor 6
ATP	Adenosine triphosphate
BBB	Blood-brain-barrier
BDNF	Brain-derived neurotrophic factor
<cb1	Cannabinoid receptor type 1
CD	Cluster of differentiation
CREB	cAMP response element-binding protein
CNS	Central nervous system
CNP	2', 3'-cyclic nucleotide 3'-phosphodiesterase
COX	Cytochrome c oxidase
CSF	Cerebrospinal fluid
DIV	Days in vitro
DNA	Desoxyribonucleic acid
EAAT2	Excitatory amino acid transporter 2
EGFP	Enhanced green fluorescent protein
EM	Electron microscopy
ER	Endoplasmatic reticulum
ESCRT	Endosomal Sorting Complex Required for Transport
EV	Extracellular vesicle

Evi	Evenness interrupted
FAT	Fast axonal transport
flox	Flanked by loxP sites
GABA	γ-aminobutyric acid
GLUT1	Glucose transporter 1
GTP	Guanosine triphosphate
h	Hour
HIV	Human immunodeficiency virus
HS	Horse serum
HSC	Heat shock cognate protein
HSP	Heat shock protein
IFN γ	Interferon gamma
IL-1ß	Interleukin 1ß
ILV	Intraluminal vesicle
KO	Knockout
LE	Late endosomes
loxP	Locus of crossover [X] in P1
MAG	Myelin-associated glycoprotein
MBP	Myelin basic protein
MCT	Monocarboxylate transporter
MHC	Major histocompatibility complex
min	Minute
miRNA	Micro ribonucleic acid
MOG	Myelin oligodendrocyte glycoprotein
mRNA	Messenger ribonucleic acid
MT	Microtubule
MTT	3-(4,5-Dimethylthiazol-2-yl)-2,5-diphenyltetrazoliumbromid
MV	Microvesicle
MVB	Multivesicular body
NAD	Nicotinamide adenine dinucleotide
NADP	Nicotinamide adenine dinucleotide phosphate
NG2	Neural/glial antigen 2

NMDA	N-Methyl-D-aspartate
NMDAR	NMDA receptor
NMJ	Neuromuscular junction
nSMase	Neutral Sphingomyelinase
OL	Oligodendrocyte
OPC	Oligodendroglial precursor cell
PD	Parkinson's disease
PDGFR	Platelet-derived growth factor
PEX5	Peroxisomal biogenesis factor 5
PLD	Phospholipase D
PLP	Proteolipid protein
PMD	Pelizaeus-Merzbacher disease
PNS	Peripheral nervous system
PrP	Prion protein
Rab	Ras-related in the brain
RNA	Ribonucleic acid
RT	Room temperature
SC	Schwann cell
SN	Supernatant
SOD	Superoxide dismutase
SPG2	Spastic paraplegia 2
Syt4	Synaptotagmin 4
Tat	Trans-activator of transcription
TDP-43	TAR DNA-binding protein 43
TfR	Transferrin receptor
WT	Wildtype

7.2 List of Tables

Table 3.1 Microscopes 23
Table 3.2 Centrifuges 23
Table 3.3 Cell culture equipment 23

Table 3.4 Other lab equipment 24
Table 3.5 Chemicals 24
Table 3.6 Kits 24
Table 3.7 Marker 25
Table 3.8 Other Materials 25
Table 3.9 Software 25
Table 3.10 Buffers, media, and solutions 26
Table 3.11 Primary antibodies 27
Table 3.12 Secondary antibodies 28
Table 3.13 Composition of enzyme mix 1 and 2 29
Table 3.14 Density of Neuronal Cultures 32

7.3 List of Figures

Figure 2-1 Glial phylogeny 2
Figure 2-2 Emergence and structure of myelin 4
Figure 2-3 Metabolic support of myelinated axons by glia 7
Figure 2-4 Exosome biogenesis and internalization 14
Figure 2-5 Reciprocal communication between neurons and oligodendrocytes 20
Figure 3-1 Cell sorting using MACS MicroBeads 30
Figure 3-2 Conversion of MTT to formazan 38
Figure 3-3 Macro for Axonal Transport Analysis 39
Figure 3-4 Example of analysing the axonal transport of single vesicles 41
Figure 4-1 Characterization of $O4^+$-oligodendrocyte cultures 42
Figure 4-2 Immunocytochemical analysis of $O4^+$-oligodendrocyte cultures 43
Figure 4-3 SOD1 is shuttled from oligodendrocytes to neurons via exosomes 45
Figure 4-4 Oligodendroglial exosomes protect neurons from oxidative stress 48
Figure 4-5 Oligodendroglial exosomes protect neurons from starvation stress 50
Figure 4-6 Oligodendroglial exosomes protect neurons during OGD 51
Figure 4-7 Kinase Screen of exosome-treated neurons 53
Figure 4-8 Exosome-dependent activation of Akt and Erk1/2 54
Figure 4-9 Exosome signalling in recipient neurons under stress conditions 54

Figure 4-10 Impact of oligodendroglial exosomes on axonal transport.....56
Figure 4-11 Oligodendroglial exosomes facilitate axonal transport under oxidative stress....57
Figure 4-12 Oligodendroglial exosomes facilitate axonal transport under starvation stress ..59
Figure 4-13 $PLP^{-/-}$ and $CNP^{-/-}$ exosomes do not protect neurons from starvation stress.....61
Figure 4-14 Dose-dependent effect of exosomes on neuronal metabolism 61
Figure 4-15 Characterization of exosomes purified by ultrafiltration 63
Figure 4-16 CNP^{null} and PLP^{null} exosomes do not mediate neuroprotection 64
Figure 4-17 PLP^{null}- and CNP^{null}-derived exosomes do not affect axonal transport 65
Figure 5-1 Composition of oligodendroglial exosomes 71
Figure 5-2 Schematic illustration of exosome-mediated neuroprotection 78

8 Publications

1. Frühbeis C, Fröhlich D, **Kuo WP** and Krämer-Albers E-M (2013) Extracellular vesicles as mediators of neuron–glia communication. Front. Cell. Neurosci. 7:182. doi: 10.3389/fncel.2013.00182

   In the nervous system, glia cells maintain homeostasis, synthesize myelin, provide metabolic support, and participate in immune defense. The communication between glia and neurons is essential to synchronize these diverse functions with brain activity. Evidence is accumulating that secreted extracellular vesicles (EVs), such as exosomes and shedding microvesicles, are key players in intercellular signaling. The cells of the nervous system secrete EVs, which potentially carry protein and RNA cargo from one cell to another. After delivery, the cargo has the ability to modify the target cell phenotype. Here, we review the recent advances in understanding the role of EV secretion by astrocytes, microglia, and oligodendrocytes in the central nervous system. Current work has demonstrated that oligodendrocytes transfer exosomes to neurons as a result of neurotransmitter signaling suggesting that these vesicles may mediate glial support of neurons.

2. Frühbeis C, Fröhlich D, **Kuo WP**, Amphornrat J, Thilemann S, et al. (2013) Neurotransmitter-Triggered Transfer of Exosomes Mediates Oligodendrocyte–Neuron Communication. PLoS Biol 11(7): e1001604. doi: 10.1371/journal.pbio.1001604

   Reciprocal interactions between neurons and oligodendrocytes are not only crucial for myelination, but also for long-term survival of axons. Degeneration of axons occurs in several human myelin diseases, however the molecular mechanisms of axon-glia communication maintaining axon integrity are poorly understood. Here, we describe the signal-mediated transfer of exosomes from oligodendrocytes to neurons. These endosome-derived vesicles are secreted by oligodendrocytes and carry specific protein and RNA cargo. We show that activity-dependent release of the neurotransmitter glutamate triggers oligodendroglial exosome secretion mediated by Ca^{2+} entry through oligodendroglial NMDA and AMPA receptors. In turn, neurons internalize the released

exosomes by endocytosis. Injection of oligodendroglia-derived exosomes into the mouse brain results in functional retrieval of exosome cargo in neurons. Supply of cultured neurons with oligodendroglial exosomes improves neuronal viability under conditions of cell stress. These findings indicate that oligodendroglial exosomes participate in a novel mode of bidirectional neuron-glia communication contributing to neuronal integrity.

3. Fröhlich D*, **Kuo WP*,** Frühbeis C, Sun JJ, Zehendner CM, Luhmann HJ, Pinto S, Toedling J, Trotter J, (2014) Multifaceted effects of oligodendroglial exosomes on neurons: impact on neuronal firing rate, signal transduction and gene regulation. Phil. Trans. R. Soc. B 369: 20130510.
   *Authors contributed equally to this study.

   Exosomes are small membranous vesicles of endocytic origin that are released by almost every cell type. They exert versatile functions in intercellular communication important for many physiological and pathological processes. Recently, exosomes attracted interest with regard to their role in cell–cell communication in the nervous system. We have shown that exosomes released from oligodendrocytes upon stimulation with the neurotransmitter glutamate are internalized by neurons and enhance the neuronal stress tolerance. Here, we demonstrate that oligodendroglial exosomes also promote neuronal survival during oxygen–glucose deprivation, a model of cerebral ischaemia. We show the transfer from oligodendrocytes to neurons of superoxide dismu- tase and catalase, enzymes which are known to help cells to resist oxidative stress. Additionally, we identify various effects of oligodendroglial exo- somes on neuronal physiology. Electrophysiological analysis using in vitro multi-electrode arrays revealed an increased firing rate of neurons exposed to oligodendroglial exosomes. Moreover, gene expression analysis and phosphorylation arrays uncovered differentially expressed genes and altered signal transduction pathways in neurons after exosome treatment. Our study thus provides new insight into the broad spectrum of action of oligoden- droglial exosomes and their effects on neuronal physiology. The exchange of extracellular vesicles between neural cells may exhibit remarkable potential to impact brain performance.

4. Krämer-Albers EM and **Kuo-Elsner WP** (2016) Extrcellular vesicles: goodies for the brain? Neuropsychopharmacology Reviews (2016) 41, 371–372; doi:10.1038/npp.2015.242

5. Frühbeis C, **Kuo-Elsner WP**, Fröhlich D, Tenzer S, Möbius W, Werner H, Trotter J, and Krämer-Albers EM (in preparation)

   Oligodendrocytes form myelin and provide trophic support to neurons ensuring long-term axonal survival. Triggered by neuronal activity, oligodendrocytes release extracellular vesicles with the properties of exosomes, which are internalized by neurons and provide support under stress conditions. Oligodendroglial exosomes carry a range of proteins including the myelin proteins PLP and CNP. Inactivation of these proteins in mice leads to degeneration of axons, which is also critical in human myelin disease. Here, we study the role of CNP and PLP in exosome release and found that cultured null oligodendrocytes secreted reduced levels of exosomes. Using the exosome pathway, null oligodendrocytes were neither able to transmit signals nor to provide protection to target neurons with the same efficiency as wild type cells. In addition, a proteomic screen revealed that the protein composition of exosomes was altered by lack of CNP and PLP. These findings indicate that transfer of cargo by oligodendroglial exosomes contributes to neuronal health.

9 Acknowledgement

10 Curriculum Vitae

11 Eidesstattliche Erklärung

Hiermit erkläre ich, Wen Ping Elsner, geboren am 23.08.1983 in Hürth, dass ich meine Dissertation selbständig und nur unter Verwendung der angegebenen Hilfsmittel angefertigt habe. Ich habe keinen anderen Promotionsversuch unternommen.

_____ _____

Ort, Datum (Wen Ping Elsner)